PLIF Investigation of the Fuel Distribution in Gasoline Direct Injection Fuel Sprays

by

Michael H. Shelby

B.S., Mechanical Engineering
University of Illinois, Urbana-Champaign
(1995)

Submitted to the Department of Mechanical Engineering
in Partial Fulfillment of the Requirements
for the Degree of

MASTER OF SCIENCE IN MECHANICAL ENGINEERING

AT THE

MASSACHUSETTS INSTITUTE OF TECHNOLOGY

May 1997

Signature of Author _____
Department of Mechanical Engineering
May 23, 1997

Certified by _____
Simone Hochgreb
Associate Professor of Mechanical Engineering
Thesis Supervisor

Accepted by _____
Ain A. Sonin
Chairman, Departmental Graduate Committee

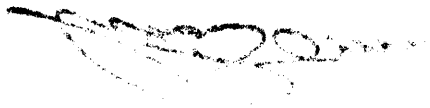

PLIF Investigation of the Fuel Distribution in Gasoline Direct Injection Fuel Sprays

by

Michael H. Shelby

Submitted to the Department of Mechanical Engineering
on May 23, 1997 in partial fulfillment of the
requirements for the Degree of

Master of Science in Mechanical Engineering.

ABSTRACT

Due to the increasing use of automobiles and the detrimental effect that exhaust emissions have on the atmosphere, researchers continue to search for methods to improve the efficiency of the internal combustion engine. One possible method of improving the specific power and the fuel economy of gasoline engines is the use of direct injection fuel systems. Injecting the gasoline directly into the combustion chamber allows the engine to operate at a higher compression ratio and improves the potential for stratified charge lean burn engines.

This work investigates the properties of fuel sprays from pressure swirl atomizer injectors of the type used in direct injection gasoline engines. An optical engine was modified for direct injection and the equipment necessary to perform Planer Laser Induced Fluorescence (PLIF) measurements of the fuel distribution inside the combustion chamber was purchased and assembled in the test facility. This document includes a description of the test equipment, LabVIEW engine control program, optical engine modifications, and preliminary results obtained with the system.

The initial spray development of three different injectors at three different fuel pressures (3.0 MPa, 5.0 MPa, and 7.0 MPa) was imaged in 30 μsec intervals. The spray development occurred in four phases: 1) Delay phase, a period of time between the rising edge of the injection signal and the first occurrence of fuel in the combustion chamber. 2) Solid jet phase, occurrence of a poorly atomized stream of liquid fuel during the first 150 μsec of the injection. 3) Wide hollow cone phase, separation of the liquid jet into a hollow cone spray once sufficient tangential velocity has been established. 4) Fully developed spray, spray cone angle is narrowed due to a low pressure zone in the center of the spray cone created by air entrainment.

The dependence of the fully developed spray cone angle on fuel injection pressure and ambient pressure was also briefly investigated. Over the range of conditions tested, the cone angle was largely insensitive to fuel injection pressure but narrowed as the ambient pressure increased. At 0.5 bar the measured cone angle was 70° and decreased to 57° when the ambient pressure was increased to 1.1 bar.

Thesis Advisor: Professor Simone Hochgreb
Title: Associate Professor of Mechanical Engineering

ACKNOWLEDGEMENTS

In working towards the completion of this project and in life, I have been supported by a number of people whom I can never properly thank. This project has been made possible by the hard work and dedication of my academic advisor, Professor Simone Hochgreb. Through her efforts, ample funding was available to acquire the equipment and services necessary for this project, and her guidance is appreciated. Professors Heywood and Cheng have also provided immeasurable assistance in the form of advice and troubleshooting in the test cell.

As do all students at the Sloan Automotive Lab, I owe a majority of my successful projects in the lab to the able help of Brian Corkum and can attribute a good number of my failures to not asking for his help soon enough. The value of the comic relief provided by Pete (liquor license) Menard is only surpassed by the value of the assistance that he provided in keeping our test cell running. The organization provided by Nancy Cook has not gone unnoticed, and is greatly appreciated.

My time at the Sloan Automotive Lab would never have been as entertaining nor as educational without my fellow students, especially those who shared the office space of 31-061. Their experiences (successful and unsuccessful) have taught me more than I could have hoped to learn in two years. I would especially like to thank Norman Peralta for his positive outlook, Robert Meyer for his German lessons (and his tolerance for what I did with them), and Brad VanDerWege for his advice and friendship.

The support and encouragement that I have received from my family was given without second thought and has made it possible for me to pursue a Master's degree. Over the years they have deserved the most thanks and often have not received it.

This work was funded by the National Science Foundation, the Department of Energy and the Warren M. Rohsenow fellowship fund.

TABLE OF CONTENTS

LIST OF TABLES

LIST OF FIGURES

CHAPTER 1

INTRODUCTION

1.1 Motivation

America's love for the automobile has grown to the point that vehicles are nearly as numerous as people (195.5 million vehicles for 260.7 million people in 1994 [1]). As the popularity of automobiles and the need for more commercial transportation has increased, consumption of fossil fuels has risen to astronomical levels. In 1994 the United States alone consumed 140,600,000,000 gallons of fuel! As more and more countries begin to develop vehicle use patterns similar to those of the United States, it is imperative that the efficiency of the Internal Combustion (IC) engine be improved. The IC engine is the most widely used power source in transportation because it offers the best balance between power density (size and weight), cost (initial and running), and availability of fuels. As the harmful effects of exhaust emissions are better understood, government bodies are consistently passing stricter legislation regarding the acceptable emission levels from all types of vehicles.

Emission levels from IC engines have been greatly reduced through improvements in engine design and the introduction of after treatment systems. Improvements in fuel metering systems, Exhaust-Gas Recirculation (EGR), combustion chamber design, and the use of 3-way catalytic converters has enabled manufactures to meet current emission regulations; however, concerns regarding "greenhouse" gas emissions such as CO_2 and total fuel consumption are increasing interest in finding more efficient IC engine designs.

1.2 Background

In spite of the advances made in pollution control systems, significant opportunity to further reduce the emission levels from IC engines and to increase the overall thermodynamic efficiency of such systems still exists. For automobile spark ignition systems, one concept currently under investigation to improve fuel economy and specific power is the Gasoline Direct Injection (GDI) engine. Modern production gasoline engines inject fuel into the intake port while the intake valve is closed. This allows the hot surfaces of the back of the intake valve and the intake port to be used to provide the energy needed to vaporize the fuel. This system eliminates much of the cylinder to cylinder variation in air fuel ratio present in a carburated or single point fuel injection systems. However, vaporization still depends on the buildup of a liquid fuel "puddle" in the intake port. The presence of this puddle makes it difficult to control the air fuel mixture accurately when the engine speed or load varies. Fuel is typically injected soon after the intake valve has closed from the previous cycle. This maximizes the time available for the fuel to vaporize, but it also makes

it more difficult to control the air-fuel ratio during transient operation (there is more of a time lag between the control action and the observed response in air fuel ratio).

A GDI fuel system can overcome many of the limitations of a port fuel injected system as well as provide some unexpected benefits. As the name implies, gasoline is injected directly into the combustion chamber in a GDI engine. As mixture preparation systems have evolved, the fuel source generally has moved closer to the combustion chamber. GDI is the natural end of that evolution. GDI fuel systems allow very precise cycle to cycle control of the amount of fuel added to the mixture because the vaporization process does not depend on the presence of a liquid puddle. But, because the fuel is added into the combustion chamber instead of into the intake port, significantly less time is available to vaporize the fuel and mix it properly with the rest of the charge (air and EGR). For this reason GDI systems typically use higher fuel injection pressures in order to create smaller diameter fuel droplets.

To date, two automotive manufactures have developed production intent GDI engines, and several others are in the process [2, 3]. Early testing indicates that a GDI fuel system can improve the Wide Open Throttle (WOT) performance of an engine by 5-10% as well as increase the fuel economy [4]. These seemingly conflicting goals are achieved because of the unique mixture preparation process of a GDI engine. In a GDI engine, the injector is typically targeted so that the majority of the fuel spray does not impinge on the surfaces of the combustion chamber. As the fuel evaporates, it cools the charge mixture by as much as 15 °C, which increases the charge density [5]. Under WOT conditions, this allows more air to be inducted into the cylinder which directly translates into an increase in maximum power. The charge cooling effect also reduces the tendency for the air/fuel mixture to self ignite, allowing a GDI engine to be designed with a higher compression ratio. This directly translates into an increase in the overall thermodynamic efficiency. Under part load conditions, with the proper charge motion, a stratified mixture can be developed. By stratifying the mixture, the engine can operate with an air fuel ratio that is overall very lean (40:1) but stoichiometric or rich in the location near the spark plug [2, 3, 6, 7]. Stratifying the mixture in this way allows the throttle to be opened eliminating much of the pumping work. The end benefit is that GDI engines operate with an efficiency closer to that of diesel engines, while maintaining drivability and emissions characteristics similar to spark ignition engines.

In order to achieve these benefits with acceptable emission levels, several challenges must be overcome. Less time is available for the air and fuel to mix in a GDI engine, therefore the spray properties of the injector are very important to the success of such a system. To operate the engine with a stratified mixture at part load and a homogeneous mixture under full load, a method for controlling the amount of air fuel mixing is needed. Typically, the amount of mixing is controlled by the injection timing. By injecting fuel early in the intake stroke, approximately 280 crank angle degrees are available to form a homogeneous mixture. For stratified operation, the injection is timed much closer to spark timing and the cylinder charge motion is shaped to bring the cloud of combustible mixture to the spark plug right at the time of spark. In order to avoid bulk quenching of the flame front and high engine-out hydrocarbon emissions, it is important that the transition from the fuel rich region to the fuel lean region is not gradual. In order to achieve these

very different operating regimes with acceptable emissions, it is necessary to have an understanding of the behavior of the fuel spray under different operating conditions.

CHAPTER 2

EXPERIMENT GOALS AND DIAGNOSTICS

In order for a GDI engine to realize the benefits of increased fuel efficiency and increased specific power, several challenges have to be overcome. Developing an injector and an in-cylinder flow field which will enable complete air utilization during full load homogeneous operation and a well contained pocket of combustible mixture during part load stratified charge operation is a difficult task. In order to achieve these goals, an understanding of the behavior of fuel injection sprays under different operating conditions is necessary. Four different factors that affect the trajectory of the fuel spray have been investigated during the course of this project. These factors are: (1) the penetration of the initial portion of the fuel spray as a function of injector and fuel pressure, (2) the angle of the fuel spray as a function of the fuel pressure and ambient pressure, (3) the spray distribution as a function of the fuel volatility and engine temperature, and (4) the behavior of the fuel spray under engine start-up fuel pressures. Some additional semi quantitative information about the droplet size obtained under different operating conditions has also been acquired, but the limited spatial resolution of the imaging system, and the high number density of the fuel spray prevents accurate droplet size measurements with this technique. By studying the behavior of the liquid fuel during the injection event, we hope to aid engine designers in constructing systems which minimize wall wetting and allow the desired air/fuel distribution to be achieved.

2.1 Description of experimental studies

2.1.1 Initial spray penetration

This study investigates the initial spray development focusing on the "pre-spray" portion of the fuel spray. At the beginning of the injection process, the fuel does not have sufficient angular momentum to achieve the hollow cone structure of the fully developed spray [8]. This initial development period consists of relatively large droplets with high axial velocities. Tracking the propagation of these early droplets and determining an injection strategy that will minimize the amount of liquid impinging on the combustion chamber surfaces will aid in reducing the hydrocarbon emissions of DI engines.

2.1.2 Spray cone angle

In addition to the early development portion of the spray, the fully developed spray is studied to determine the effect of varying the fuel injection pressure and the ambient pressure on the cone angle. The angle at which the fuel leaves the injector has a direct effect on where the fuel ends up in the cylinder and must be understood if wall wetting is to be avoided.

2.1.3 Engine temperature and fuel volatility

The overall structure of the spray is also investigated in relation to the operating temperature of the engine and the volatility of the dopant. The vaporization characteristics of the fuel being used and the thermal state of the mixture present in the combustion chamber at the time of injection will affect how far a fuel droplet will travel before it is vaporized. The penetration of the bulk of the fuel spray is determined by the initial momentum present in the spray and how quickly the spray is vaporized.

2.1.4 Start-up fuel pressure operation

When the engine is first started, the mechanical high pressure fuel pump can not deliver the normal operating fuel pressure. One strategy, which has been used by Mitsubishi, is to use the low pressure fuel feed pump to start the engine [3]. In this study, the spray character of the Zexel injectors (see section 3.7 for a description of the injector hardware) is investigated with a fuel pressure of 0.3 MPa to emulate the low start-up pressure.

2.2 Diagnostic Selection

In order to investigate the properties of the fuel spray that were mentioned in the previous section, it is necessary to have a diagnostic tool that can simultaneously measure the fuel distribution on a 2-dimensional plane. The most common systems used for this type of measurement include mie scattering, Planer Laser Induced Fluorescence (PLIF), and exciplex fluorescence. Each of these diagnostics has its advantages and its drawbacks.

Mie scattering is the simplest of the possible systems. When light passes through the fuel droplets, a portion of the light is redirected, or scattered away from the axis of travel. This scattered light is then collected and information about the presence or absence of fuel droplets can be inferred. One major drawback to this system is that the strength of the scattered signal depends on the size of the droplet, with smaller droplets scattering more light than larger droplets. This technique has been used widely to image sprays but is not applicable to vapor measurements.

Planer Laser Induced Fluorescence (PLIF), makes use of compounds which can be excited to a higher energy state by ultraviolet laser light and then return to their ground state by emitting light. This light is collected and the amount of the compound present in the measurement volume is proportional to the intensity of fluorescent light received. This technique can be used to study both the liquid and the vapor phase of fluorescent compounds. The strength of the fluorescence can be affected by several factors. The concentration of the fluorescent compound, collision quenching with other molecules, temperature, pressure, and laser intensity can all affect the amount of fluorescent light. The use of PLIF in combustion systems and the fluorescent properties of many substances are well described in the literature. [9, 10, 11, 12, 13, 14]

The third technique, exciplex fluorescence, is similar to PLIF except that a compound, or mixture of compounds, is chosen that emits a different wavelength of light in the vapor phase than it does in the liquid phase. This property makes the exciplex technique very useful for studying the evaporation and mixture preparation of fuel-air mixtures. The major difficulty of using the exciplex system is finding a compound that has sufficient spectral separation in the fluorescence between the liquid and the vapor phase and evaporative properties similar to those of gasoline. A mixture of 2.9% benzene and 2.0% triethylamine has been suggested, but there is still significant overlap in the emission spectrum of the vapor and liquid phase [15].

The technique we have selected for studying the fuel distribution in direct injection fuel sprays is Planer Laser Induced Fluorescence (PLIF). The general method for measuring the two dimensional distribution of fuel inside of a spray is as follows. A compound that will fluoresce when struck with ultraviolet laser light is added to the fuel to act as a tracer. Slightly before the image is taken, a pulsed sheet of laser light is directed through the center of the fuel spray. A high speed camera is then used to image the resulting fluorescence. The acquired image is a 2-dimensional cross section of the fuel spray. Table 2.1 is summary of the tests which were run during these investigations.

Table 2.1 Test matrix

Study	Injector	Fuel pres. (MPa)	SOI (CA)	Image timing	Dopant
Initial spray penetration	20° Zexel	3,5,7	630	330-1050μs ASOI(Δt 30 μs)	3-pentanone
	60° Zexel	3,5,7	630	330-1050μs ASOI(Δt 30 μs)	3-pentanone
	Chrysler	3,5,7	630	170-970μs ASOI(Δt 30 μs)	3-pentanone
Cone angle	60° Zexel	1,2,3,4,5,6,7	630	640 CA	3-pentanone
	60° Zexel	5	10	20	3-pentanone
	60° Zexel	5	30	40	3-pentanone
	60° Zexel	5	60	70	3-pentanone
	60° Zexel	5	90	100	3-pentanone
Temperature volatility	20° Zexel	5	630	640 (cold to hot)	3-pentanone
	20° Zexel	5	630	640(cold to hot)	acetone
	60° Zexel	5	630	640(cold to hot)	3-pentanone
	60° Zexel	5	630	640(cold to hot)	acetone
	60° Zexel	5	630	645 (hot)	acetone
	60° Zexel	5	600	606(cold to hot)	acetone
	60° Zexel	5	600	607(cold to hot) horizontal	acetone
	60° Zexel	5	600	607(cold to hot) horizontal	3-pentanone

CHAPTER 3

EQUIPMENT

The PLIF technique can be used throughout the engine cycle and the equipment necessary for PLIF measurements can also be used for exciplex and for mie scattering (a visible light source is needed for mie scattering). A simple schematic diagram of the PLIF system can be found in Figure 3.1 and a more detailed description of the system hardware, connections, operation, and software settings can be found in Appendix 1. The basic components that make up the PLIF system are an ultraviolet laser, a high speed camera, and a suitable dopant to trace the fuel.

3.1 Laser

A Lambda Physik Compex 102 was purchased and installed for the purposes of this study. The Compex 102 is an excimer laser operating at 308 nm (with XeCl gas mixture), 20 Hz maximum repetition rate, and 240 mJ maximum pulse energy. The beam exits the laser in a rectangular shape having dimensions of 22 mm tall by 7 mm wide. The beam is shaped by a pair of cylindrical lenses (focal length 157.1 mm and 52.3 mm) and a slit changing the beam dimensions to 30 mm by 0.5 mm. Approximately 20% of the energy emitted by the laser is actually transmitted to the test volume. The greatest loss of energy occurs when the final width of the beam is set by passing it through the slit.

3.2 Camera system

The camera system selected for this project consists of a Princeton Instruments Intensified Charge Coupled Device (ICCD) camera. This system was chosen for its wide dynamic range (16 bit, 65536 gray levels), extremely short exposure times (50 nano seconds to several seconds), and its ability to function as a timing device for the rest of the instrumentation. The camera system consists of a Pentium PC computer, a Princeton Instruments ST138 camera controller, a Princeton Instruments PG200 pulse generator, and a Princeton Instruments 576SE ICCD detector. The CCD array has 384 rows and 576 columns of pixels, yielding a spatial resolution of approximately 0.8 mm when coupled with a 60 mm Nikkor camera lens. The major limitation of the system for imaging engine processes is that it requires approximately two seconds between pictures to transfer the image data from the camera to the memory of the computer. This limitation prevents more than one image from being taken in an engine cycle. In fact, at 1000 rpm at least 16 engine cycles occur between pictures. If higher framing rates are required for a future experiment, it is possible to operate the camera in "Frame Transfer" mode with the present equipment (see Princeton Instruments manuals for a description). In "Frame Transfer" mode, only a portion of the CCD array is used to acquire an

image, and then the image is rapidly shuffled from the exposed portion of the array to the unexposed portion. Several pictures can be taken in rapid succession at the cost of resolution.

3.3 PLIF timing modes

For the data presented in this work, two different methods of synchronizing the engine and the data acquisition system have been used. The most common method used to synchronize the PLIF system and the engine operation was a DCI counter (external counter with reset, count, and output connections) to count engine crank angle and to trigger the PG200 at the desired crank angle. This method works well for acquiring images at a known crank angle, but because the engine RPM is not constant some variability in the acquired images was observed when time based events (i.e. fuel injection pulse) where imaged. The crank angle at which the DCI counter triggers the PG200 can be adjusted between images while the camera is transferring the image to the computer. By sweeping crank angle in this manner, a "movie" of the fuel injection pulse or any other event can be built up in one data file.

In the initial spray characterization experiments, images where acquired in 30 μsec increments timed from the rising edge of the injection control signal. In order to time the experiment in this manner, the injection signal is connected to the PG200 *trigger in* BNC port and a table of gate delay and delay trigger values are programmed into the PG200 (see PG 200 manual, functions 102 and 103). Once started, the PG200 will continue to cycle through the values in the table. For this series of images the engine was started, the *start acquisition* button on camera software was pressed and then after the camera had taken one image, the start sequence function on the PG200 was executed. This timing method was initiated because there was some variability and lack of temporal resolution when timing pictures from the crank angle signal.

3.4 Dopants

At the heart of the PLIF technique is the choice of the fluorescent compound or dopant. A seemingly infinite number of compounds will fluoresce if excited by the proper wavelength. In some cases, pump gasoline provides an adequate signal, but the fluorescent compounds within gasoline have not been well characterized [16]. A good dopant yields sufficient signal strength, is insensitive to temperature and pressure fluctuations, and reliably follows the substance to be measured. For fuel tracing, a number of aldehides and ketones have been investigated by several researchers [10, 11, 12, 17] For the tests conducted in this study, two different ketones were selected. Acetone was used to represent the more volatile components present in gasoline, while 3-pentanone was used to trace the behavior of the mid-range compounds (see Table 3.1 for dopant properties). All testing was conducted with a 10:1 mixture of iso-octane and dopant by volume. This mixture strength gave adequate signal levels for the spray visualization and relatively low signal levels for the vapor phase measurements. The properties of these dopants and iso-octane can be found in table 3.1. Absorption and emission spectra can be found in the literature for several

ketones [14]. The absorption spectrum for acetone and 3-pentanone ranges from 240 nm to 320 nm. The peak absorption band for both dopants occurs near 280 nm but the absorption is still significant at 308 nm. The peak emission band is near 420 nm for all of the ketones studied [14].

Table 3.1 Dopant properties [18]

Compound	Boiling point °C	Vapor pressure (kPa @ 300 °C)	Heat of vaporization (kJ/mol @ 300 °C)	Flash point °C
Iso-octane	99	6.8	351	-7
Acetone	56	32.1	308	-17
3-pentanone	102	5.0	382	6

The intensity of the fluorescence produced by the compound depends on many factors. Ambient pressure, temperature, concentration, and laser intensity are some of the variables that affect the signal strength. For some compounds, the excited molecules can release their excess energy through collisions with other molecules, a process called quenching. The pressure dependence of acetone has been studied by Yuen et al. [19] and they determined that acetone is not significantly affected by small pressure changes in the range of pressures encountered in these experiments and thus does not have any significant quenching partners.

3.5 Optical engine

The spray visualization experiments were conducted inside of a running engine that has been extensively modified for optical access (Figure 3.2). The engine has a square cross section which allows complete optical access through two of the side walls and a 75.6 mm x 72.6 mm viewing area through a third window. The third window was added for this project and it allows the fluorescence to be viewed at 90 degrees from the path of the laser light. Dimensions and specifications for the engine are given in Table 3.2. The overall compression ratio for the engine is 8.0, which is significantly lower than that of several of the prototype DI engines currently operating at 11-12:1. The compression ratio can easily be increased by placing spacers underneath the piston, however, sealing the engine becomes progressively more difficult as the peak pressures increase. The engine can be operated in either a port fuel injected configuration or a direct injection configuration . The engine is controlled by a LabVIEW based computer program, which allows the spark timing, injection timing and injection duration to be set arbitrarily. A detailed explanation of this program can be found in Appendix 2.

Table 3.2 Optical engine parameters

Parameter	Description
Cross Section	82.55 mm x 82.55 mm
Stroke	114.3 mm
Displacement	0.77 liters
Compression ratio	8
Number of valves	2
Head geometry	flat
Piston geometry	flat

The modifications required for operating the optical engine with direct injection included constructing a new high pressure fuel system and providing a mounting location for the injector within the cylinder head. Given the difficulty of locating replacement parts for our engine and the extensive amount of rework that would be required to mount the injector in an optimal location (near the center of the combustion chamber), an adapter was made so that the spark plug hole could be used for the injector (drawings for the adapter can be found in Figures A3.7 and A3.8 in Appendix 3). The spark plug was then relocated to the opposite side of the combustion chamber in what was previously a pressure transducer hole. No effort was made to shape the intake flow for stratified charge operation so all testing was conducted with a homogenous charge strategy. For a detailed exploration of the mixture preparation process in stratified charge engines, extensive rework or replacement of the engine would be required to achieve more representative in-cylinder flows.

3.6 High pressure fuel system

The high fuel pressures required for direct injection were generated using a compressed nitrogen cylinder and a hydraulic accumulator. Figure 3.3 shows the components of the fuel system and the connections between them. This type of system has several advantages over a mechanical pump. By using a high pressure nitrogen cylinder to pressurize the entire fuel system, the fuel pressure can be set independently of the engine operating condition. Mechanical fuel pumps generally do not deliver full pressure during engine start-up, using the compressed nitrogen fuel system makes it possible to test the injector at the fuel pressure obtained during cranking for an extended period of time. The accumulator fuel system also has few wetted components making flushing the system easier when changing fuels. The nitrogen and the fuel are separated by a Greer hydraulics accumulator (part # -1 800575) which prevents the nitrogen from being absorbed by the fuel while it is under pressure.

Operating procedure:

Since the fuel system is operated at relatively high pressures, care should be taken when using the system to prevent discharging the fuel into the test cell and creating an extreme fire hazard. The procedure for refilling the fuel system is as follows:

Purge the leftover fuel:

1) Close the nitrogen cylinder valve.
2) Bleed the system down to atmospheric pressure by opening the bleed valve located next to the pressure regulator.
3) Place the fill tube in a container appropriate for waste fuel.
4) Open the fuel fill valve located next to the fuel injector and the valve on the end of the fill tube.
5) Turn the pressure regulator to the lowest pressure setting.
6) Re-open the nitrogen cylinder valve.
7) Close the bleed valve and slowly pressurize the system (~0.5 MPa is sufficient). This will empty the remaining fuel into the waste container.
8) Remove the fill tube from the waste container and close the nitrogen cylinder.
9) Open the bleed valve and return the system to atmospheric pressure.

Prepare system for fuel fill:

1) Attach the vacuum pump to the nozzle located on the bleed valve and evacuate nitrogen side of the fuel system.
2) Close the bleed valve and remove the vacuum pump. The accumulator bladder is now fully inflated.
3) Attach the vacuum pump to the fuel fill line and evacuate the fuel side of the system. Be sure to use a liquid trap and allow the pump to run for several minutes to facilitate the evaporation of any remaining fuel in the system.
4) Close the valve attached to the end of the fuel fill line and remove the vacuum pump. The system is now ready to be re-filled.

Filling the fuel system:

1) Submerse the fuel fill line in the new fuel-dopant mixture.
2) Open the valve on the end of the fuel fill line and allow the atmospheric pressure to push the fuel up into the accumulator. Take care not to allow any air into the system.
3) Close the valve on the fuel fill line.
4) Close the fuel fill valve located adjacent to the fuel injector.
5) Re-open the valve on the fuel fill line. (Prevents pressure from building up in the plastic line if there is a leak past the fuel fill valve.)
6) Pressurize the system to the desired operating pressure.

To date, the fuel system has been used over a pressure range of 0.3 MPa to 7.0 MPa. The fuel system components are all rated for at least 13 MPa.

3.7 Fuel injectors

The injectors used for this study include two manufactured by Zexel Incorporated and one donated by Chrysler Corporation (see Table 3.3 for series numbers). All three of the injectors are pressure swirl atomizers which impart a significant amount of rotational momentum to the fuel as it is injected. Each injector produces a hollow cone spray with a characteristic cone angle. The nominal cone angle for the Chrysler injector was 50° while the Zexel Injectors were nominally 20° and 60°. See Figure 3.4 for a photograph of the injectors (the 20° and 60° Zexel injectors are identical externally, so only one is shown

in the figure). Fuel delivery curves were provided by Zexel for both injectors and a linear approximation to those curves is provided in Table 3.3. Because it is desirable to be able to inject fuel late into the intake stroke, direct injection generally requires a higher fuel pressure. This higher fuel pressure is used to finely atomize the spray so that less time is required to vaporize the fuel. Calculations performed by Lee Dodge indicate that the Sauter Mean Diameter (SMD) should not exceed 15 μm in order for all of the fuel to be vaporized by the 90% burned point in the heat release process. In order to achieve this level of atomization with a pressure swirl atomizer, a pressure drop of 4.9 MPa is required across the injector [20].

The injectors are driven by hardware donated by each of the manufactures. The Zexel system requires a negative logic TTL signal (injects when control signal goes to 0 volts) and the Chrysler driver is capable of processing negative or positive TTL level signals. See Figure 3.5 for the wiring diagram for the injector driver installation.

Table 3.3 Injector hardware

Injector	Series number	Fuel delivery (mm^3/stroke)
20° Zexel	HFI-2.1: 960040-2350	$Q=15.39T_{pw}-1.56$
60° Zexel	HFI-2.1: 960040-2330	$Q=14.87T_{pw}-1.17$
Chrysler	TF-003	not available

(T_{pw} = injection pulse width in msec)

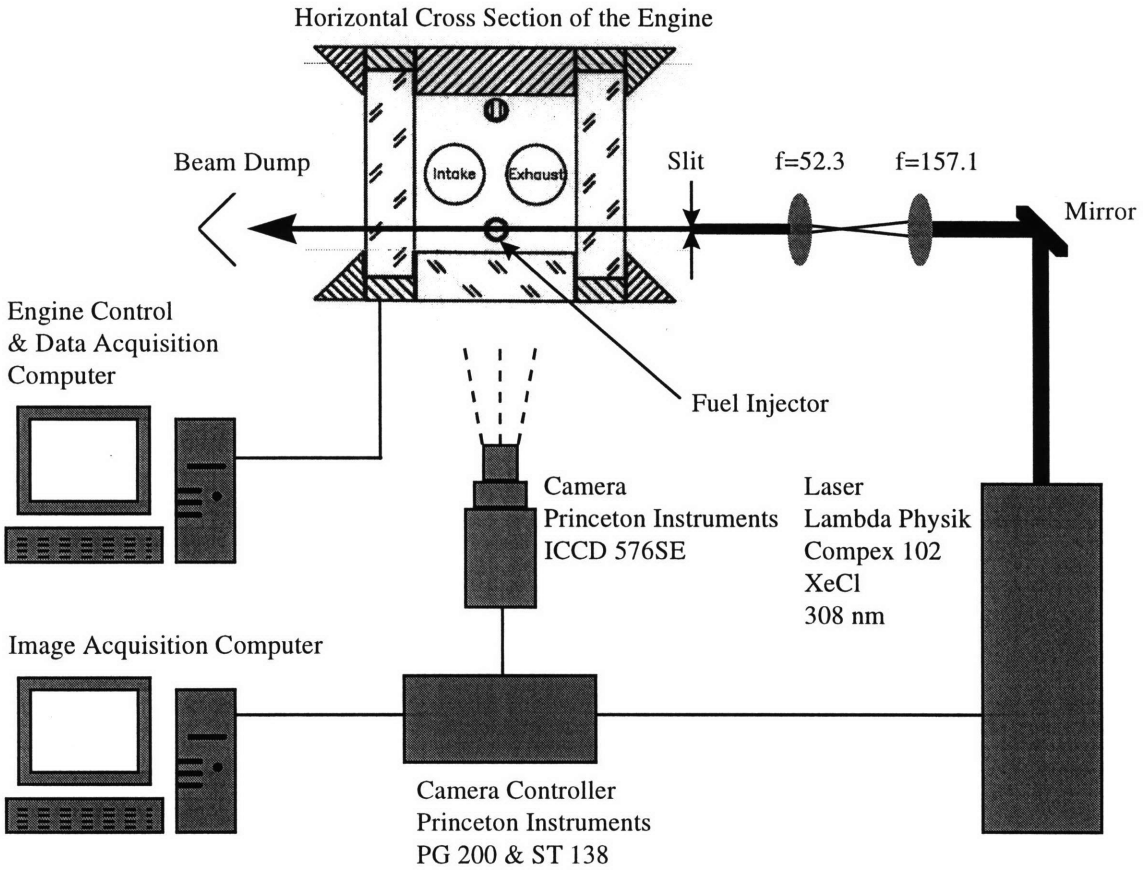

Figure 3.1 Schematic of the PLIF system

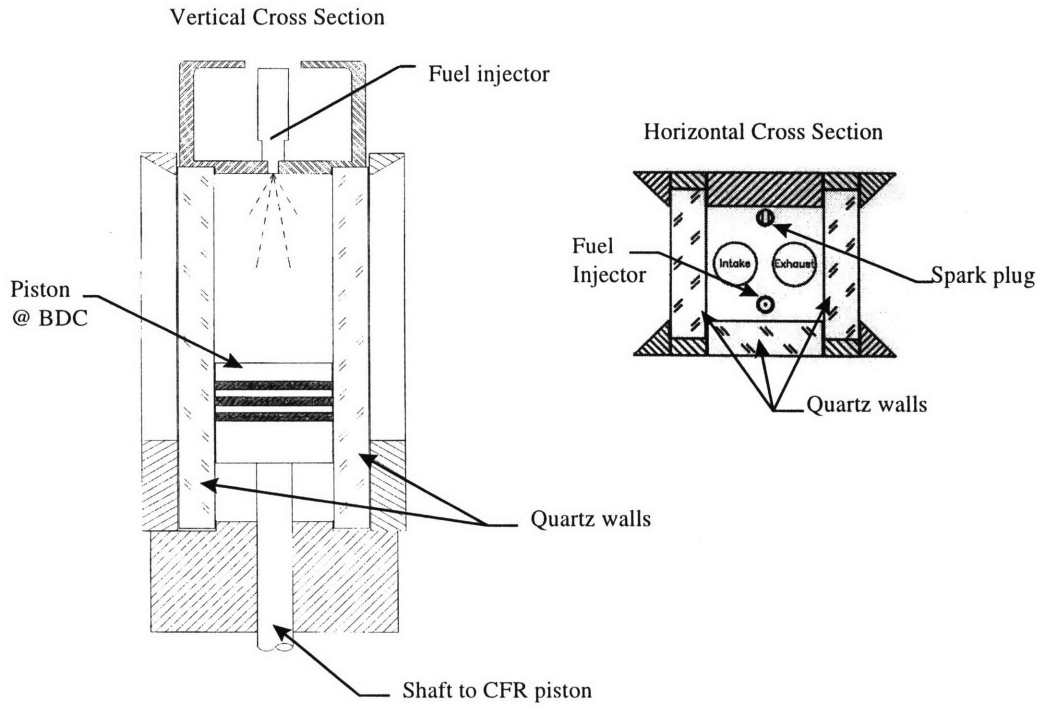

Figure 3.2 Schematic of the optical engine

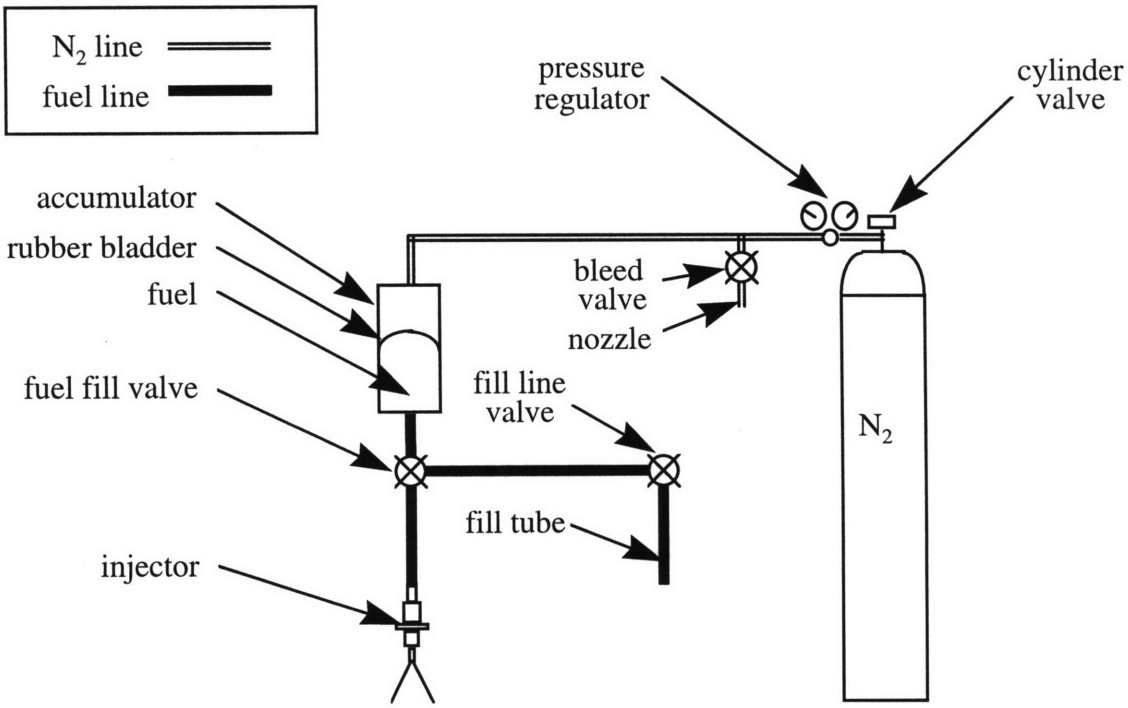

Figure 3.3 High pressure fuel system

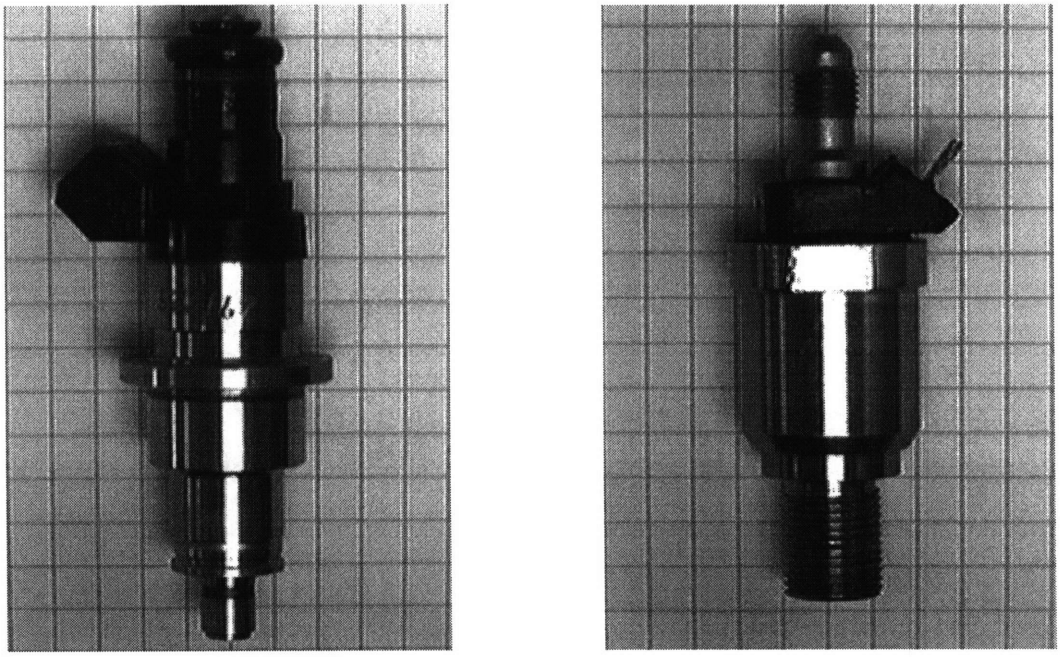

a) Zexel injector

b) Chrysler injector

Figure 3.4 High pressure swirl injectors

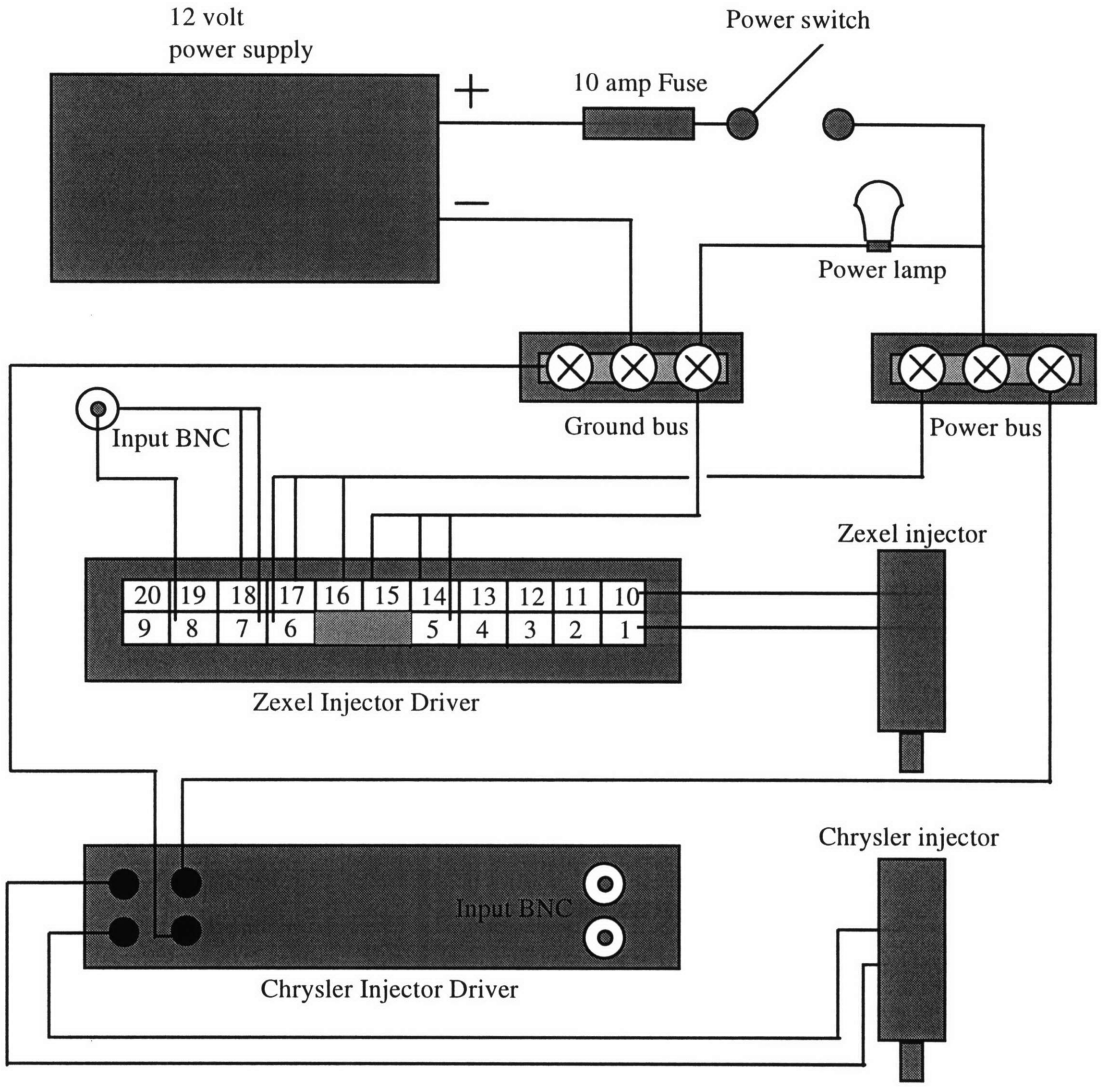

Figure 3.5 Injector driver wiring diagram.

CHAPTER 4

INITIAL SPRAY DEVELOPMENT RESULTS

For testing the initial spray development, images where acquired in 30 μsec intervals timed with the PG200 triggered from the injection TTL signal. Due to the low framing rate of the camera system, each image was acquired in a different engine cycle. A selection of images from these series can be found in figures 4.1-4.3. Figure 4.1 is a collection of images taken with the Chrysler injector comparing the operation of the injector at different fuel pressures. The three columns in the figure correspond to the three injection pressures tested (3 MPa, 5 MPa, and 7 MPa) and each row is 60 μsec later in the injection event. A background signal caused by residue on the camera lens (originally attributed to impurities in the quartz window) can be seen on all of the images presented in this series. This background appears as droplets outside of the main spray and is repeated in each frame.

These images indicate that the spray development occurs in four distinct phases. The first phase is a delay period between when the signal to inject is delivered to the injector driver and fuel is first detected by the LIF system. The delay period is a function of the injector design and the voltage applied to the coil by the injector driver. The Chrysler injector and the Zexel injector were controlled by drivers donated with the respective injectors. The Chrysler injector protruded into the combustion chamber so that the injector tip is clearly visible in the images, while the Zexel injectors where slightly recessed. Using the spray velocity measurements, which will be described shortly, the inability to see the Zexel injector tip can easily be corrected for. The delay period for the 20° and 60° Zexel injectors was 310 μsec and 360 μsec respectively while the delay period for the Chrysler injector was 180 μsec. When compared to the crank angle time scale, this delay period is quite significant at high engine RPM and should be taken into account if accurate injection timing is required (e.g. for stratified charge operation). At 6000 RPM, the injection delay period is 12.6 crank angle for the Zexel system and 6.5 crank angle for the Chrysler system. Fortunately a homogenous charge, early injection strategy is generally used at high engine speeds, which is less sensitive to injection timing [3].

The second phase is a high momentum large droplet phase which occurs before the spray develops enough angular momentum to form a hollow cone profile. Figure 4.4 is a schematic of the interior of a pressure swirl atomizer taken from Lefebvre [21]. Inside the injector tip is a swirl chamber where a steady vortex is developed during the injection event. The pintle seat is downstream of the swirl chamber and the swirl vanes are upstream. Before the pintle is lifted and fuel flow is established, the fuel within the swirl chamber is relatively stagnant. When the pintle is first lifted, this portion of the fuel does not have enough tangential velocity to form a hollow cone spray and is injected directly along the axis of the injector with relatively high velocities. This phase of the spray is more pronounced for the Zexel injectors than it is for the Chrysler injector. The penetration for this portion of the spray has been plotted for each injector at all three fuel pressures in Figures 4.5-4.7. Linear curve fits where used to establish the velocities of the initial portion of the spray. The results from these plots are summarized in Table 4.1.

Table 4.1 Initial spray velocities

Fuel pressure MPa	3	5	7
Injector	m/sec	m/sec	m/sec
Chrysler	62	86	93
20° Zexel	63	88	93
60° Zexel	70	78	86

The third phase of the spray occurs once sufficient angular velocities have been produced in the swirl chamber to overcome the surface tension of the fuel, and a hollow cone spray develops. For all three injectors at 5 MPa fuel pressure, the hollow cone structure is first observed 150 μsec after fuel is first detected with the PLIF system.

The fourth phase of the spray is a narrowing of the spray cone. Once the hollow cone structure of the spray has been developed, a flow pattern is set up in the ambient air due to entrainment. Aerodynamic drag and the conservation of momentum causes the gasses in the region of the spray to follow the spray. Since the spray is shaped as a hollow cone, a low pressure region is created at the center of the spray (Figure 4.8). This low pressure zone causes the fully developed spray to contract. This can best be observed with the pictures taken with the Chrysler injector (Figure 4.1, rows 8-11, 3 MPa). When the spray cone first opens, the air entrainment has not been established and the cone angle is significantly wider than when the spray is fully developed.

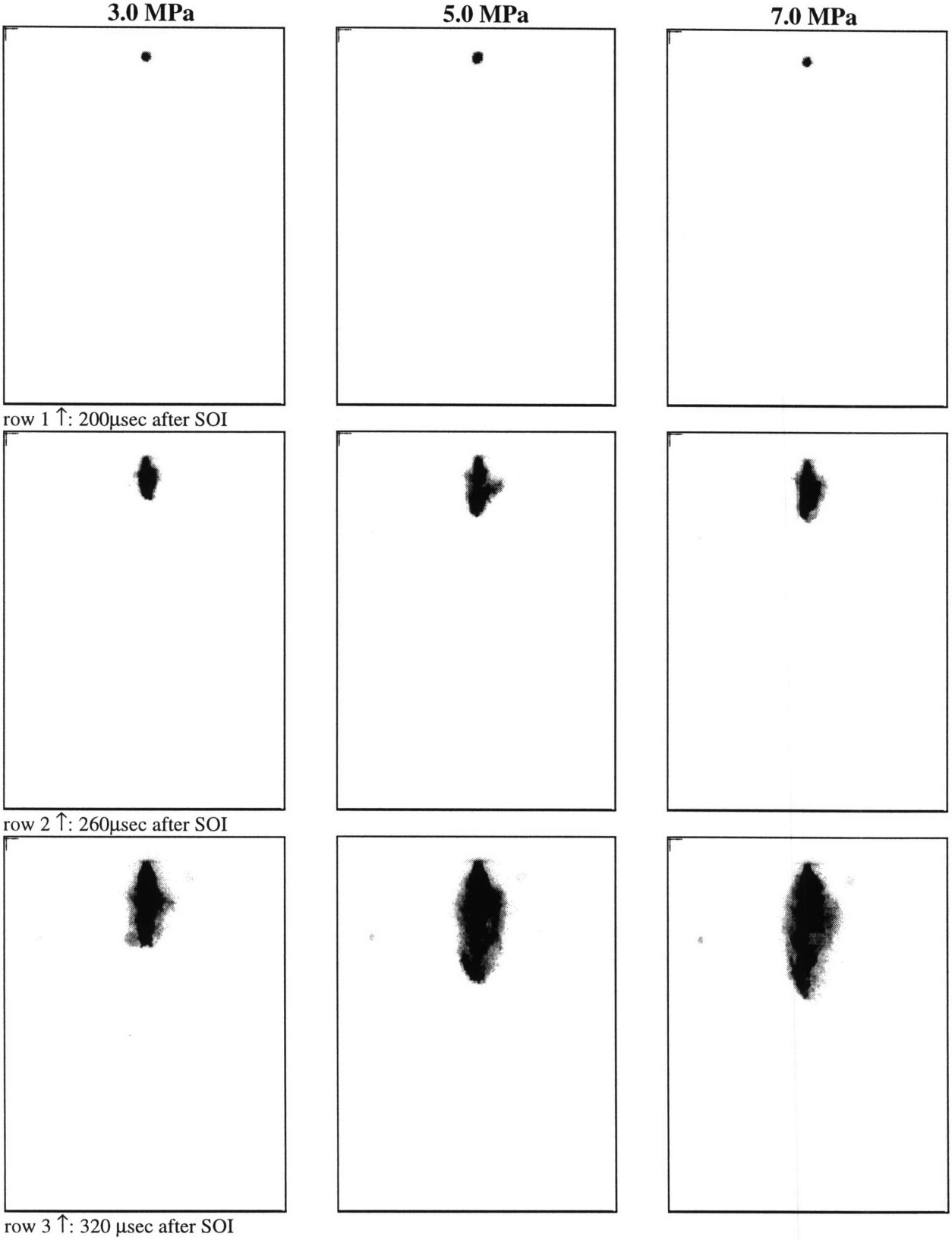

Figure 4.1 **Early spray development with the Chrysler injector (continued on the following 3 pages)**
P_{amb} = 0.5 bar; SOI = 90 ATCI; 167 μsec = 1 crank angle

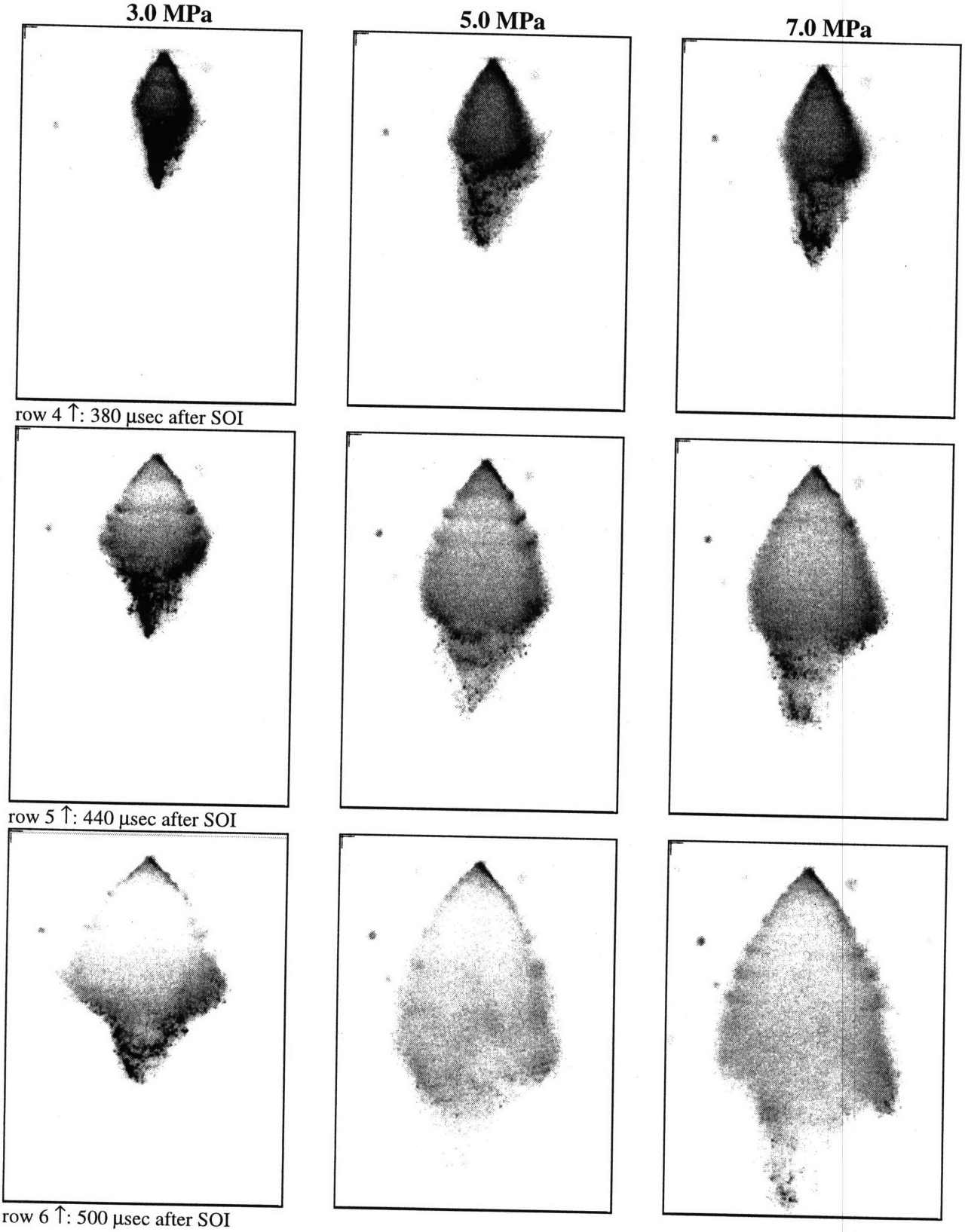

Figure 4.1 continued **Early spray development with the Chrysler injector**
P_{amb} = 0.5 bar; SOI = 90 ATCI

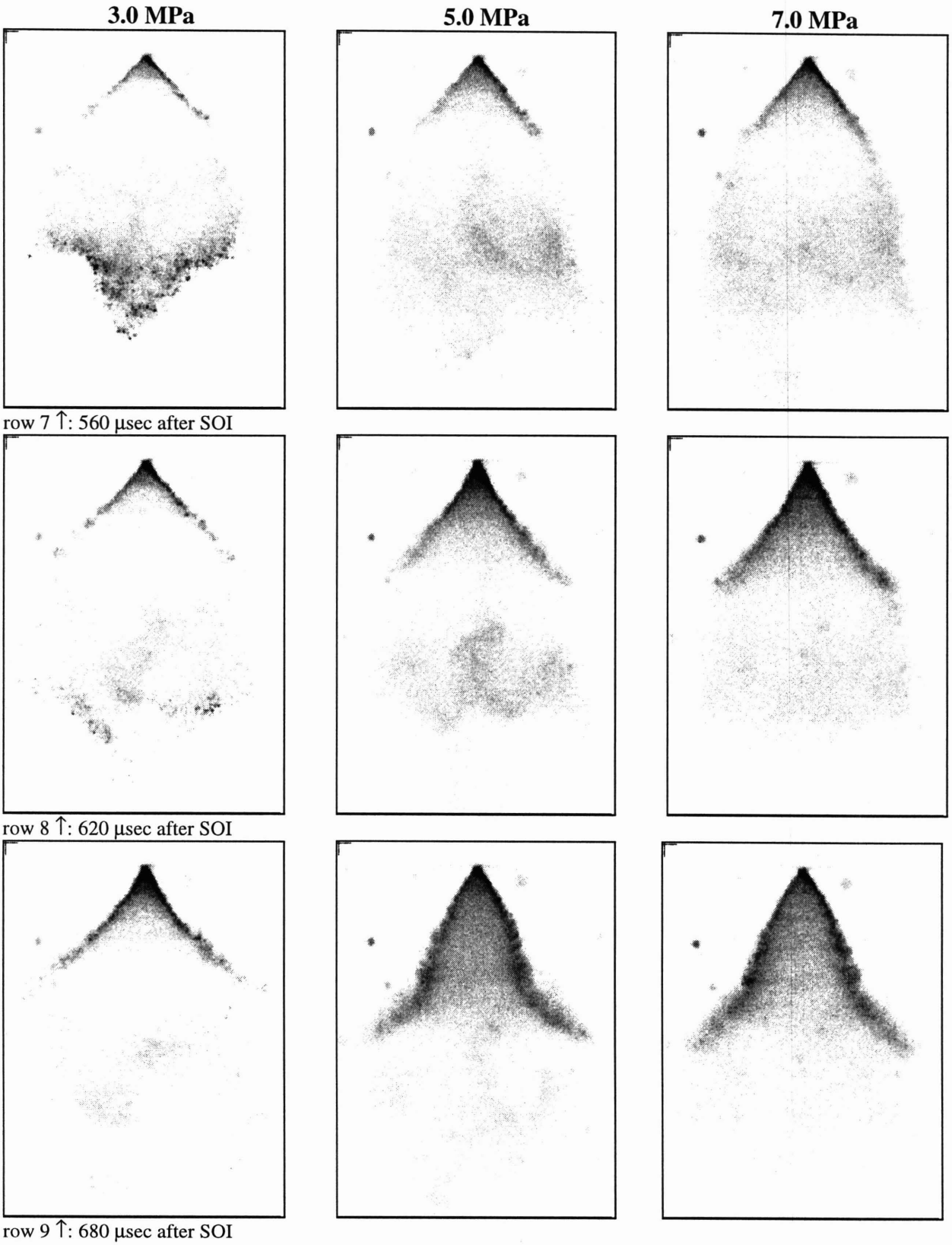

Figure 4.1 continued **Early spray development with the Chrysler injector**
P_{amb} = 0.5 bar; SOI = 90 ATCI

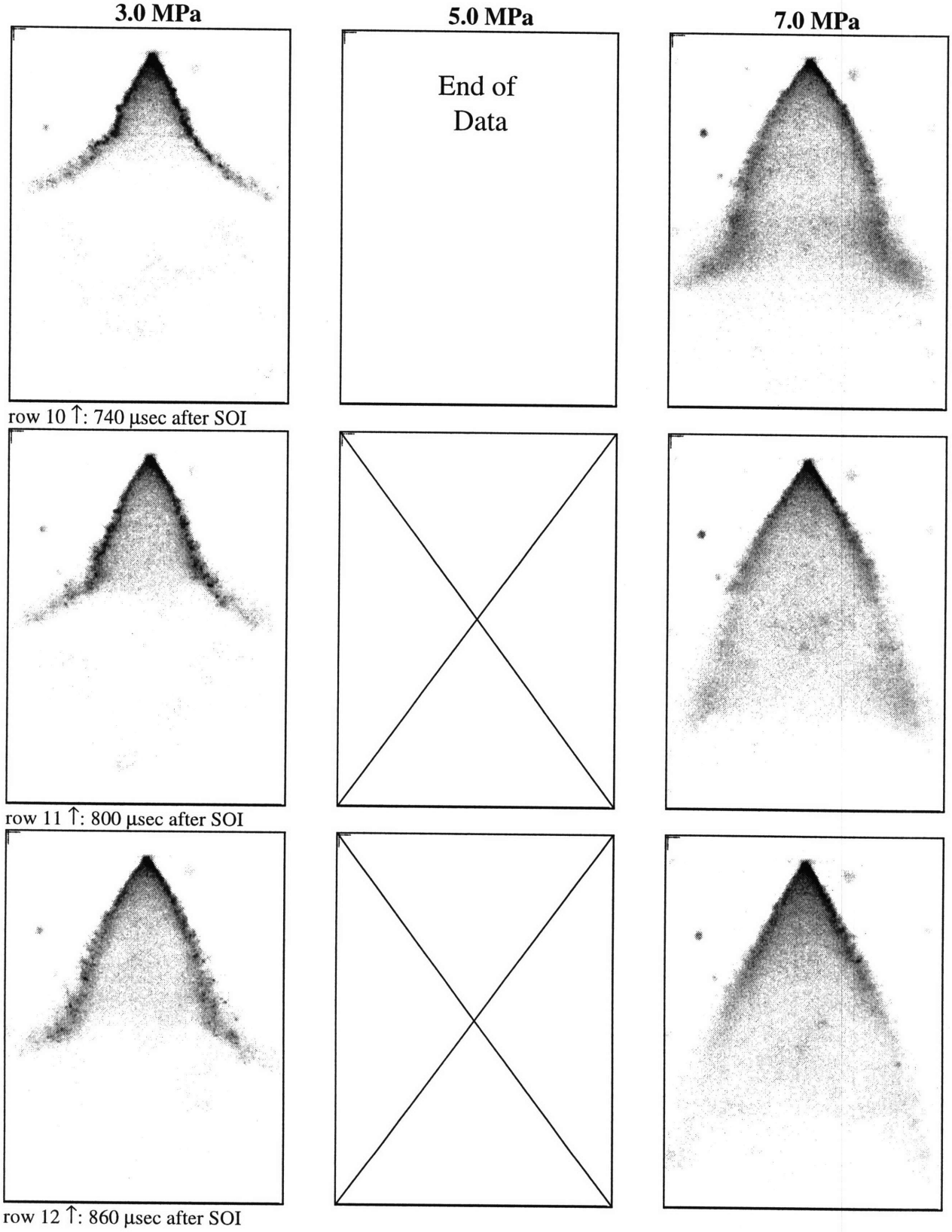

Figure 4.1 continued **Early spray development with the Chrysler injector**
P_{amb} = 0.5 bar; SOI = 90 ATCI

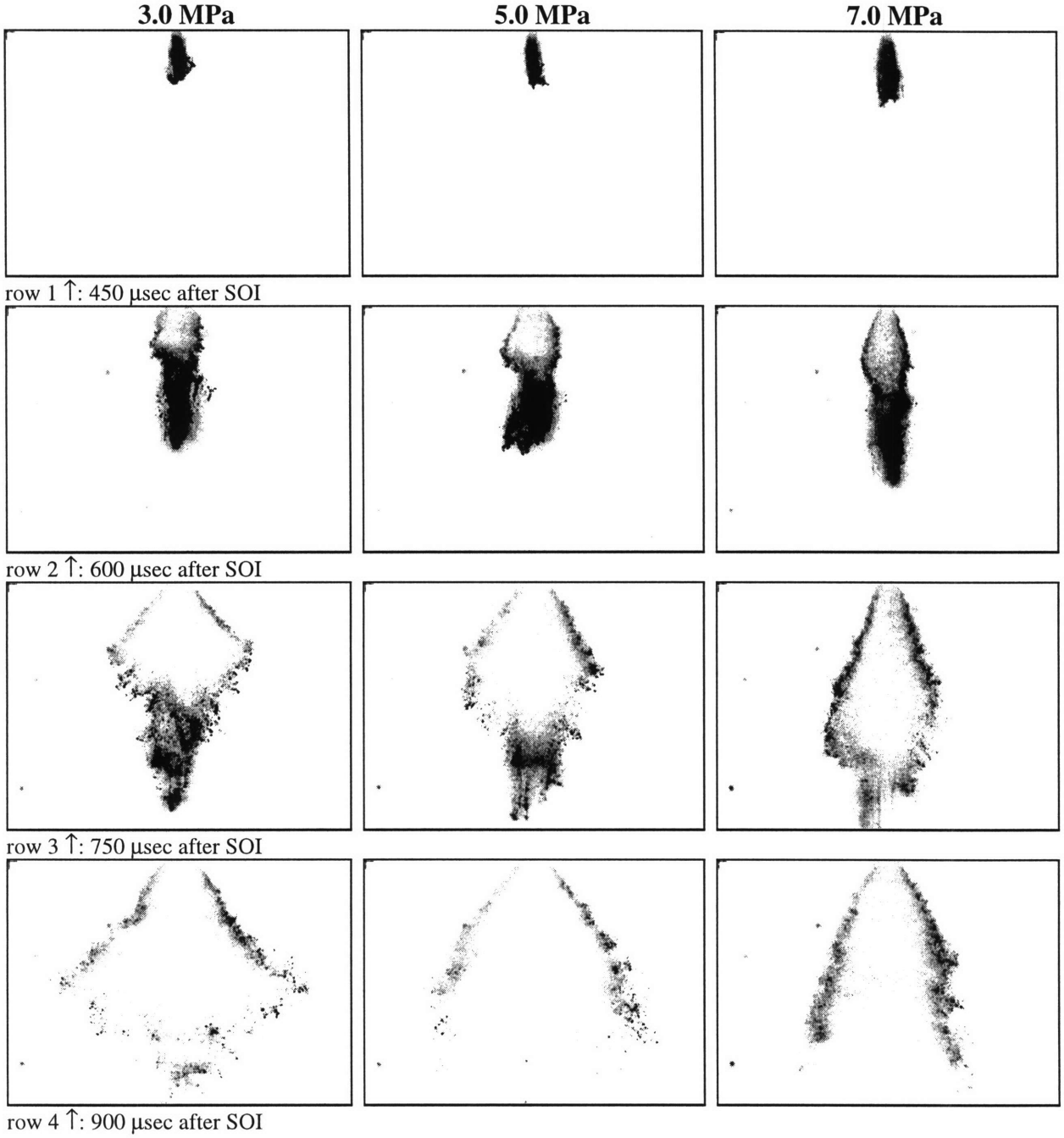

Figure 4.2 **Early spray development with the 60° Zexel injector**
P_{amb} = 0.5 bar; SOI = 90 ATCI
Intensity range 5,000-20,000

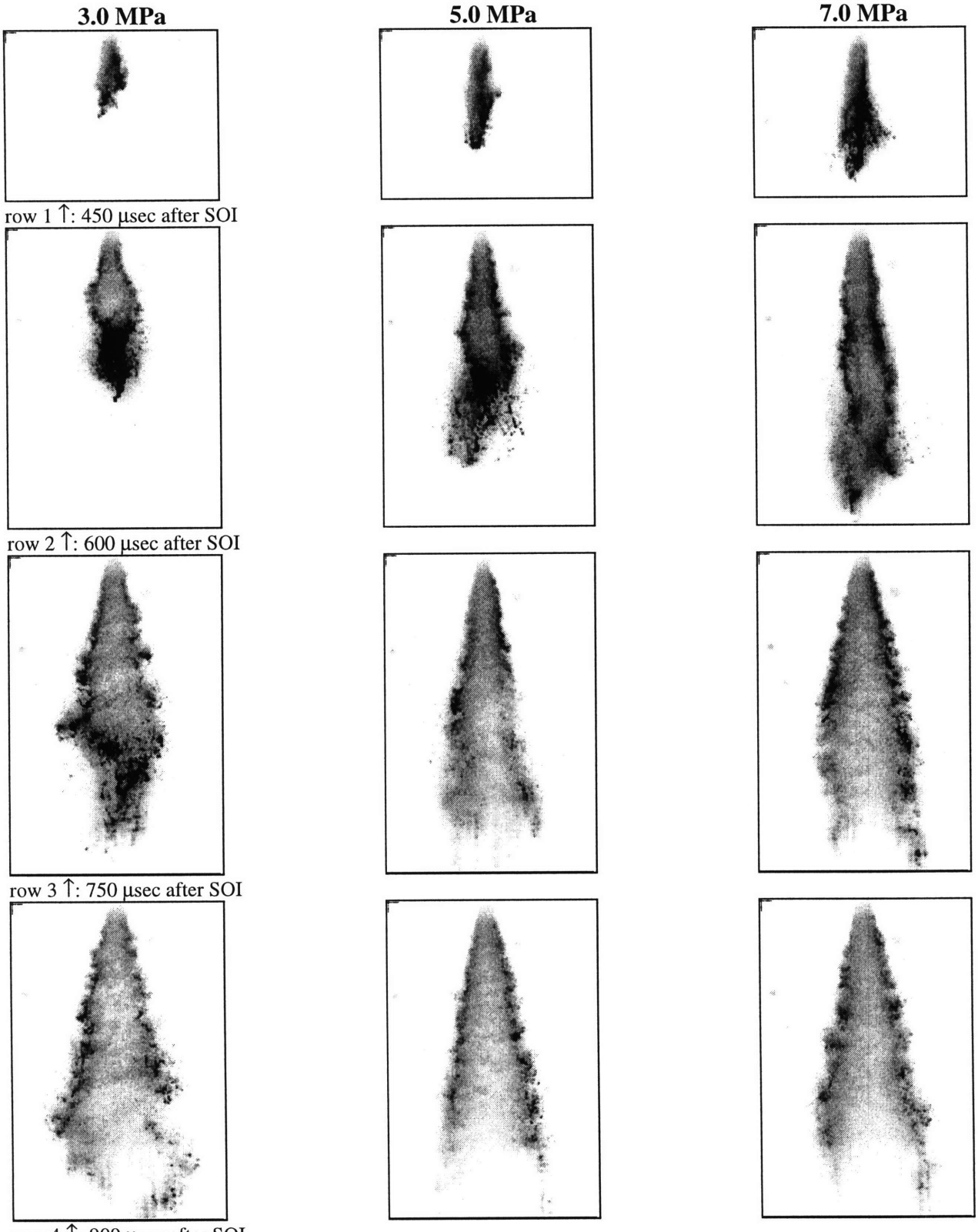

Figure 4.3 **Early spray development with the 20° Zexel injector**
P_{amb} = 0.5 bar; SOI = 90 ATCI
Intensity range 5,000-50,000

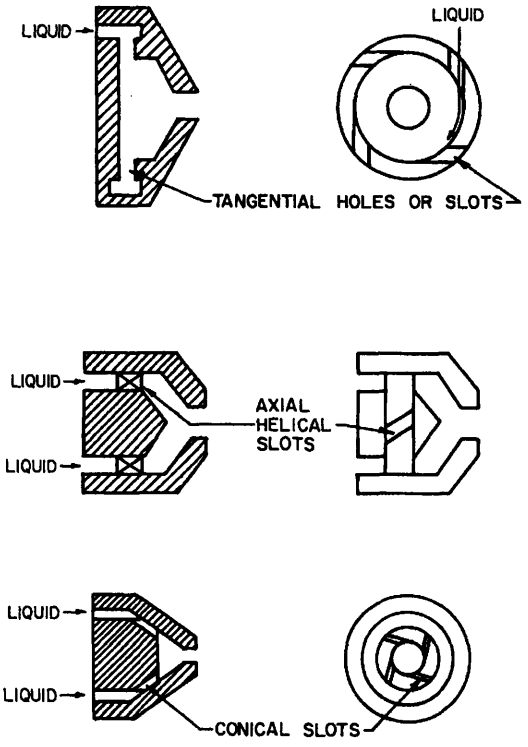

Figure 4.4 Designs of simplex swirl atomizers [21]

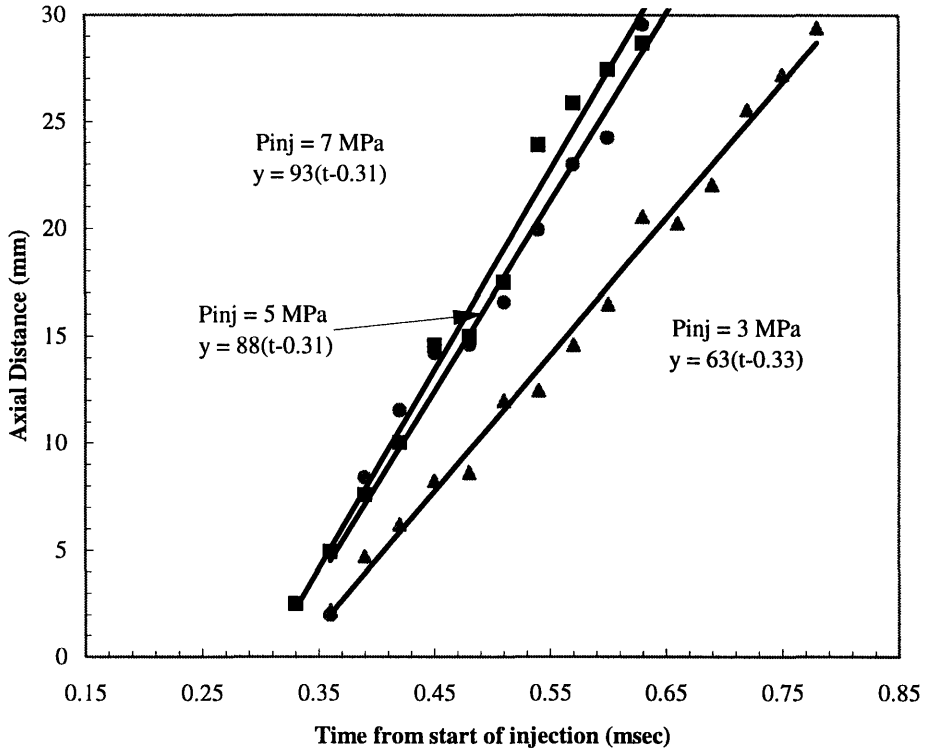

Figure 4.5 20° Zexel injector spray penetration (Ambient pressure: 0.5 bar)

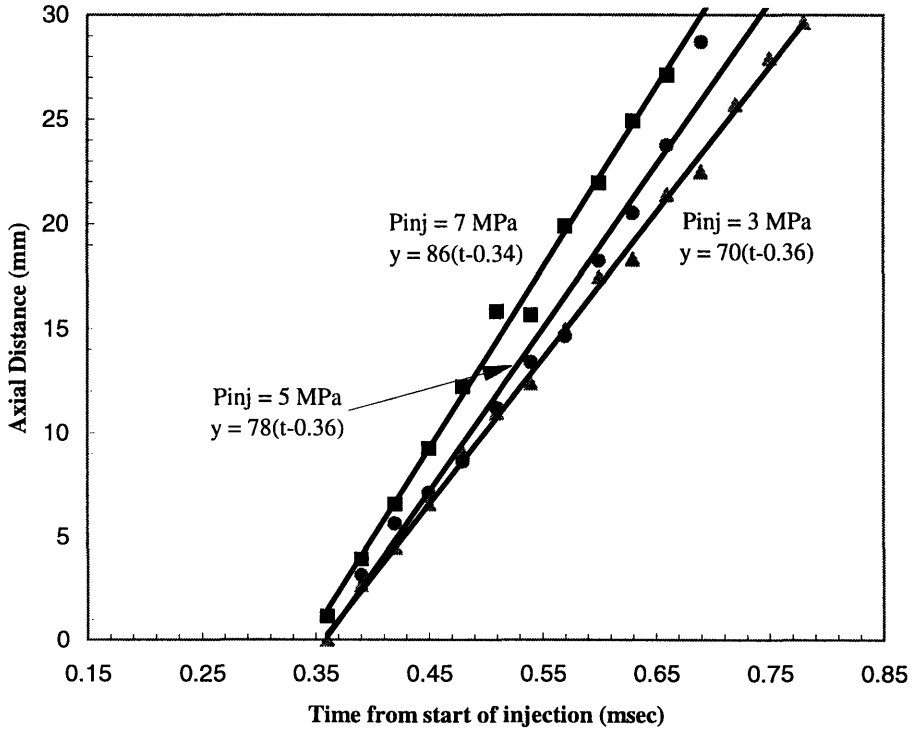

Figure 4.6 60° Zexel injector spray penetration (Ambient pressure: 0.5 bar)

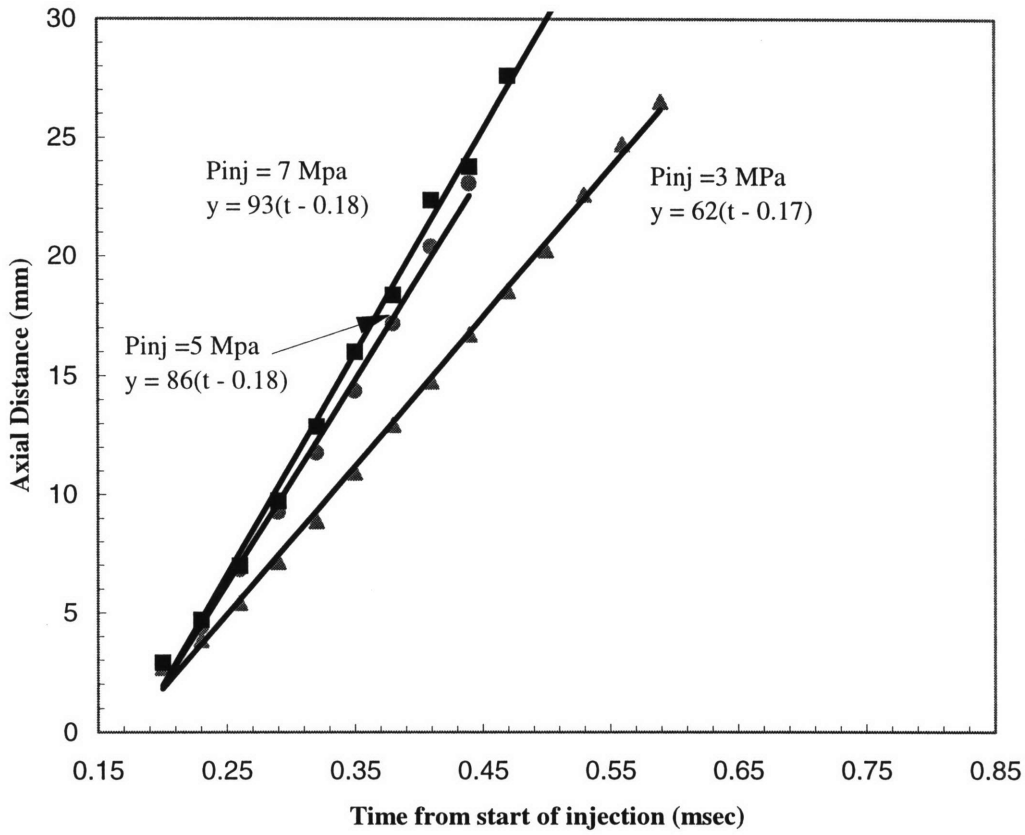

Figure 4.7 Chrysler injector spray penetration (Ambient pressure: 0.5 bar)

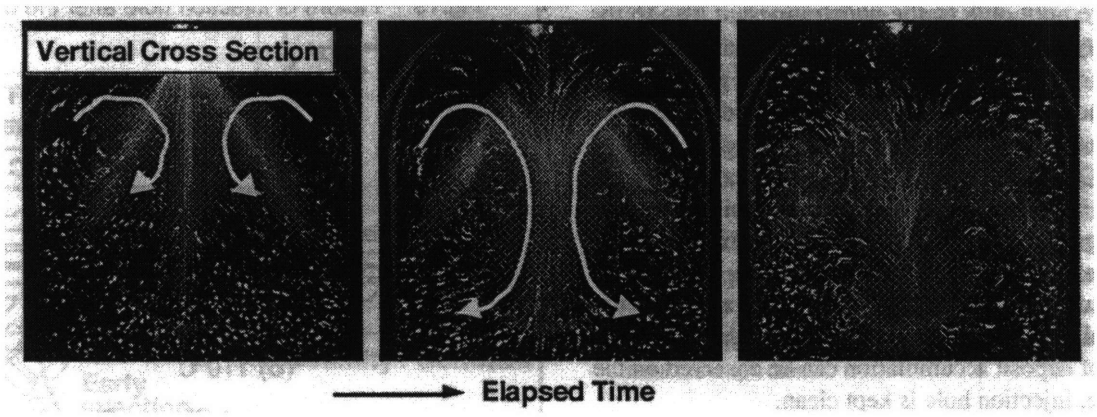

Figure 4.8 Air entrainment into the fuel spray (Ambient pressure: 0.1 MPa) [3]
Visualized using polymer micro-balloons in air.

CHAPTER 5

SPRAY CONE ANGLE RESULTS

The effect of ambient and fuel pressure on the spray cone angle for pressurized swirl atomizers is known to be different than that for simple orifice injectors [21]. In the first part of this study the ambient pressure was held constant at 0.5 bar and the fuel pressure was varied from 1 MPa to 7 MPa. Images for the second portion of the study were taken with the fuel injection pressure set at 5 MPa and the ambient air pressure ranging from 0.5 bar to 1.1 bar. Sample images from this study are shown in Figures 5.1 and 5.2. The cone angles where measured by drawing lines through the dense portion of the sprays and measuring the angle between the lines.

Over the range of pressures investigated in this study, the fuel injection pressure appears to have only a modest effect on the cone angle (Figure 5.1). The effect of the ambient pressure was much more pronounced (Figure 5.2). These results agree with what has been observed by other researchers [22, 23]. The cone angle is determined by the ratio of the axial and tangential velocity of the fuel as it leaves the injector orifice and the pressure distribution of the ambient air. The axial and tangential velocities are affected similarly by an increase in fuel pressure, so little change in cone angle should occur. As the ambient pressure is increased, the amount of air entrained in the spray increases and the pressure differential between the interior of the cone and the exterior of the cone increases. This causes a decrease in the cone angle as the ambient pressure increases.

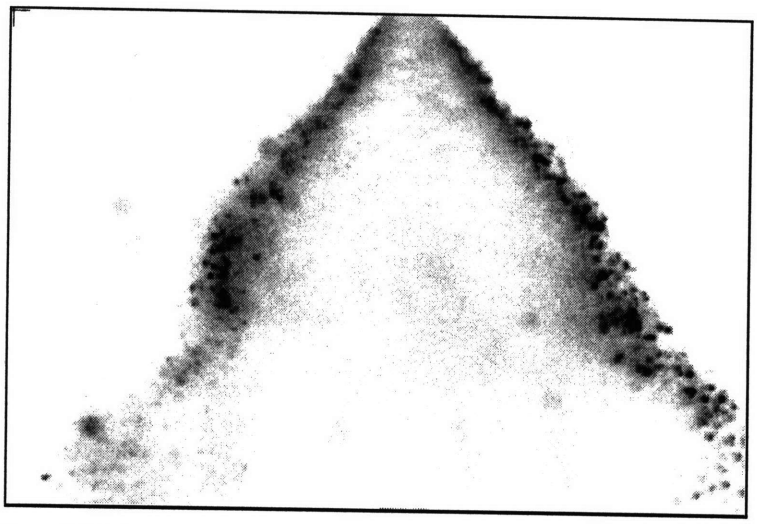

P_{inj} = 2.0 MPa, P_{amb} = 0.5 bar, Cone angle = 70°

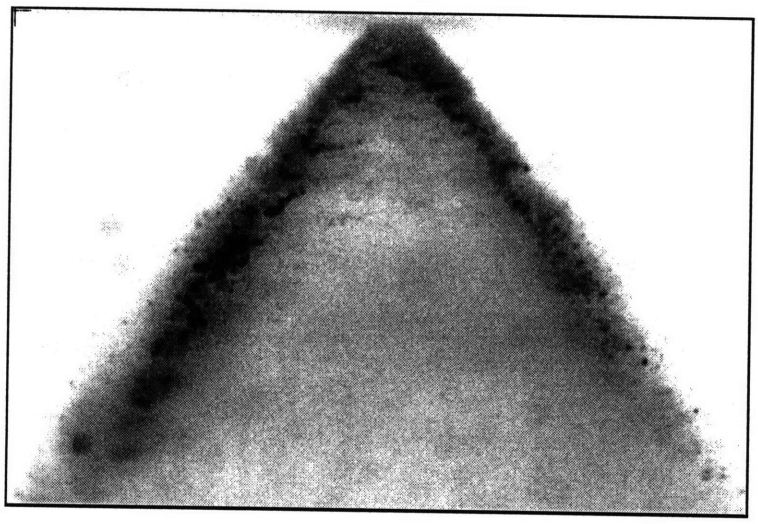

P_{inj} = 5.0 MPa, P_{amb} = 0.5 bar, Cone angle = 70°

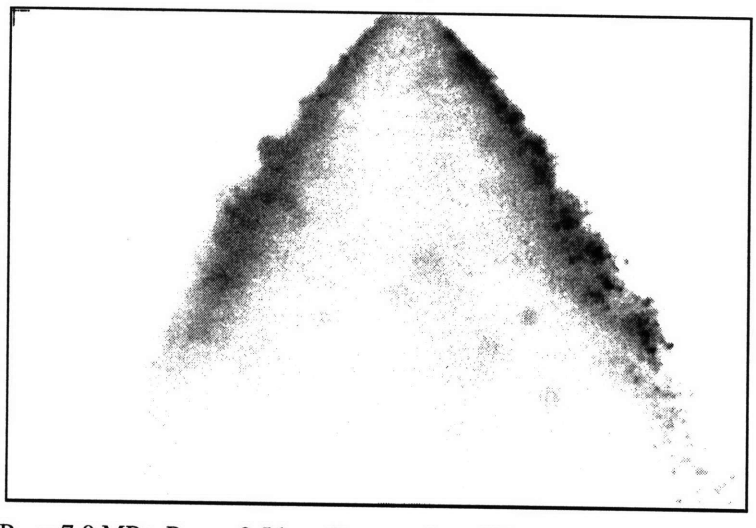

P_{inj} = 7.0 MPa, P_{amb} = 0.5 bar, Cone angle = 67°

Figure 5.1 Variation in spray cone angle versus fuel injection pressure.

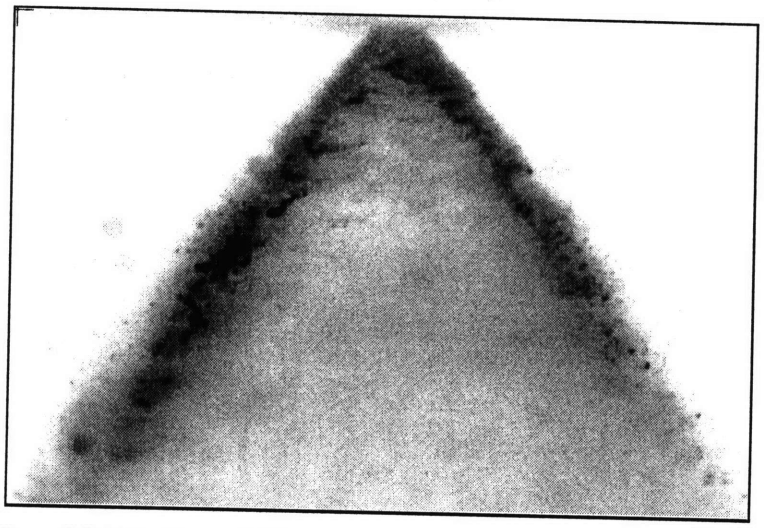

P_{inj} = 5.0 MPa, P_{amb} = 0.5 bar, Cone angle = 70°

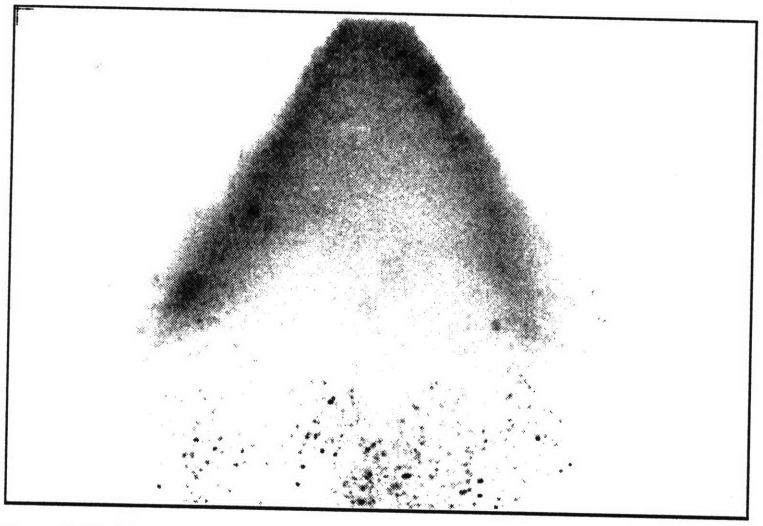

P_{inj} = 5.0 MPa, P_{amb} = 1.0 bar, Cone angle = 63°

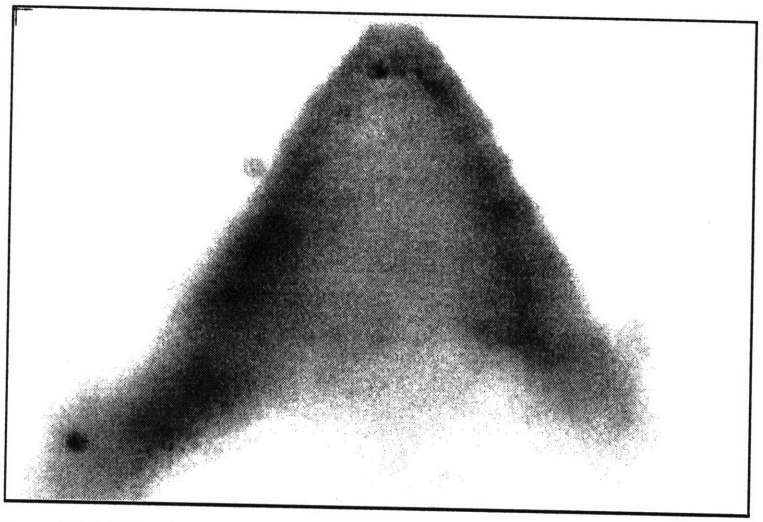

P_{inj} = 5.0 MPa, P_{amb} = 1.1 bar, Cone angle = 57°

Figure 5.2 Variation in spray cone angle versus ambient pressure.

CHAPTER 6

ENGINE TEMPERATURE AND FUEL VOLATILITY RESULTS

When the engine was converted to direct injection and the first PLIF pictures were taken, some unexpected results were observed. In certain pictures the spray appeared as expected, a distinct hollow cone structure with the fuel concentrated at the edges of the spray. While in other frames, the spray appeared as a collapsed jet with the fluorescence in the center of the spray. It was later discovered that the images in which the spray appeared "collapsed" were taken after the engine had been running for some time, and the images which were acquired shortly after start-up appeared as hollow cone sprays.

An experiment was set up in which the PLIF system acquired pictures 6 crank angle after the start of injection once every second as the engine warmed up after a cold start. The injection timing was set to be 60° after top center of the intake stroke and the dopant used was acetone. This set of data, displayed in Figure 6.1, clearly shows a transition of the fluorescence from the edges of the spray to the center of the image as the engine warms up. In images taken on a horizontal plane 15mm below the head surface, the same trend was observed (see Figure 6.2 for imaging plane). This experiment was repeated using a less volatile dopant, 3-pentanone, and the trend was not observed (see Table 2.2 for properties of the fuels and dopants). Figure 6.3 is a comparison of the horizontal PLIF images taken during the warm-up period with acetone and 3-pentanone. This data indicates that the more volatile dopant was rapidly vaporizing and being drawn into the center of the spray by the entrained air flow field, while the less volatile dopant did not vaporize as rapidly.

At this time it was decided to instrument the engine with a thermocouple (Omega, Part #:KMTSS-020U-6) and quantify the temperature at which the transition occurred with the acetone dopant. The location of the thermocouple is shown in Figure 6.4 and a typical temperature history for a start-up experiment is shown in Figure 6.5. The thermocouple was located as close to the injector as was feasible without modifying the injector itself. When the experiment was repeated to measure the temperature at which the transition occurred, the collapse was not observed using either acetone or 3-pentanone. A comparison between the first data set demonstrating the collapsed cone and the second data set is shown in Figure 6.6. After reviewing the data, there are a few possible explanations for the differences in the observed sprays.

1) Start Of Injection was 90° into the intake stroke in the second set of experiments compared with 60° ATCI for the first. The start of injection was delayed with the second set of images to prevent the spray from impinging on the piston, and to correspond more closely with the timing that provides the greatest improvement in volumetric efficiency [4]. With the earlier start of injection, the ambient charge temperature is higher because a majority of the charge would have consisted of residual gas from the

previous cycle. A higher ambient temperature would facilitate the evaporation of the acetone. Once the acetone is vaporized the entrained air flow field could carry the vapor to the center of the spray.

2) The second set of images was acquired later relative to the start of injection by approximately 700 μsec (4 crank angle). The images were acquired later to insure that the spray had fully developed (the pre-spray is still visible at the bottom of the images in the first set of data). Since the tip of the injector is exposed to the combustion chamber, it will be significantly hotter than the rest of the injector (the temperature distribution inside the injector was investigated on the Mitsubishi engine [3]). The fuel that is stationary near the tip of the injector between cycles may be heated to a significantly higher temperature than the fuel that passes through the injector later in the injection. The first set of data was taken at the beginning of the injection process, which would correspond to fuel that was near the tip of the injector (and therefore heated more) between cycles. If the temperature of the acetone is raised well above the boiling point (56° C) the acetone may rapidly boil when injected into the cylinder.
3) The very first set of images (vertical cross sections with acetone) was taken without the accumulator in the fuel system. The effect of nitrogen absorption into the fuel and the subsequent desorbtion is unknown. The horizontal images in which the collapse is evident (Figure 6.3, Acetone column) were taken with the accumulator fuel system, but it is possible that the fuel system was not properly purged of air. If a significant amount of nitrogen or air was absorbed by the fuel when the fuel was pressurized, the sudden drop in pressure experienced by the fuel during injection may cause the nitrogen to rapidly desorb from the fuel. Rapid desorption of a gas could finely atomize the spray.

A limited number of experiments could be used to determine which, if any, of these factors caused the transitional behavior of the spray. The first test would be to use the accumulator fuel system, acetone dopant, 60° ATCI SOI, and 66° ATCI image timing and see if the fluorescence signal transitions to the center. If it does this indicates that the cause is either the ambient air temperature or the fuel temperature. If no transition is observed, the experiment should be repeated with air purposely introduced into the fuel system.

If the transition is observed with the start of injection at 60° ATCI and 66° ATCI image timing, the next step would be to acquire images at different times relative to the start of injection while the engine is hot. This can be done by changing the value on the DCI box between images (see section 3.3). The effect of the ambient air temperature can be investigated by adjusting the start of injection crank angle. The charge temperature in the cylinder will steadily decrease as air is inducted into the cylinder because the residual mass fraction will decrease as fresh air is added.

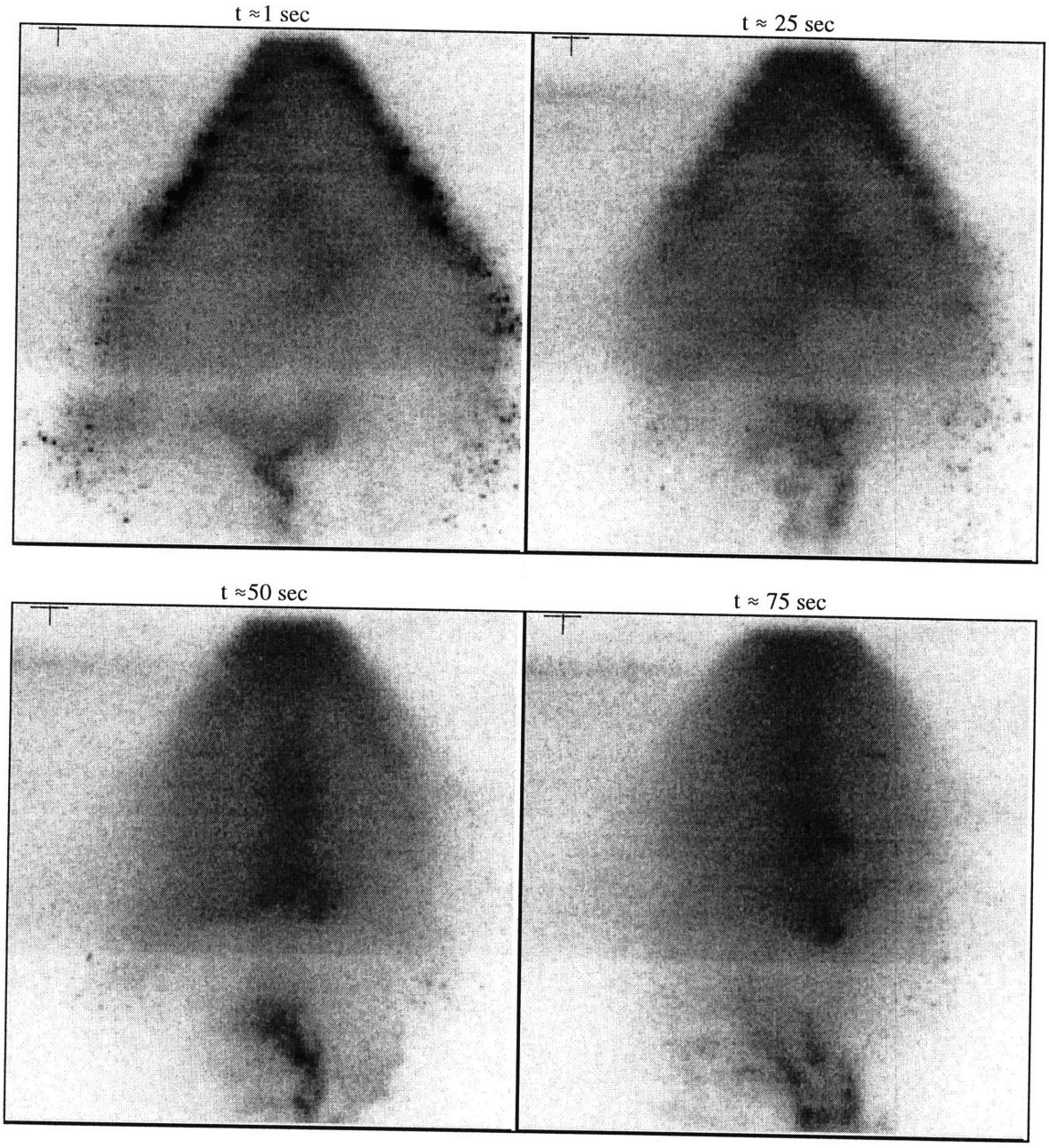

Figure 6.1 Transitional behavior of the spray images doped with acetone over time. Engine was started at t=0.

SOI: 60° ATCI

Image: 66° ATCI

Iso-octane & acetone (10:1)

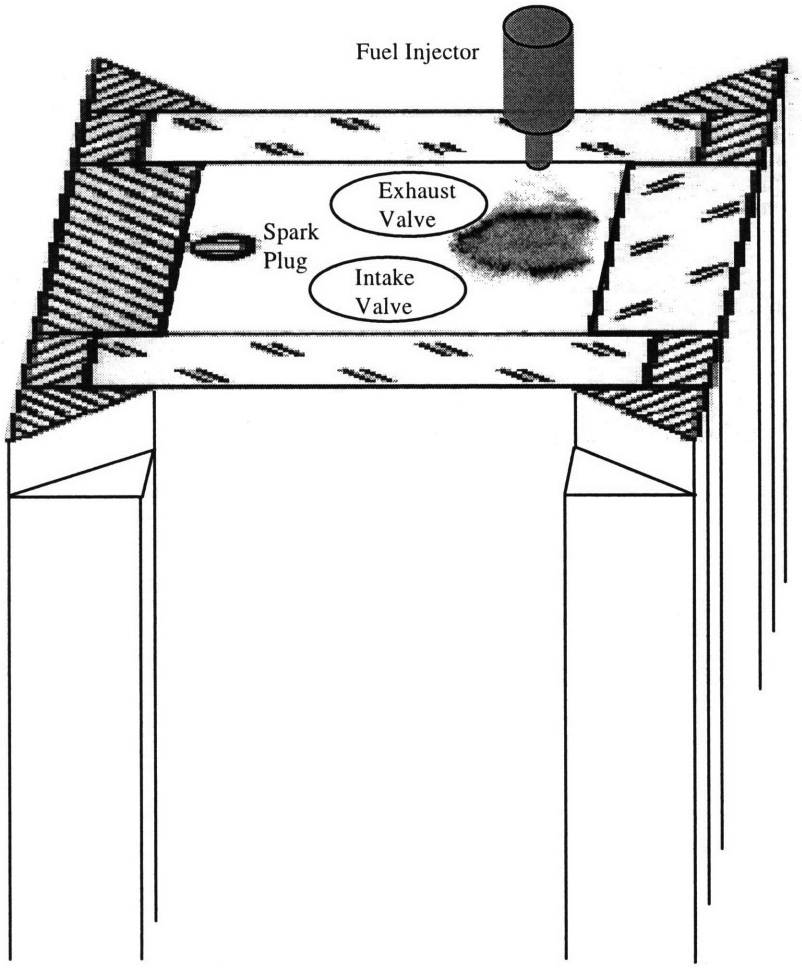

Figure 6.2 Image location for horizontal PLIF pictures. (Not to scale)

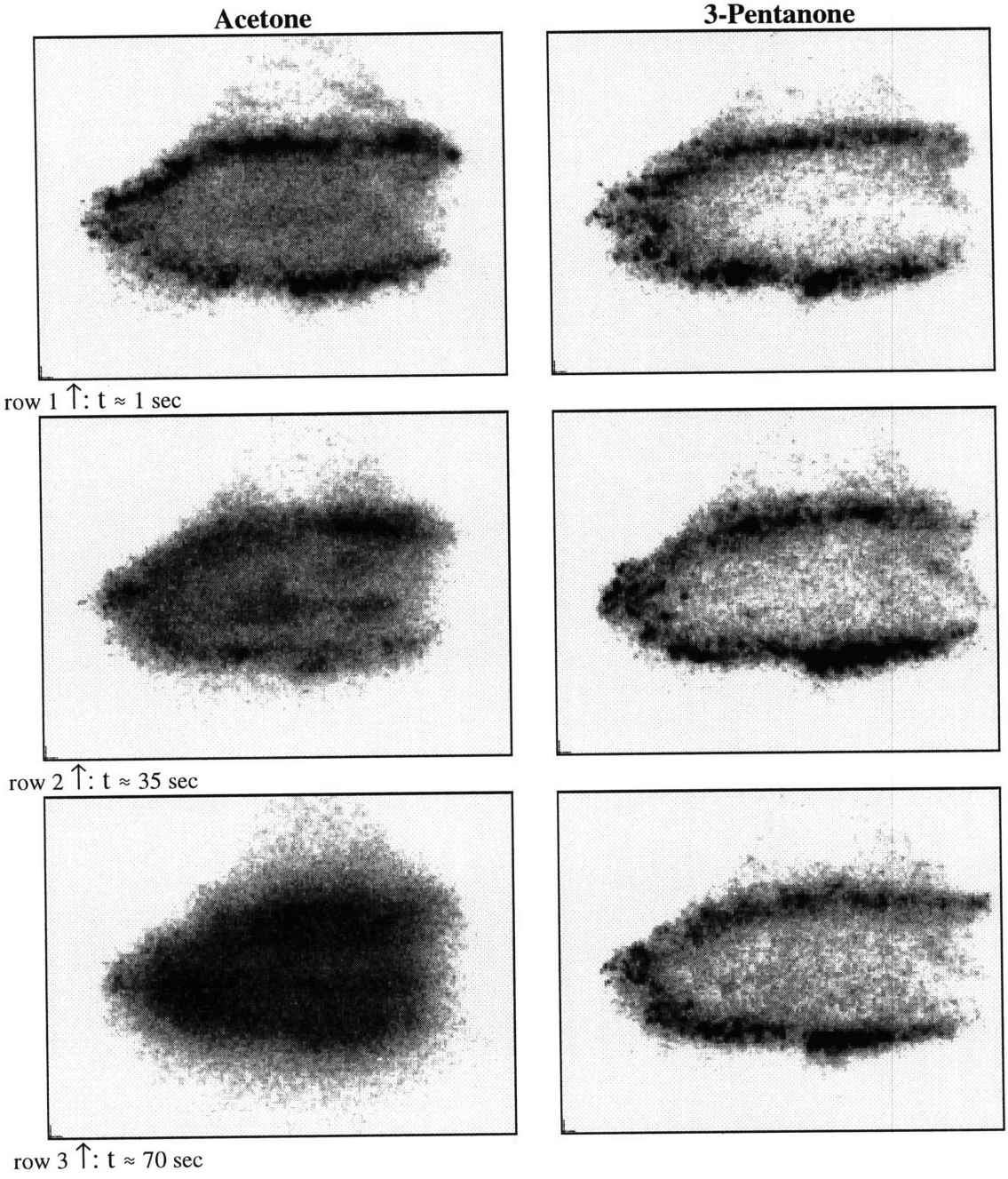

Figure 6.3 Warm-up comparison of images taken with acetone and 3-pentanone. Image location is 15 mm below the surface of the cylinder head. Engine was started at t=0 sec.

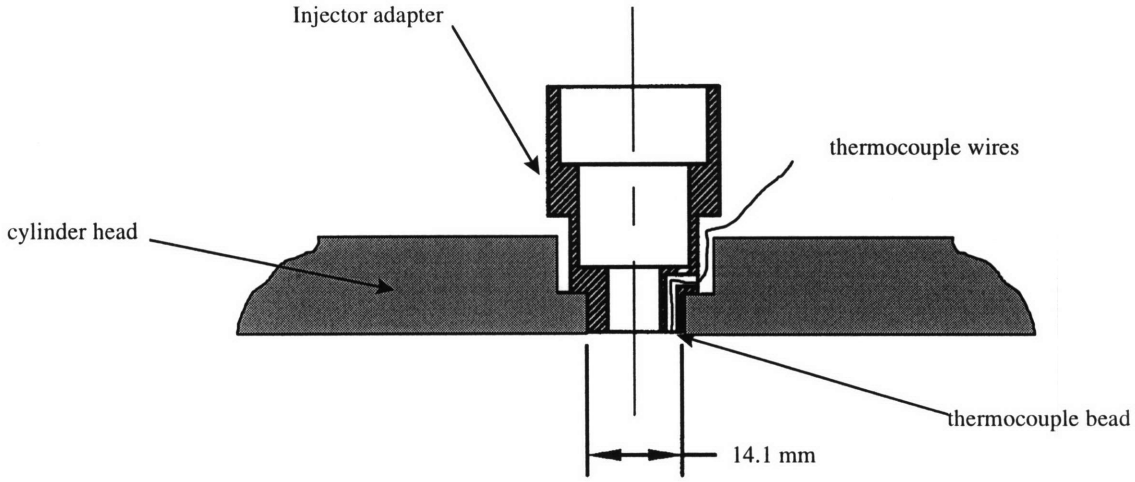

Figure 6.4 Thermocouple location.

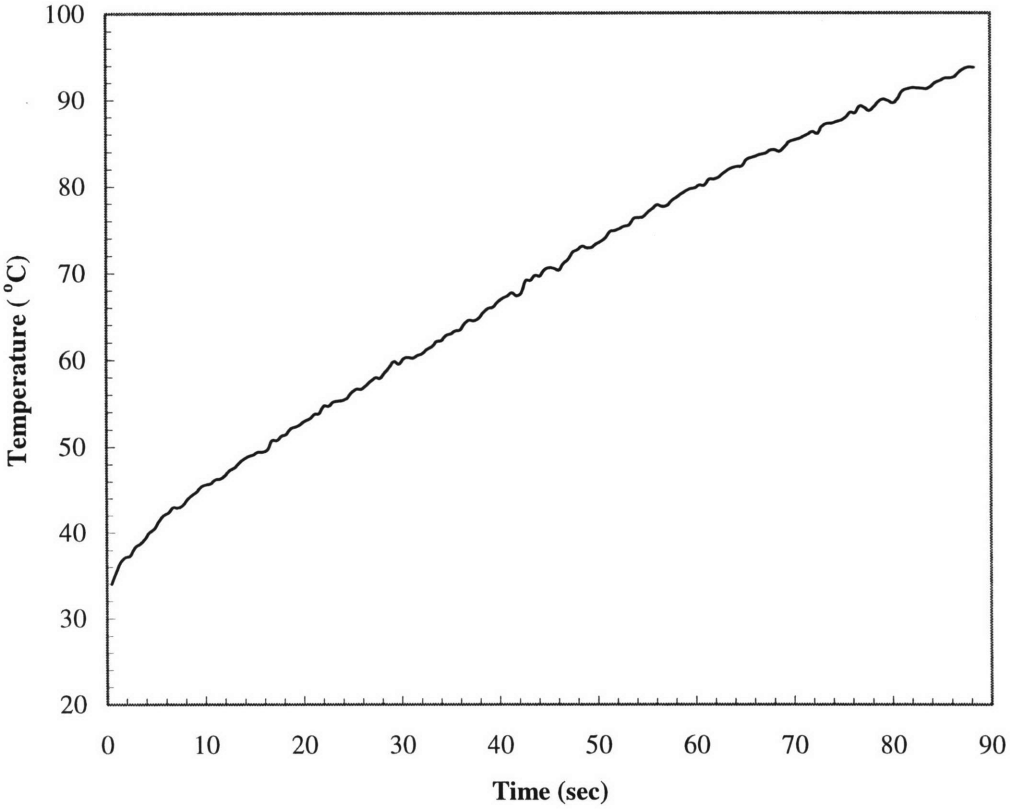

Figure 6.5 Typical temperature history at the injector exit during a warm-up experiment.

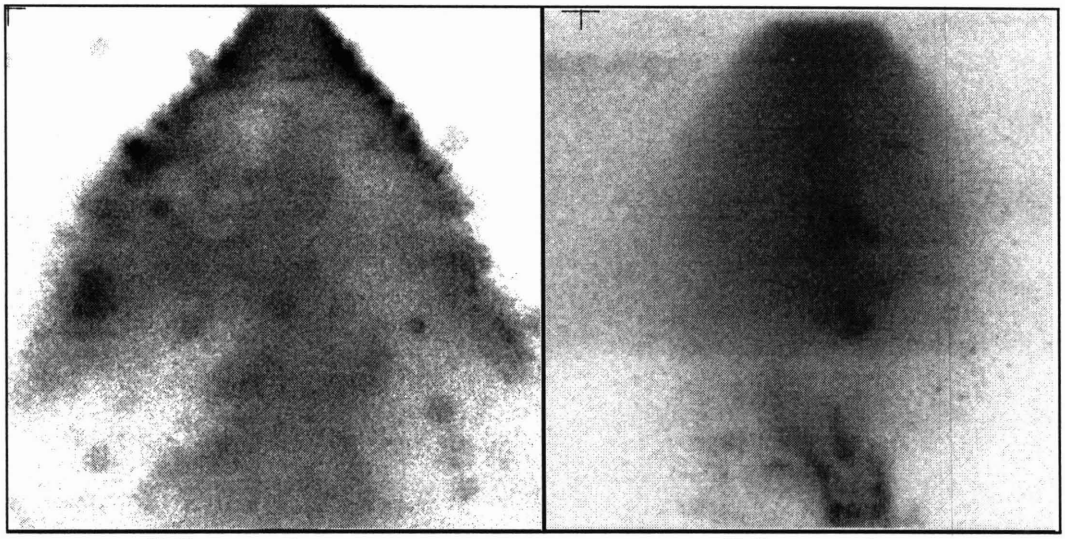

Fully warmed up
Dopant: Acetone
Image: 105° ATCI
SOI: 90° ATCI

Fully warmed up
Dopant: Acetone
Image 66° ATCI
SOI: 60° ATCI

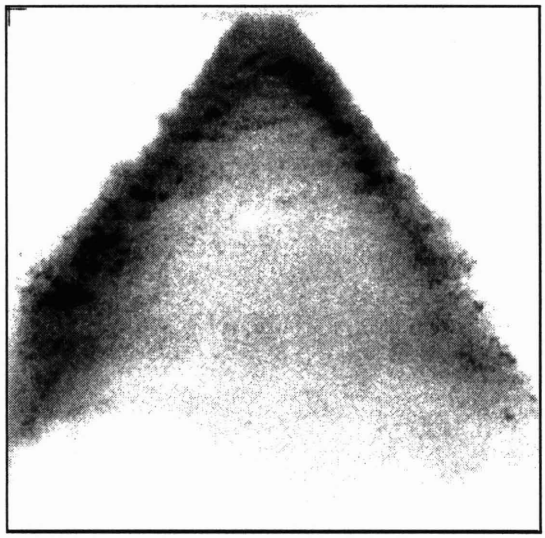

Fully warmed up
Dopant: 3-pentanone
Image: 100° ATCI
SOI: 90° ATCI

Figure 6.6 Fully warmed up images with and without the collapsed cone structure.

CHAPTER 7

START-UP FUEL PRESSURE RESULTS AND INJECTOR COMPARISONS

7.1 Start-up fuel pressure results

In most GDI systems a mechanical fuel pump is used to create the high injection pressures required for direct injection. This presents a problem at start-up because the engine RPM is generally too low during cranking for the mechanical high pressure pump to develop normal fuel pressure. One strategy for overcoming this difficulty is to allow the electric fuel feed pump, located in the gasoline tank, to supply the fuel pressure during start-up [3]. The operating pressure of the fuel feed pump is generally about 0.3 MPa. Figure 7.1 shows the 60° and the 20° Zexel injectors operating with 0.3 MPa fuel pressure. For this set of images the engine shaft encoder was used to time the data acquisition. When this timing method is used, care must be taken when comparing images of the injection event. Because the engine RPM is not entirely constant, two images taken the same number of crank angle after start of injection may not correspond to the exact same time (microseconds) relative to start of injection. Both injectors were still able to develop the hollow cone structure, but the atomization is noticeably worse. The injection duration required to inject an amount of fuel is proportional to the square root of the injection pressure [21]. Therefore the injection duration required for a stoichiometric mixture is approximately four times as long when operating from the fuel feed pump.

7.2 Injector spray comparisons

From the PLIF images, it is possible to compare the fuel spray atomization and uniformity in a qualitative manner. Both the Zexel and the Chrysler injectors are undergoing further development and the comparisons made in this section only refer to the models tested (see Table 3.3 for injector series numbers). Figure 7.2 shows a graph of the intensity values along a line drawn though the dense portion of the fuel spray for all three injectors. The spray character of the Chrysler injector is noticeably different from that of the two Zexel injectors. The amount of variation in the intensity values measured along the spray is much less for the Chrysler injector than for either of the Zexel injectors. This indicates that the spray from the Chrysler injector is more finely atomized. Large (relative to the camera resolution) droplets appear as peaks on the intensity graph. The intensity curves for both of the Zexel injectors show large variations along the fuel spray indicating that course droplets are present within the spray (the 20° injector spray appears slightly less atomized that the 60° spray). The peaks on the intensity curve for the Chrysler injector are much smaller in magnitude and the intensity seems to drop with distance from the injector. This decrease in intensity could be attributed to the atomization of the spray and the entrainment of surrounding air. As air is entrained, the number density of dopant molecules within a unit volume decreases, which in turn decreases the fluorescence signal measured from that volume. For a more quantitative comparison of the atomization from the injectors, a different measurement technique should be used.

The large scale spatial uniformity of the sprays can also be compared qualitatively using the PLIF images. As can be observed from the images taken with the 60° Zexel injector, (Figures 4.2, 5.1, 5.2, 6.1, 6.3, 7.1) there is often a lack of symmetry in the fuel spray and noticeable regions of high fluorescence intensity indicating a non-uniform spray. Images acquired with the 20° Zexel injector (Figures 4.3, 7.1) show similar features. These non-uniformities may not be significant for the operation of the engine but they do appear to include some larger fuel droplets. The appearance of the spray from the Chrysler injector is more uniform and very symmetric (Figures 4.1, 7.1). It should be noted that the fuel flow rate from the Chrysler injector is approximately 30% lower than that from the Zexel injectors. If a higher rate injector is required, it may be necessary to trade off some of the finer atomization properties of the Chrysler injector for a higher flow rate.

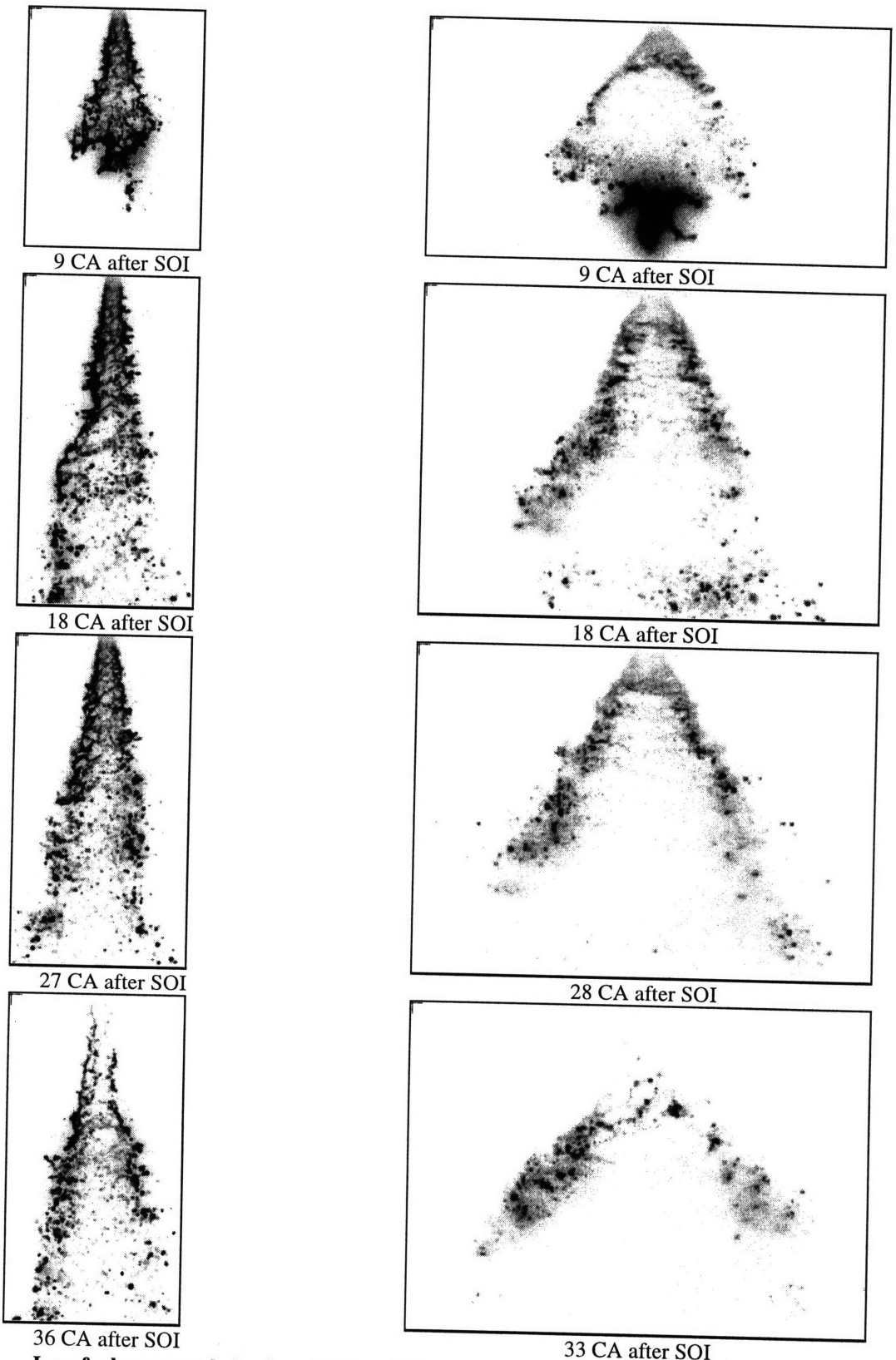

Figure 7.1 **Low fuel pressure behavior of 20° and 60° Zexel injectors**
P_{inj} = 0.3 MPa; P_{amb} = 0.5 bar; SOI = 90 ATCI
Intensity range 5,000-50,000 20°, 5,000-40,000 60°

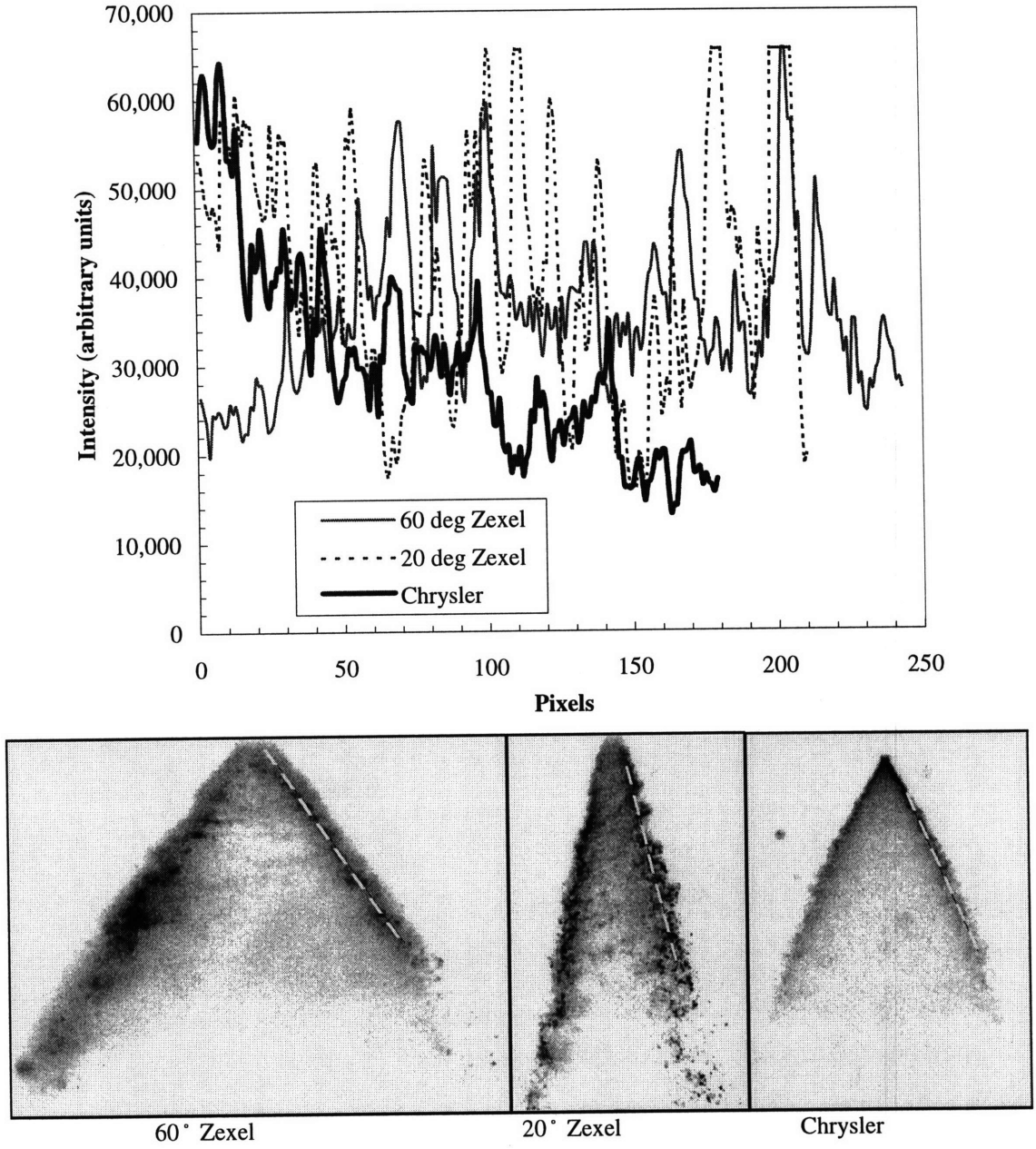

Figure 7.2 Graph of intensity values along the injector spray for all three injectors
Images from which the intensity values were measured are shown below the graph.
P_{inj} = 5.0 MPa

CHAPTER 8

SUMMARY AND CONCLUSIONS

During the course of this project, an optical engine has been modified to operate with a direct injection fuel system and the equipment necessary to perform PLIF measurements has been installed. Early experimental work has been conducted with the system to investigate the behavior of direct injection fuel sprays under different operating conditions. The development of the spray and the steady state cone angle were investigated over a range of fuel injection pressures. The dependence of the spray structure on the volatility of the dopant and the temperature of the engine was also examined. The results from these studies are summarized below.

1) The spray development occurs in four distinct phases.
   a) *Delay phase*: This is the period of time between when the signal to inject is sent to the injector driver and fuel is first detected with the PLIF system. The delay phase for the 20° and 60° Zexel injectors was 310 μsec and 360 μsec respectively. With the Chrysler injector, the delay phase was 180 μsec.
   b) *Liquid jet phase*: Before the spray develops sufficient angular momentum to form a hollow cone, fuel leaves the injector along the centerline of the spray in a poorly atomized stream. The velocity of the pre-spray for the 20° and 60° Zexel injectors was 88 m/s and 78 m/s respectively (P_{inj} = 5.0 MPa). The velocity of the pre-spray for the Chrysler injector was 86 m/s at the same fuel injection pressure.
   c) *Wide spray cone phase*: When the hollow cone structure first develops, the included angle of the fuel spray is significantly wider than the fully developed spray.
   d) *Fully developed phase*: Once a conical spray structure has developed, entrainment of the ambient air causes a low pressure zone to develop in the center of the fuel spray. This causes the spray cone angle to decrease for the steady state spray.
2) Over the range of fuel injection pressures tested (1 MPa – 7 MPa), the spray cone angle is insensitive to changes in the fuel injection pressure. The measured cone angle varied 3° over the range of pressures tested, which is within the accuracy of the method used to measure the angles.
3) As the ambient pressure within the cylinder increases from 0.5 bar to 1.1 bar, the measured cone angle decreases from 70° to 57°.
4) In some images taken with a high volatility dopant (acetone) the location of the fluorescence signal was seen to transition from the edges of the hollow cone to the center of the spray as the engine warmed up. Experimental evidence suggests that acetone rapidly vaporizes and is drawn to the center of the spray by the entrained air flow field. This was not observed in data taken with 3-pentanone, which is less volatile. Data taken under slightly different conditions (at a later injection timing) with acetone did not show as pronounced a transition.

REFERENCES

[1] "1996 Motor Vehicle Facts and Figures." AMMA (1996).

[2] Harada, J., et al., "Development of Direct Injection Gasoline Engine." *SAE Paper No. 970540* (1997).

[3] Iwamoto, Y., et al., "Development of Gasoline Direct Injection Engine." *SAE Paper No. 970541* (1997).

[4] Anderson, R., et al., "Understanding the Thermodynamics of Direct Injection Spark Ignition (DISI) Combustion Systems: An Analytical and Experimental Investigation." *SAE Paper No. 962018* (1996).

[5] Han, Z., Reitz, R., Yang, J., Anderson, R., "Effects of Injection Timing on Air-Fuel Mixing in a Direct-Injection Spark-Ignition Engine." *SAE Paper No. 970625* (1997).

[6] Lake, T., Sapsford, S., Stokes, J., Jackson, N., "Simulation and Development Experience of a Stratified Charge Gasoline Direct Injection Engine." *SAE Paper No. 962014* (1996).

[7] Tomoda, T., et al., "Development of Direct Injection Gasoline Engine - Study of Stratified Mixture Formation." *SAE Paper No. 970539* (1997).

[8] Parrish, S., Farrell, P., "Transient Spray Characteristics of a Direct-Injection Spark-Ignited Fuel Injector." *SAE Paper No. 970629* (1997).

[9] Bräumer, A., et al., "Quantitative Two-Dimensional Measurements of Nitric Oxide and Temperature Distributions in a Transparent Square Piston SI Engine." *SAE Paper No. 952462* (1995).

[10] Itoh, T., et al., "Development of a New Compound Fuel and Fluorescent Tracer Combination for Use with Laser Induced Fluorescence." *SAE Paper No. 952465* (1995).

[11] Lawrenz, W., et al. "Quantitative 2D LIF Measurements of Air/Fuel Ratios During the Intake Stroke in a Transparent SI Engine." *SAE Paper No. 922320* (1992).

[12] Reboux, J., Puechberty, D., "A New Approach of Planner Laser Induced Fluorescence Applied to Fuel/Air Ratio Measurement in the Compression Stroke of an Optical S.I. Engine." *SAE Paper No. 941988* (1994).

[13] Crosley, D., Smith, G., "Laser-induced fluorescence spectroscopy for combustion diagnostics." *Optical Engineering*, Vol. 22 No. 5 (1983).

[14] Hansen, D., Lee, E., "Radiative and nonradiative transitions in the first excited singlet state of symmetrical methyl-substituted acetones." *The Journal of Chemical Physics*, Vol. 62, No. 1 (1975).

[15] Münch, K., Krämer, H., Leipertz, A., "Investigation of Fuel Evaporation Inside the Intake of a SI Engine Using Laser Induced Expiplex-Fluorescence with a New Seed." *SAE Paper No. 961930* (1996).

[16] Drake, M., Fansler, T., Franch, D., "Crevice Flow and Combustion Visualization in a Direct-Injection Spark-Ignition Engine Using Laser Imaging Techniques." *SAE Paper No. 952454* (1995).

[17] Swindal, J., et al., "In-Cylinder Charge Homogeneity During Cold-Start: Studied with Fluorescent Tracers Simulating Different Fuel Distillation Temperatures." *SAE Paper No. 950106* (1995).

[18] Smith, B., Srivastava, R., Thermodynamic Data for Pure Compounds, *Part A, Hydrocarbons and Ketones*. Amsterdam; Elsevier, 1986.

[19] Yuen, L., Peters, J., Lucht, R., "Pressure Dependence of Laser-Induced Fluorescence from Acetone." Combustion Institute Central States Section, May 1996.

[20] Dodge, L., "Fuel Preparation Requirements for Direct-Injected Spark-Ignition Engines." *SAE Paper No. 962015* (1996).

[21] Lefebvre, A., Atomization and Sprays. New York; Hemisphere Publishing Inc., 1989.

[22] Zhao, F., Yoo, J., Lai, M., "Spray Dynamics of High Pressure Fuel Injectors for DI Gasoline Engines." *SAE Paper No. 961925* (1996).

[23] Fraidl, G., Piock, W., Wirth, M., "Gasoline Direct Injection: Actual Trends and Future Strategies for Injection and Combustion Systems." *SAE Paper No. 960465* (1996).

[24] Johansson, B., Neij, H., Juhlin, G., Aldén, M., "Residual Gas Visualization with Laser Induced Fluorescence." *SAE Paper No. 952463* (1995).

[25] Green, R., Cloutman, D., "Planer LIF Observations of Unburned Fuel Escaping the Upper Ring-Land Crevice in an SI Engine." *SAE Paper No. 970823* (1997).

[26] Zhao, F., Lai, M., Harrington, D., "A Review of Mixture Preparation and Combustion Control Strategies for Spark-Ignited Direct-Injection Gasoline Engines." *SAE Paper No. 970627* (1997).

[27] Han, Z., et al., "Modeling the Effects of Intake Flow Structures on Fuel/Air Mixing in a Direct-Injected Spark-Ignition Engine." *SAE Paper No. 961192* (1996).

[28] Salters, D., Williams, P., Greig, A., Brehob, D., "Fuel Spray Characterization within an Optically Accessed Gasoline Direct Injection Engine Using a CCD Imaging System." *SAE Paper No. 961149* (1996).

[29] Jackson, N., Stokes, J., Whitaker, P., Lake, T., "Stratified and Homogeneous Charge Operation for the Direct Injection Gasoline Engine - High Power with Low Fuel Consumption and Emissions." *SAE Paper No. 970543* (1997).

[30] Kuma, T., et al., "Combustion Control Technologies for Direct Injection SI Engine." *SAE Paper No. 960600* (1996).

[31] Yamauchi, T., Wakisaka, T., "Computation of the Hollow-Cone Sprays from a High-Pressure Swirl Injector for a Gasoline Direct-Injection SI Engine." *SAE Paper No. 962016* (1996).

[32] Pontoppidan, M., Gaviani, G., Bella, G., Rocco, V., "Direct Fuel Injection - A Study of Injector Requirements for Different Mixture Preparation Concepts." *SAE Paper No. 970628* (1997).

[33] Karl, G., Kemmler, R., Bargende, M., Abthoff, J., "Analysis of a Direct Injected Gasoline Engine." *SAE Paper No. 970624* (1997).

[34] Ohsuga, M., et al., "Mixture Preparation for Direct-Injection SI Engines." *SAE Paper No. 970542* (1997).

APPENDIX 1

PLIF SETUP

A1.1 Physical connections

The PLIF system consists of several pieces of equipment which must work together properly if images are to be acquired at the correct time. If you are going to use the PLIF equipment, please take the time to review the operating manuals for each piece of the camera system. The camera can be damaged by misuse and is very expensive to repair. The laser can damage the operator which is very expensive to repair as well. This appendix is intended to supplement the manuals and give information that is relevant to the PLIF application of the equipment. There are many connections between the camera controller, pulse generator, computer, and engine shaft encoder and a diagram of those connections is shown in Figure A1.1. A brief explanation of each device, and the connections made to it will be given in this appendix.

1) DCI box: This is a counter box which has *Crank Angle*[1] and *BDC* as inputs. The DCI box is used to count engine crank angle and trigger the PG200 at the crank angle a picture is desired. As the engine is currently configured, 0 CA corresponds to BDC of the intake stroke. The "low" dial indicates the crank angle at which the DCI box will trigger the PLIF system. The "high" dial should be set to any value larger than 720 (this prevents the reset signal from accidentally triggering the PG200).
2) PG200: This is an accurate, flexible, programmable pulse generator. The PG200 is used to synchronize the operation of the laser, intensifier, and the CCD chip. The PG200 is triggered by the DCI box and sends out trigger signals to the laser, and the camera controller (ST138). The PG200 also produces the high voltage (200 Volts) signal which operates the camera intensifier. The high voltage *GATE OUT 1* on the PG200 is wired to the *GATE* BNC connector on the rear of the ICCD camera. A special BNC cable is used for this connection because of the high voltage. The *DELAY TRIGGER OUT* connector on the front of the PG200 is typically wired to the *EXT. TRIG.* connector on the laser. *AUX. DLY'D TRIG OUT* on the back of the PG200 is wired to *EXT. SYNC* on the back of the ST138. *INHIBIT* (bar) *IN* on the front panel of the PG200 is wired to *NOTSCAN* on the rear of the ST138.
3) ST138: The ST138 is responsible for activating the CCD chip (the actual light collecting device) in the camera and transferring image data to the computer. A large 50 pin cable connects the ST138 and the camera, and a "taxi" cable connects the ST138 and the computer. The signal to start acquiring an image is received by the ST138 at the *EXT. SYNC* BNC. The ST138 sends a signal to *INHIBIT* (bar) *IN* on the PG200 from *NOTSCAN* while information is being read from the CCD. This prevents the PG200 from triggering the system and re-exposing the array in the middle of the data transfer operation.

[1] Italicized words refer to the names of BNC connectors on the device.

4) ICCD 576SE: This is the ICCD camera. The connections include the high voltage gate signal from *GATE OUT 1* on the PG200 to *GATE* on the camera, and a 50 pin cable to the ST138.
5) Laser: For the purposes of acquiring data, the laser is controlled by a signal on the *EXT. TRIG.* BNC located on the back panel of the laser. The laser trigger signal is generated by the PG200.
6) Computer: The computer is connected to the PLIF system by means of the "Taxi" cable which runs between the Princeton Instruments board inside the computer and the ST138.

A1.2 Equipment settings

After all of the hardwire connections have been made, there are several settings which should be checked.

1) PG200 settings: The experiment timing is shown in Figure A1.2. The PG200 settings control most of the timing parameters and are shown in Table A1.1.

Table A1.1 PG200 settings

Function	PLIF Setting	Focus Setting
Auxiliary Delay Trigger (function 16)	1 μsec	1 μsec
Delay Trigger	2 μsec	2 μsec
Gate Delay	2.9 μsec	2.9 μsec
Gate Width	15 μsec	250 μsec
Gate Sync (function 15)	0,0 (both disabled)	0,0 (both disabled)
Trigger Mode	External	Internal

2) ST138 Settings: The only controls on the ST138 are for the peltier cooler for the ICCD camera. To reduce the amount of Dark Charge (signal that the camera records even with the lens cap on) that the camera records, the cooler can be switched on. The dial on the front of the ST138 is calibrated in negative degrees Celsius (i.e. a setting of 20 yields a temperature of -20° C). The cooler should always be OFF unless NITROGEN AND COOLING WATER are flowing to the camera. The nitrogen prevents moisture from freezing to the CCD chip and the cooling water prevents the warm junction on the cooler from overheating. Generally, a setting of 10 is sufficient to reduce the background noise below 1000-2000 counts.
3) Software Settings: The image acquisition and processing is done with Winview which was written by Princeton Instruments. The software settings necessary for the system to operate are shown in figures A1.3-A1.6. The values in the Hardware Setup window (A1.3) should not be changed unless new equipment is added. Auto Store can be turned off while focusing the camera so that the system will take and display an unlimited number of pictures; with Auto Store off, only the picture that is on the screen is saved, so when an experiment is run Auto Store should be turned on.

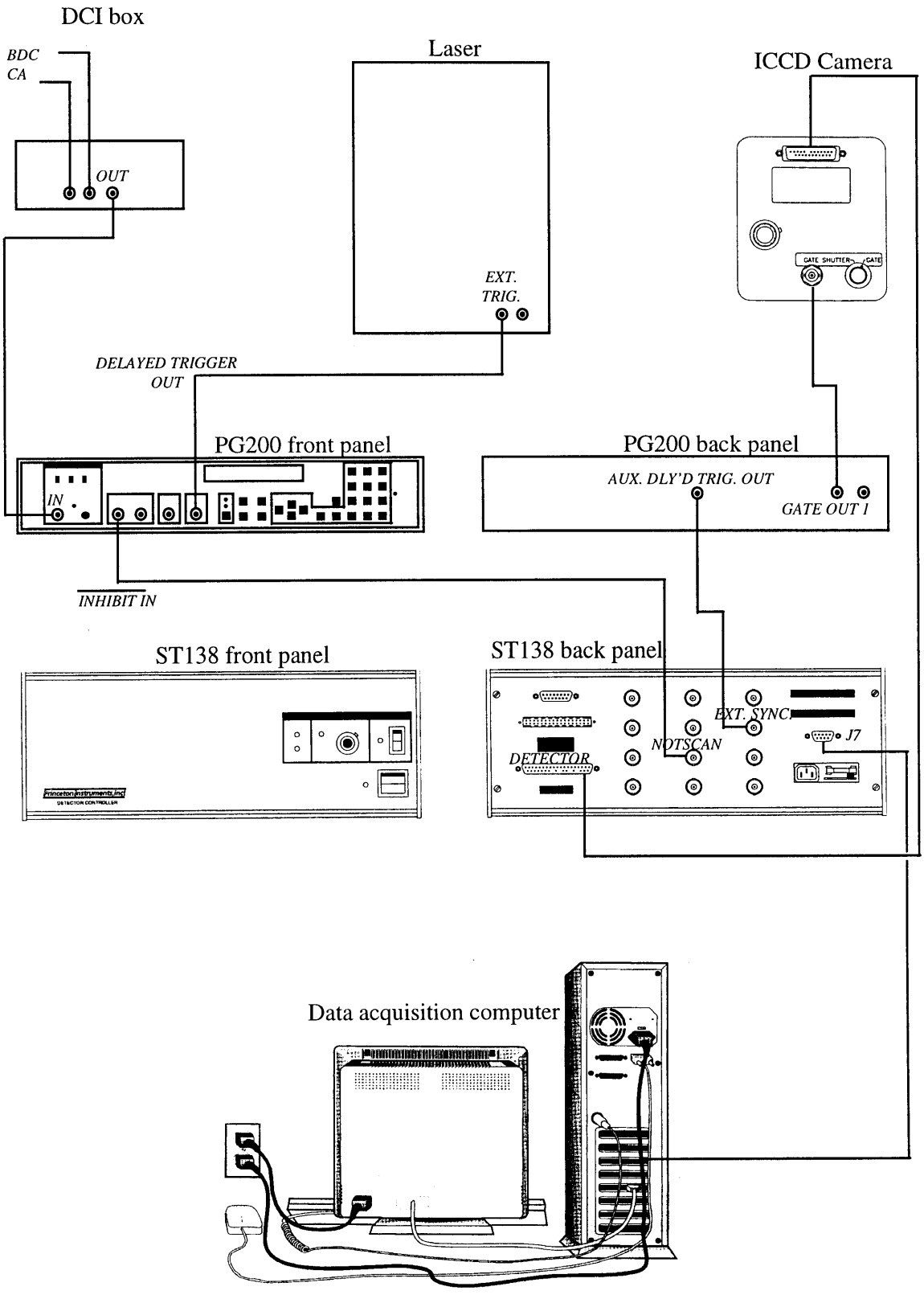

Figure A1.1 PLIF equipment connections.

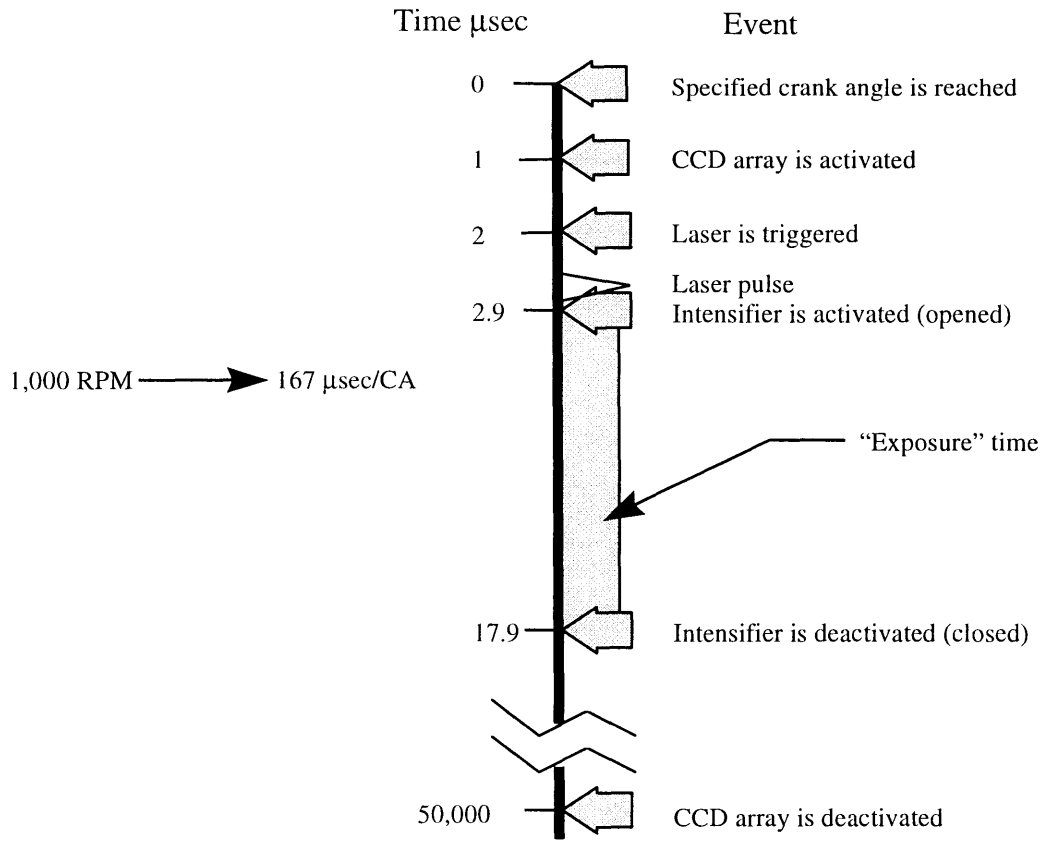

Figure A1.2 Experiment timing diagram.

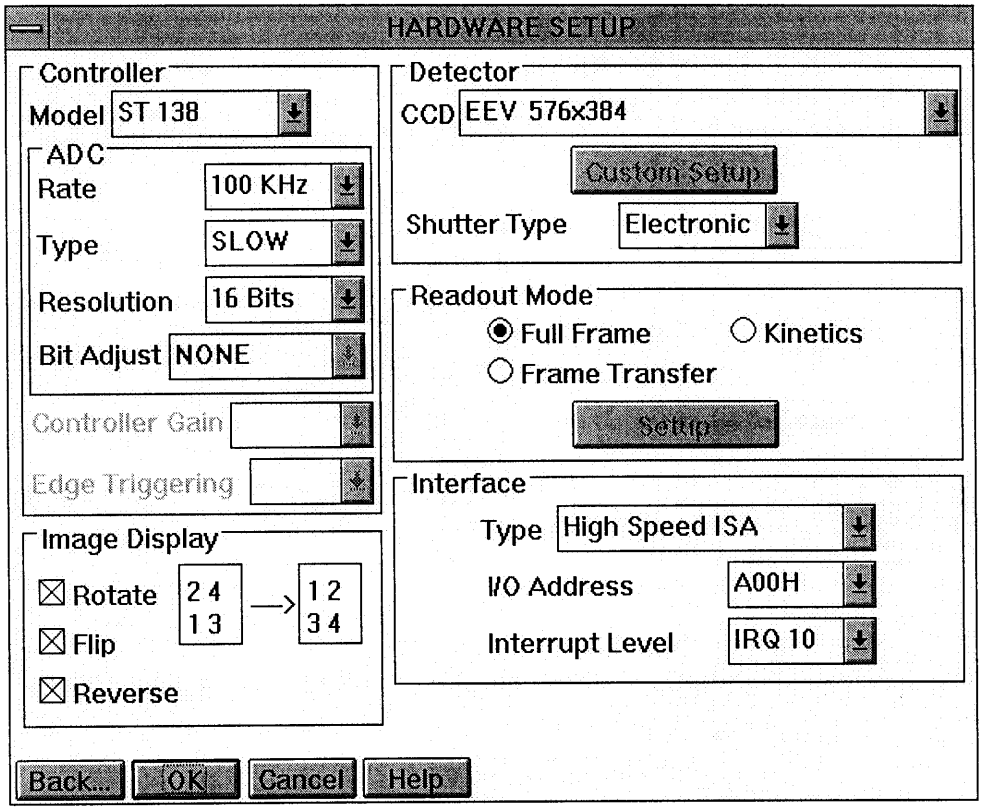

Figure A1.3 Winview hardware setup window.

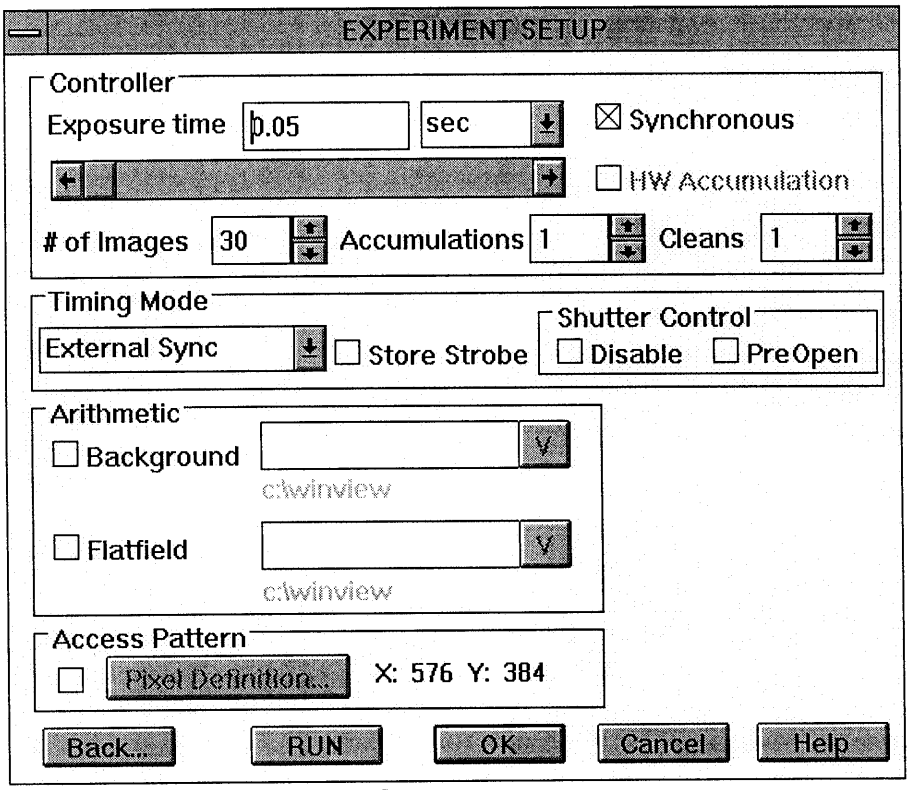

Figure A1.4 Winview experiment setup window.

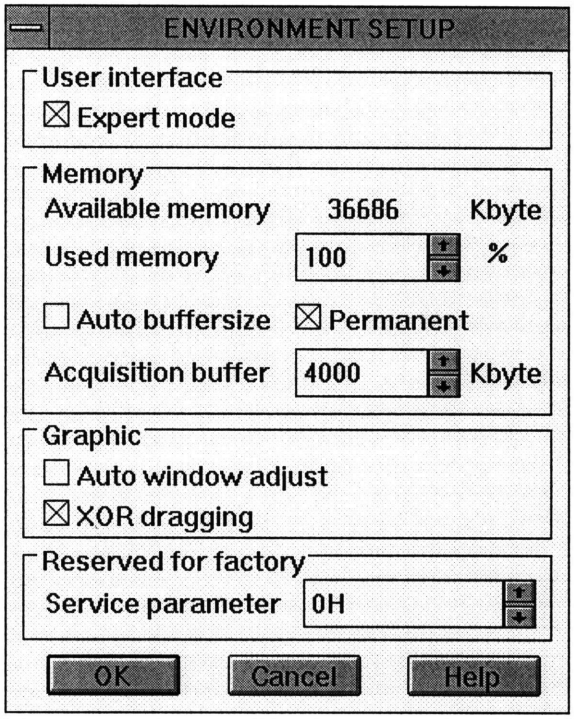

Figure A1.5 Winview environment setup window.

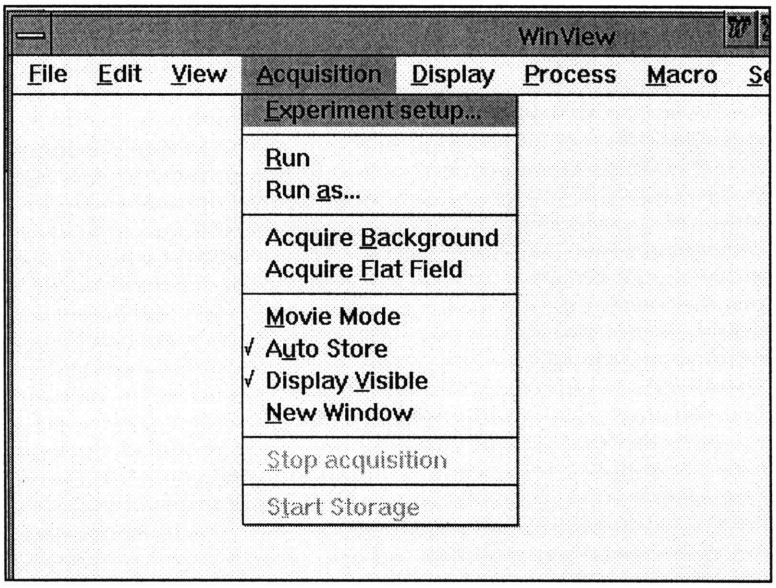

Figure A1.6 Location of Auto Store setting.

APPENDIX 2

LabVIEW ENGINE CONTROL PROGRAM

A2.1 Background

Due to numerous difficulties and lack of flexibility with the purpose built controller previously used to control the square piston optical engine, a new LabVIEW based engine control system has been developed. The program controls spark timing, injection timing, and injection duration. LabVIEW is a software package written by National Instruments that comes with an extensive library of pre-built subroutines related to the acquisition and processing of data using a computer. Programs within LabVIEW are referred to as VI's or Virtual Instruments, because one of the primary uses of LabVIEW is to emulate common laboratory equipment (oscilloscope, function generator, multimeter, etc.) using a computer and a Data AcQuisition (DAQ) board. LabVIEW uses a graphical programming language where subroutines appear as icons and the flow of information is represented by wires. This system is user friendly and has some advantages over text-based programming languages such as C or FORTRAN. LabVIEW comes with many pre-built subroutines which make common DAQ operations, such as acquiring data and writing data to a file, easier to program.

For our purposes, we needed a controller that would take Crank Angle (CA) and Bottom Dead Center (BDC) pulses as inputs and output TTL control signals for the fuel injector and the ignition coil. The engine controller programmed for these experiments was designed to be as simple to use and modify as possible. The system runs completely open loop, so the spark timing, injection timing and injection duration are all set in software by the user.

A2.2 Equipment

The engine controller consists of a personal computer, LabVIEW software, and a National Instruments timing board with a 50 pin connector block. The computer is a 120 MHz Pentium with 16 megabytes of RAM. The timing board is a PC-TIO-10 National Instruments board, which consists of 10 programmable 16 bit timers (2 Am9513A chips) and 16 TTL level digital I/O lines. Data acquisition is accomplished using a Lab-PC-1200+ also from National Instruments. All programming was done using LabVIEW Full Development System for Windows 95, version 4.0.1 (S/N G10X46192).

A2.3 Theory of operation

In order to understand the engine control program, it is necessary to understand how the digital counters on the PC-TIO-10 timing board operate. Each counter has three pins associated with it on the connector block. The three pins are the Gate, Clock, and the Output pins. The Gate and Clock pins operate

as inputs to the counter and the Output pin is the output. There are many options within LabVIEW for how the Gate pin can be used, but for understanding the basic operation of the engine control program it is sufficient to think of the Gate pin as a reset function. When the signal on the Gate pin transitions from 0 volts to 5 volts the counter begins to count transitions from 0 volts to 5 volts (rising edges) on the Clock pin. The output can then be programmed to behave in a number of different ways. The most common output strategy is for the counter to count a certain number of "delay pulses", and then set the output high for a software specified number of pulses (pulse width).

For a basic engine control program, three counters are used. The first counter is used to charge the ignition coil and set the spark timing. The inputs to this counter are CA and BDC on the Clock and Gate pins respectively. The counter resets on the BDC signal and begins to count CA. The output of this counter is configured to be TTL level high, which charges the ignition coil, until the counter reaches the value of the spark timing. The ignition coil initiates a spark when the control signal transitions from high to low.

The operation of the second counter is very similar except that it is used to control the injection timing. For this counter the inputs are also CA and BDC on the Clock and Gate pins. The output of this counter is programmed to be low for counts less than injection timing and high for counts greater than injection timing. This counter is used as the reset for the third counter. The third counter is used to create an injection control pulse based on time not crank angle. The Gate pin of the third counter is wired to the output of the second counter so that the third counter is reset when the proper CA is reached. The third counter uses an internal clock for the Clock signal so that the injection pulse width can be accurately resolved. The output of the third counter is set to be high (or optionally low) until the end of injection duration period is reached.

A2.4 LabVIEW engine control program

A2.4.1 Configuration

The LabVIEW engine control program is capable of generating either high TTL pulses (on=5 volts), or low TTL pulses (on=0 volts) for both the spark and injection signal. The controls for determining which logic is used are located to the right of the main display within the "T10 CA controller.vi" (Figure A2.1). It is very important to use the correct polarity for the fuel system that you are using, otherwise the injector will inject fuel continuously. The port fuel injection system uses high TTL logic while the Zexel direct injection system uses low TTL logic. The spark signal polarity for the square piston engine should always be set to low TTL logic unless the output of the controller is being sent through a NOT gate to isolate the signal. The injection timing and spark timing are set relative to the BDC pulse. Currently, BDC for the square piston engine corresponds to BDC of the intake stroke. Therefore 25° spark advance from TDC corresponds to a spark timing of 155.

A2.4.2 Operation

The program is located within a LabVIEW library called "skip fire controller". Within the library are two files, "T10 CA controller.vi" and "skip config.vi". The engine control front panel is located in the "T10 CA controller.vi" file. Once the program has been loaded, enter the values for the spark timing, injection timing, and injection duration that are appropriate for your operating conditions and press the "Start" button. The switches for the ignition and the fuel injection allow the fuel injection to be turned off independently of the spark, however, if the ignition is turned off the injection signal will also be disabled to prevent flooding the engine with fuel. The monitored inputs (inputs that the program continuously monitors for changes and reconfigures the counters to reflect changes) to the program are the Ignition switch, Fuel Injection switch, Spark Timing, Start of Injection, and Injection Duration. The program does not monitor the TTL polarity settings or the skip fire controls, so if a change is made to one of those controls a monitored control must also be changed before the counters will be reconfigured.

The controller is capable of operating in a skip fire mode where several firing cycles are followed by several motoring cycles. There are some limitations to what values can be used with the present program. The number of cycles to skip and the number of cycles to fire can be any number larger than 3. LabVIEW limits the minimum count on a counter to 3. The Trigger Cycle is used to allow the synchronization of an external device to the engine firing cycles. The Trigger Cycle transitions from low to high at BDC of the firing cycle specified in the Trigger Cycle input on the front panel. For example if the # to skip, # to fire, and Trigger Cycle inputs where 10,10, and 5 respectively, then the controller would disable the fuel injection for 10 cycles, enable the fuel injection for the next 10 cycles and on the 5^{th} firing cycle the voltage on the Trigger Cycle BCN connector would transition from 0 volts to5 volts. After the 10 firing cycles, the Trigger Cycle voltage would return to 0 volts and the process would repeat.

A2.4.3 Code explanation

A diagram of the engine controller program, "T10 CA controller.vi", is displayed in Figures A2.2–A2.5. In order to understand the elements which make up the program, it would be extremely beneficial for the reader to use the help within LabVIEW to get descriptions of the individual elements that make up the program. This can be done by opening the engine control program, stopping the execution, selecting the *Show Diagram* option under the *Windows* pull down menu and selecting *Show Help* under the *Help* menu. To display information about an icon, simply select it with the mouse and a description of the icon will appear in the help window.

A2.4.3.1 T10 CA controller.vi program

The program is laid out in a "sequence structure", which looks like a frame of film, and consists of one or more subdiagrams, or frames, that execute sequentially. The engine control program consists of 4 frames numbered from 0 to 3.

Frame 0 (Figure A2.2):

This frame was included to fix a problem that was encountered when the data acquisition system was added to the engine control computer. In order to synchronize the data acquisition system to the engine, the crank angle signal was used to set the scan clock on the LAB-PC-1200+ board. The difficulty encountered was that the pin used to set the scan clock was grounded until the data acquisition program was started. This effectively grounded the crank angle signal and brought it below the level that the TIO-10 board recognized as a clock signal and prevented the counters from counting crank angle.

The fix was to configure the LAB-PC-1200+ board to recognize the scan clock as an input in the engine control program so that the pin would not be grounded while the engine control program is running. So this frame configures the LAB-PC-1200+ to use the I/O connector to set the scan clock.

Frame 1 (Figure A2.3):

Frame 1 is used to prevent the program from running until the Start button is pressed. This is accomplished by placing the Boolean control (start button) inside of a while loop. The while loop continues to loop until the start button is pressed; when the start button is pressed, the Boolean value is TRUE. This value is then run through a NOT gate and into the loop control. When the loop control receives a FALSE signal it exits the while loop.

Frame 2 (Figure A2.4):

The main function of frame 2 is to monitor the Ignition Switch, Fuel Injection switch, ignition timing, fuel injection timing and the fuel injection duration inputs on the front panel. If the user changes one of these values, the subroutine "skip config.vi" is called and the counters are reconfigured to reflect the new values. If the user has not modified any of the monitored inputs, the program measures the engine RPM and displays the value on the front panel.

While the engine controller is running the program operation stays within the WHILE loop found in frame 2. The arrow blocks found on the edges of the WHILE loop are called shift registers and they are used to pass values from one iteration of the loop to the next iteration. These are used to compare the value of the monitored variables with the values obtained the last time the loop was run. If the values of the monitored variables have changed then one of the comparitors (triangles with equal signs on the inside) will return false and the "skip config.vi" subroutine will

be called. If all of the monitored parameters are the same as they were the last time the loop was executed, the TRUE condition of the case statement is executed and the RPM is measured and displayed.

The section of the code within the WHILE loop but below the case statement is used to obtain the "task ID's" for the counters used for the spark timing, injection timing and the injection duration. The task ID's are necessary so that the counters can be stopped in Frame 3. The task ID's are initialized to 0 and then they receive a value from the "skip config.vi" subroutine. The "Max & Min" VI's are necessary because the case statement requires each case to have the same number of outputs. Therefore the TRUE condition in the case statement outputs 0 for the Task ID's, and the maximum function along with shift registers are used to keep track of the task ID's.

The while loop in Frame 2 will operate continually until the stop button is pressed on the front panel. Once the stop button is pressed the program will execute Frame 3.

Frame 3 (Figure A2.5):

The purpose of frame three is to stop the counters used to trigger the spark and fuel injection, and to return the LAB-PC-1200+ board to its original state. If the polarity of the output is set to low, then the output of the counter will be set high when the counter is stopped, this prevents triggering the fuel injector continuously when the program is stopped.

A2.4.3.2 Skip config.vi

Within skip config.vi are the VI's that configure the counters on the TIO-10 board. The wiring diagram for the PC-TIO-10 connector block can be found in Figure A2.6. A diagram for skip config.vi can be found in Figures A2.7–A2.8. The overall structure of the subroutine consists of a TRUE/FALSE case statement. The TRUE case is used when the skip fire switch on the front panel of the engine control program is turned on. And the false cased is used when skip fire is turned off.

TRUE case (Figure A2.7):

The TRUE portion of the case statement is used when it is desirable to operate the engine in a skip fire manner. When the engine is skip firing, several firing cycles are followed by several non-firing cycles. This allows the engine to be operated longer without overheating and can also be used to purge the residual gas from the cylinder. Skip firing is accomplished by deactivating the high frequency pulse train generator, which prevents the counter responsible for triggering the fuel injector from counting.

The primary element used to configure the counters is the "Generate Delayed Pulse.vi." The triggering options, TTL polarity, counter number, pulse delay, pulse width, and clock source are all selected with this sub-vi.

Counter #1: Spark Timing

Counter #1 is used to control the spark timing. When the Ignition switch on the front panel is in the on position this counter is configured to restart counting on each rising edge of the BDC signal. The counter's clock source is the external clock pin, which is wired to the CA (crank angle) signal from the engine. The counter is typically configured for low TTL pulses (controlled on the front panel of the engine control program) so the output is high during the delay phase (charges ignition coil) and low during the pulse width. The delay is then set to be the number of crank angle between BDC and the desired spark timing. The width is configured to be the rest of the engine cycle (720 minus spark timing).

When the ignition switch is turned off on the front panel, the spark counter is configured so that it only counts pulses while the BDC signal is high. Since the BDC signal is shorter than a crank angle, the counter never counts any crank angle and the level remains high.

Counter #8: Injection Timing

Counter #8 operates in the same manner as Counter #1 except that the output is used to gate another counter. Counter #8 is configured for high TTL pulses (the default), so the output transitions from low to high when the Injection timing crank angle is reached and stays high until the end of the cycle. On the connector block, the output of Counter #8 is wired to the gate of Counter #2.

Counter #3: Skip Fire Counter

Counter #3 is used to count engine cycles. Counter #3 is configured to start counting on the rising edge of the BDC signal and it counts cycles by monitoring the number of times Counter #8 tries to gate the injection timing counter. The output of Counter #3 is low for the number of motored cycles and high for the number of firing cycles. The output of Counter #3 is used to gate the cycle trigger counter (#9) and the high frequency timing clock (Counter #4).

Counter #4: Timing Clock

Counter #4 is used to generate a 40KHz clock signal that is used by Counter #2 to time the injection pulse width. The output square wave is generated whenever the gate signal is high, i.e. whenever the output of Counter #3 is high.

Counter #2: Injection Duration

Counter #2 is used to time the injection duration relative to a clock signal that is generated by counter #4. The gate signal for Counter #2 is generated by Counter #3 and the clock signal is generated by Counter #4. This counter is triggered every engine cycle, but the clock signal from Counter #4 is only active during the firing cycles, therefore the injection pulse is only delivered during the firing cycles. The output for Counter #2 is the signal that is sent to the injection driver.

Counter #9: Cycle trigger

The purpose of counter #9 is to provide a trigger for external data acquisition devices (e.g. the LIF system) on a specified firing cycle. The clock source to the counter is the BDC signal and the counter is gated by the output of counter #3. The counter transitions from low to high on BDC of the specified cycle. The output is wired to a BNC connector on the connector box.

FALSE case (Figure A2.8):

When the skip fire feature of the engine controller is turned off the counter configuration is much simpler and easier to understand. Only three counters are needed, and the purpose of each is described below.

Counter #1:

This counter operates in the same manner as it does in the TRUE case.

Counter #8:

This counter operates in the same manner as it does in the TRUE case.

Counter #2:

The operation of Counter #2 is similar in the FALSE case and in the TRUE case. The only difference is that the clock source is internal and the pulse width and delay are given in seconds. The "Delay Pulse Generator.vi" determines the best clock speed to achieve the desired timings and Counter #4 is not used.

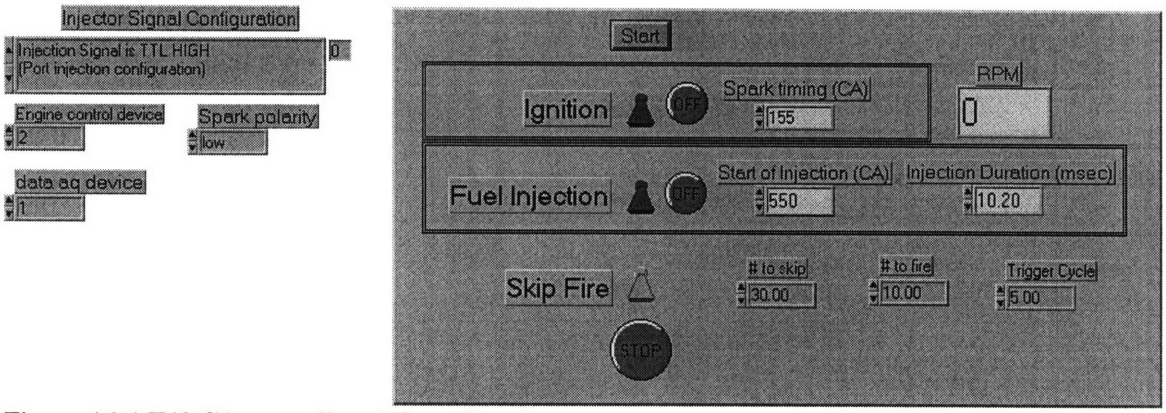

Figure A2.1 T10 CA controller.vi Front Panel

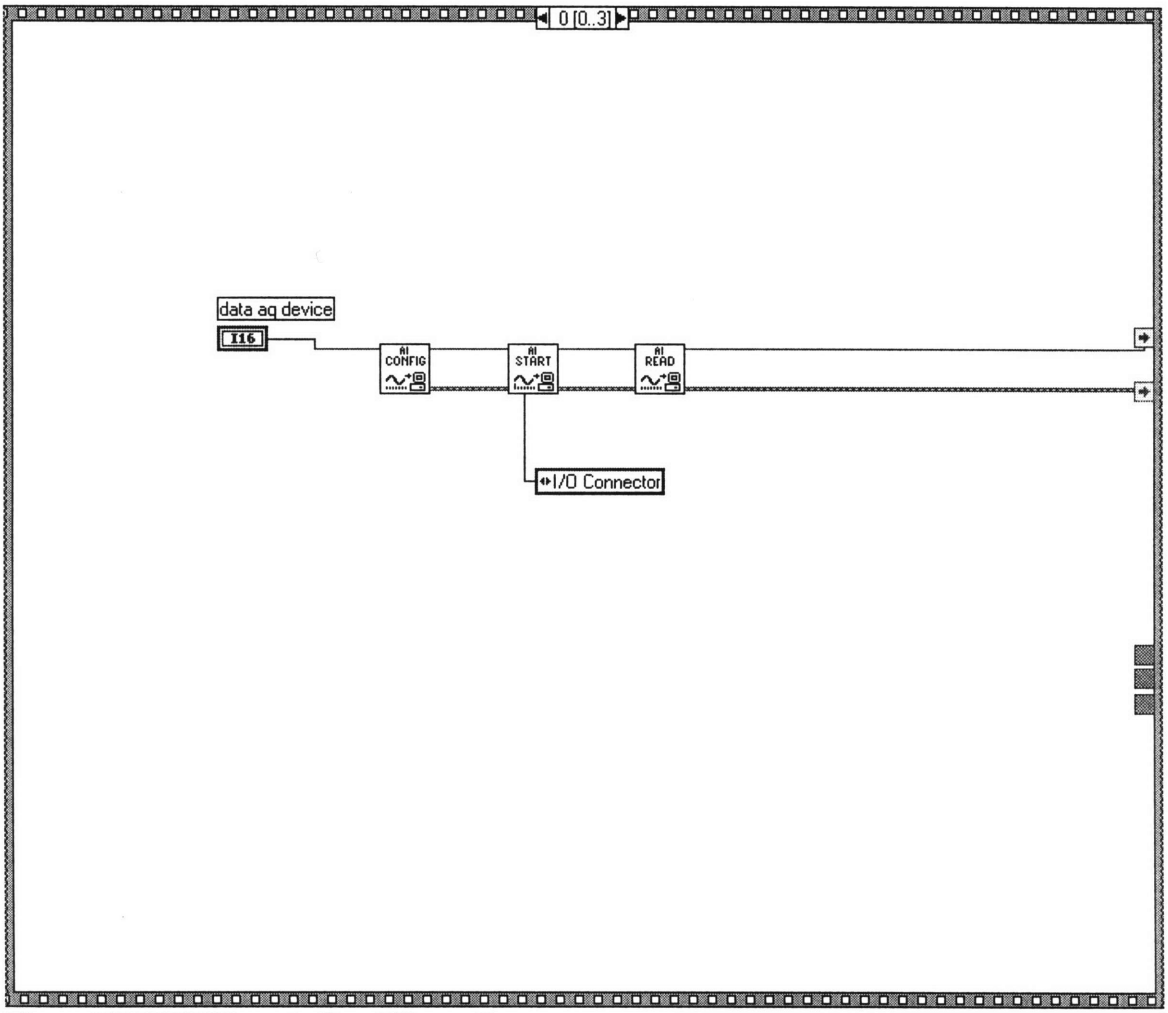

Figure A2.2 T10 CA controller.vi Frame 0

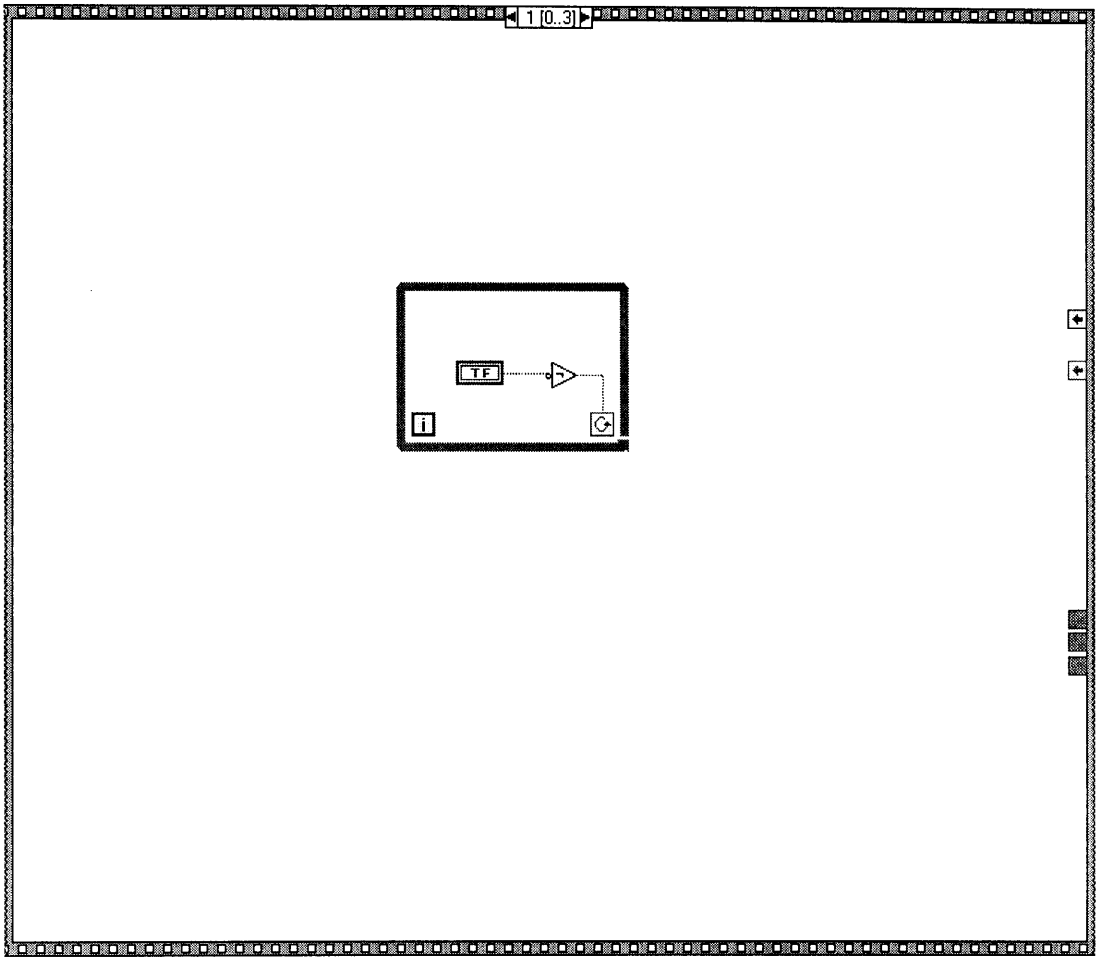

Figure A2.3 T10 CA controller.vi Frame 1

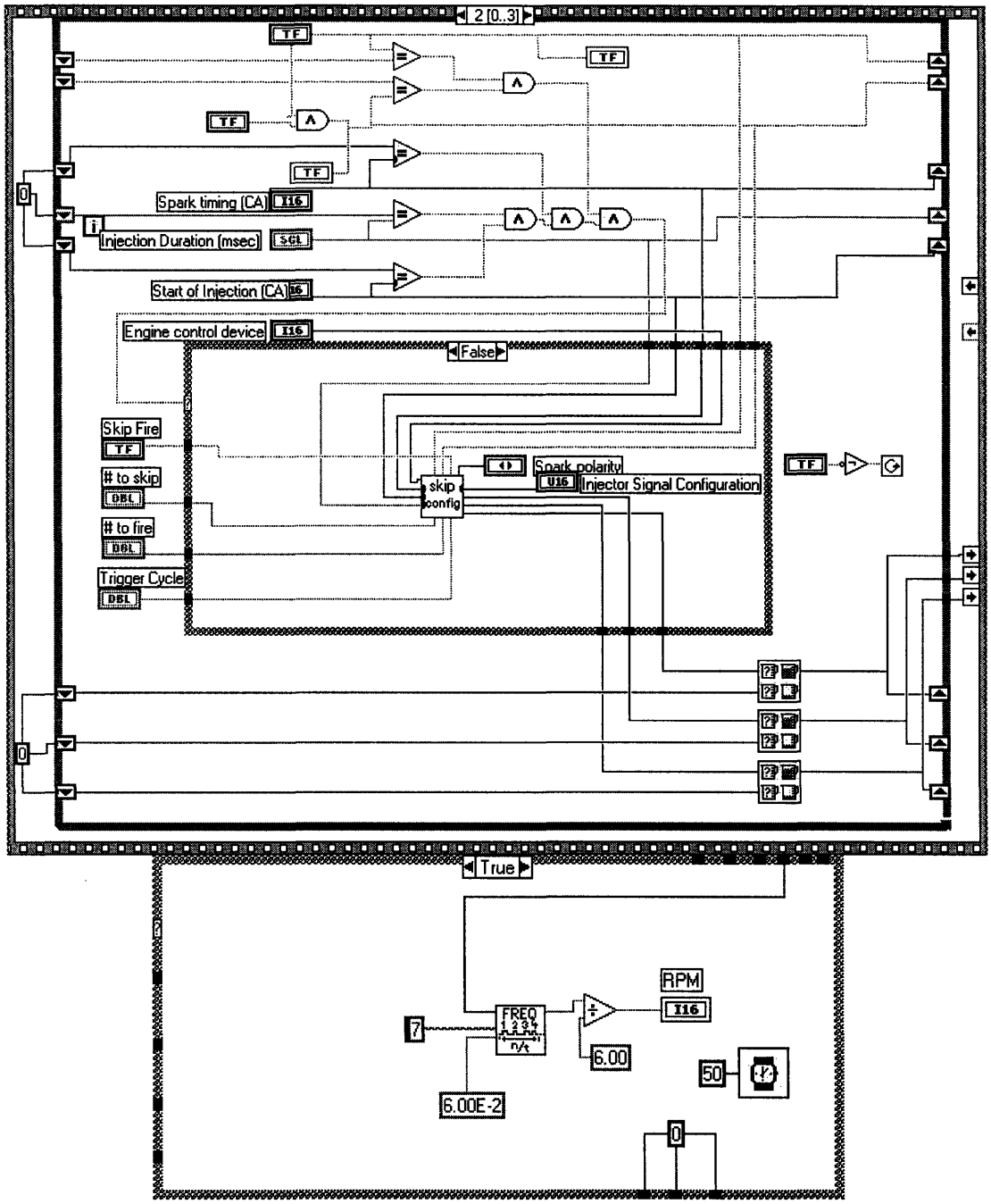

Figure A2.4 T10 CA controller.vi Frame 2

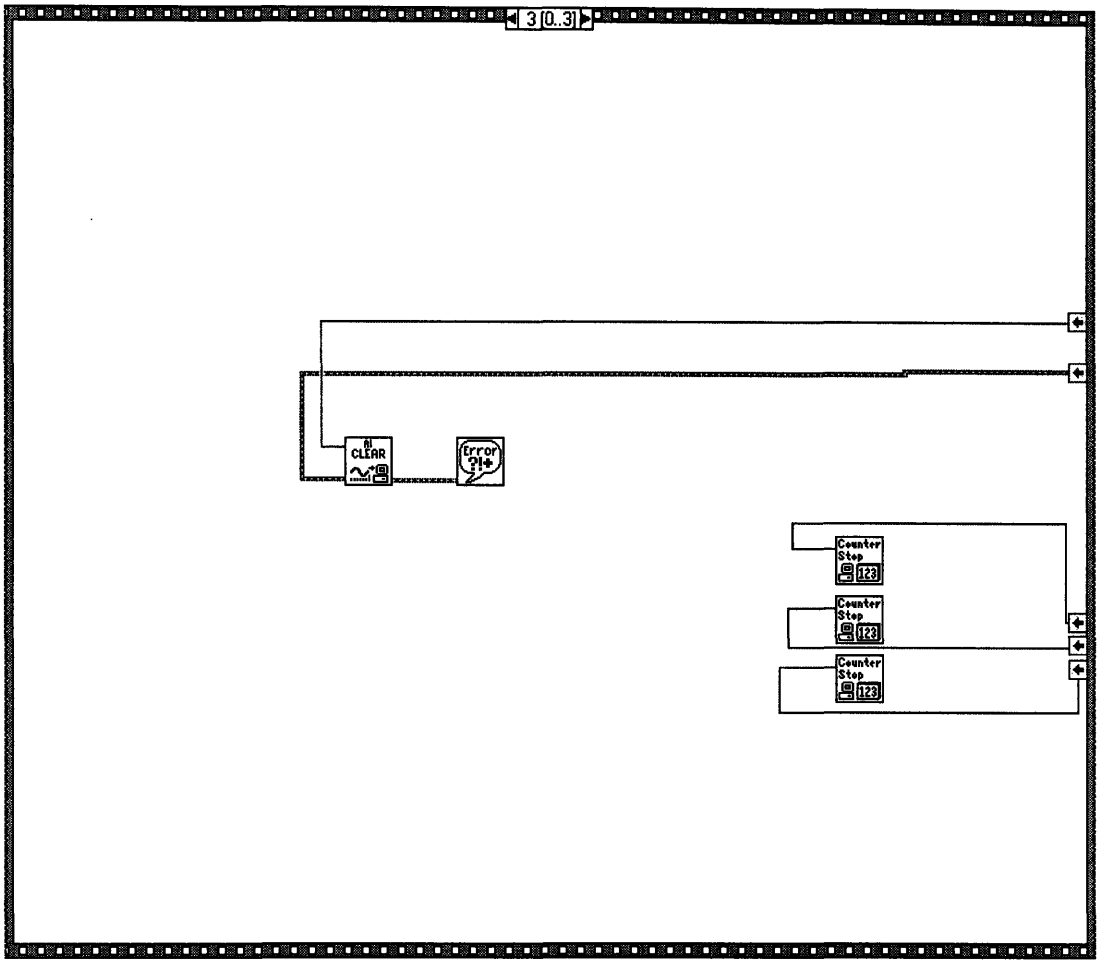

Figure A2.5 T10 CA controller.vi Frame 3

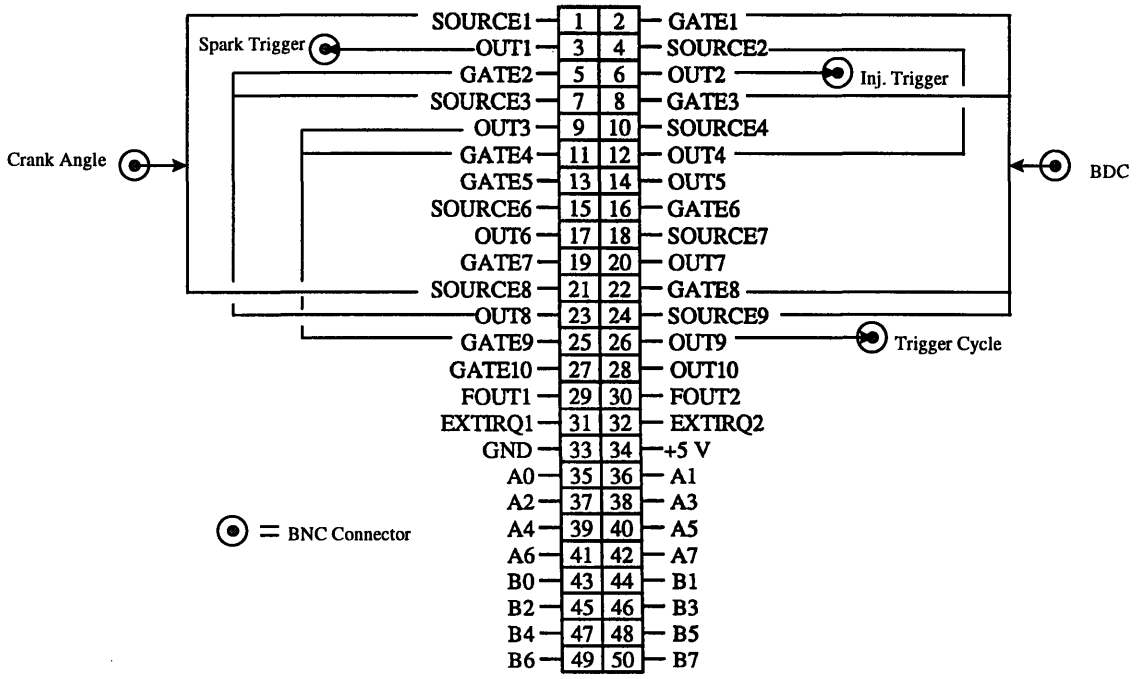

Figure A2.6 Wiring diagram for PC-TIO-10 connector block

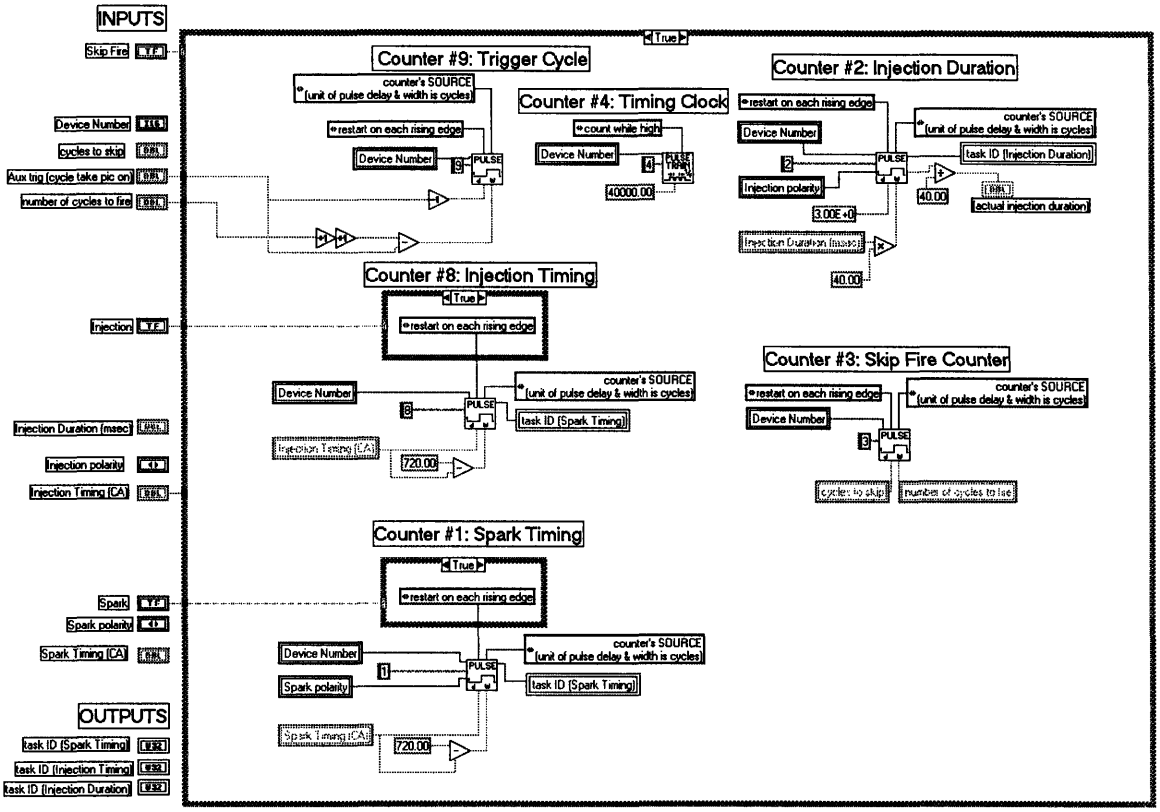

Figure A2.7 Skip fire config.vi: True case

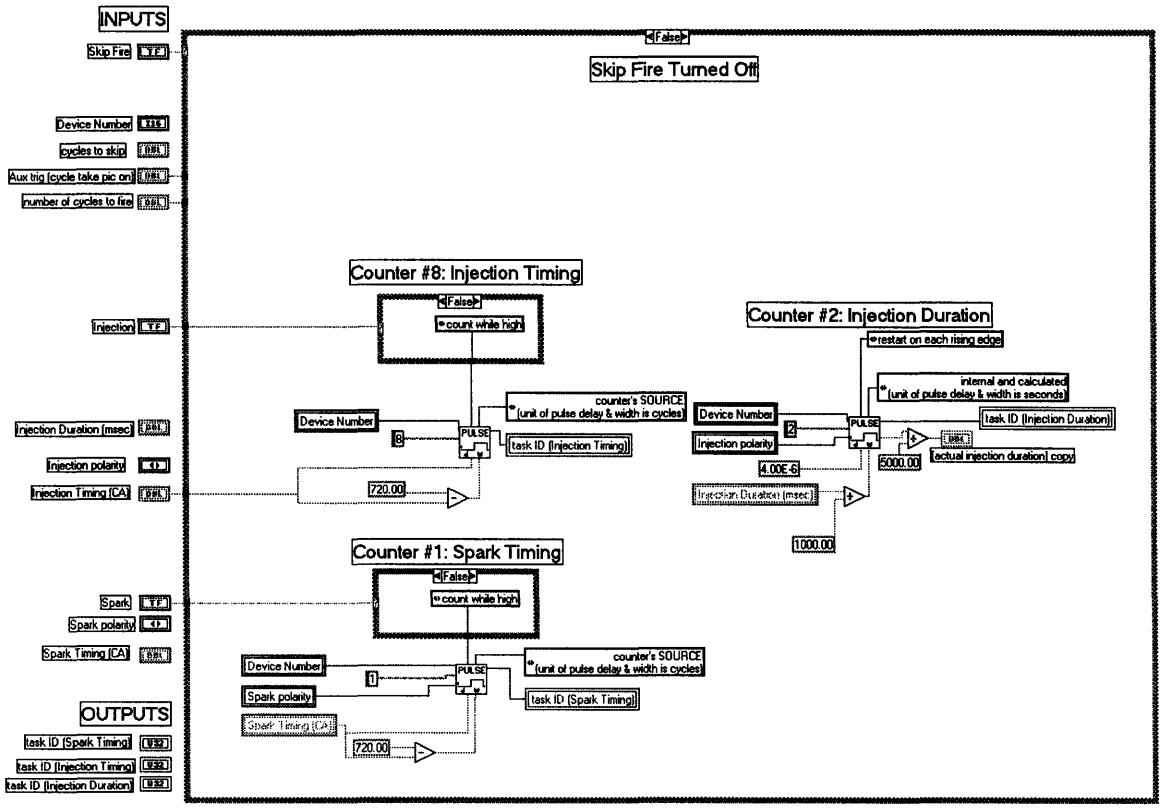

Figure A2.8 Skip fire config.vi: False case

APPENDIX 3

ENGINE MODIFICATION DRAWINGS

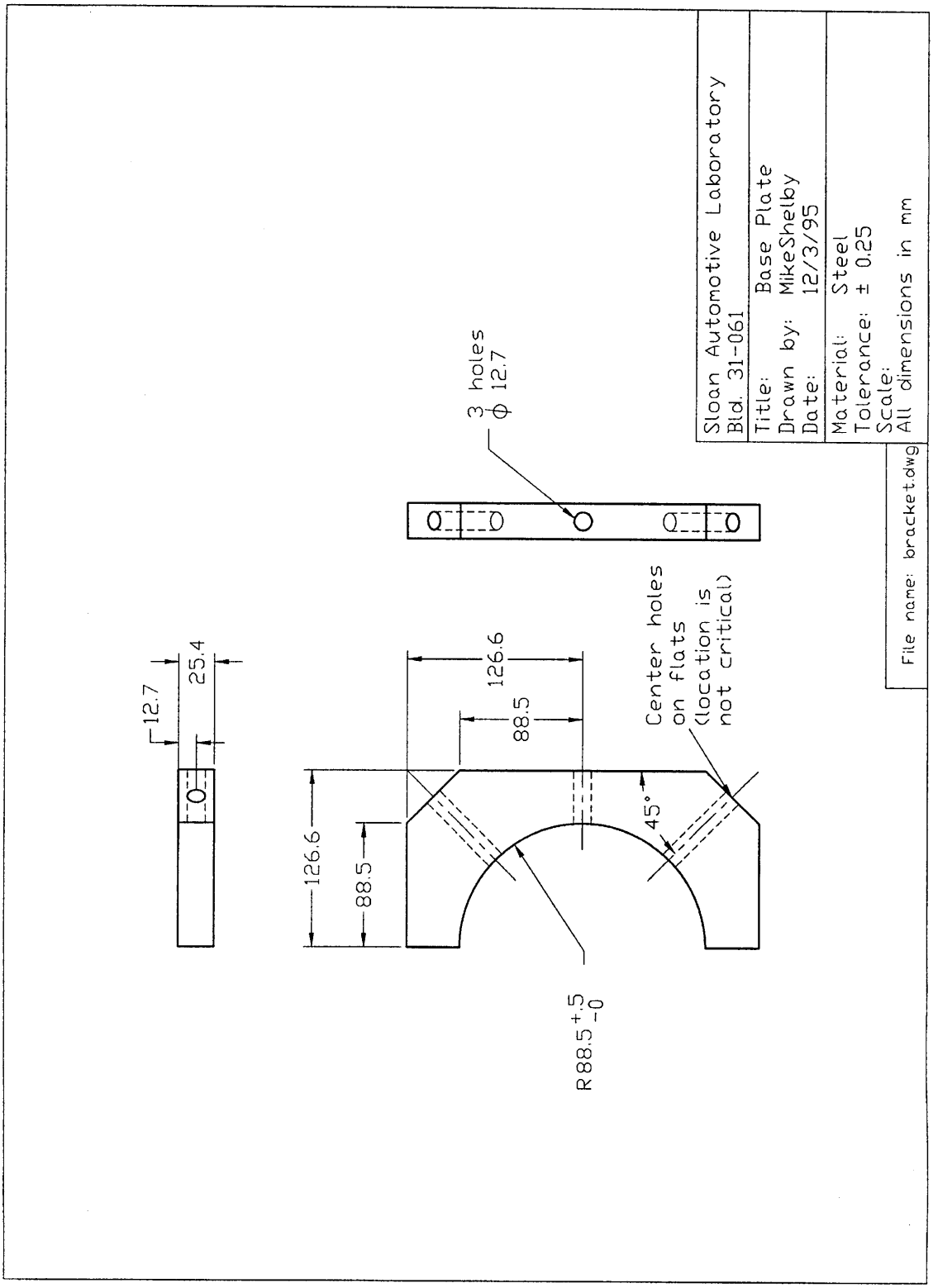

Figure A3.1 Base plate drawing

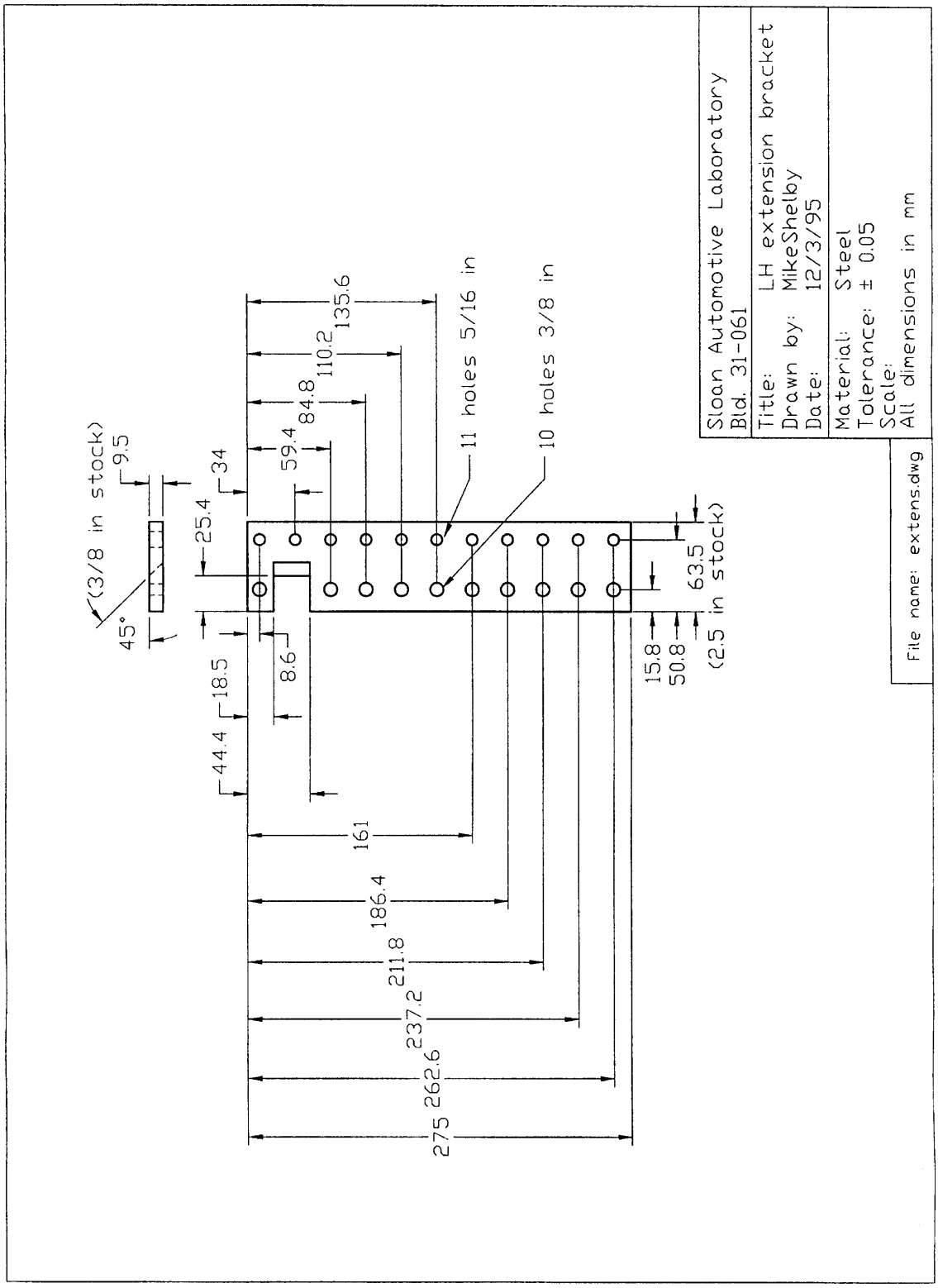

Figure A3.2 Left extension bracket drawing

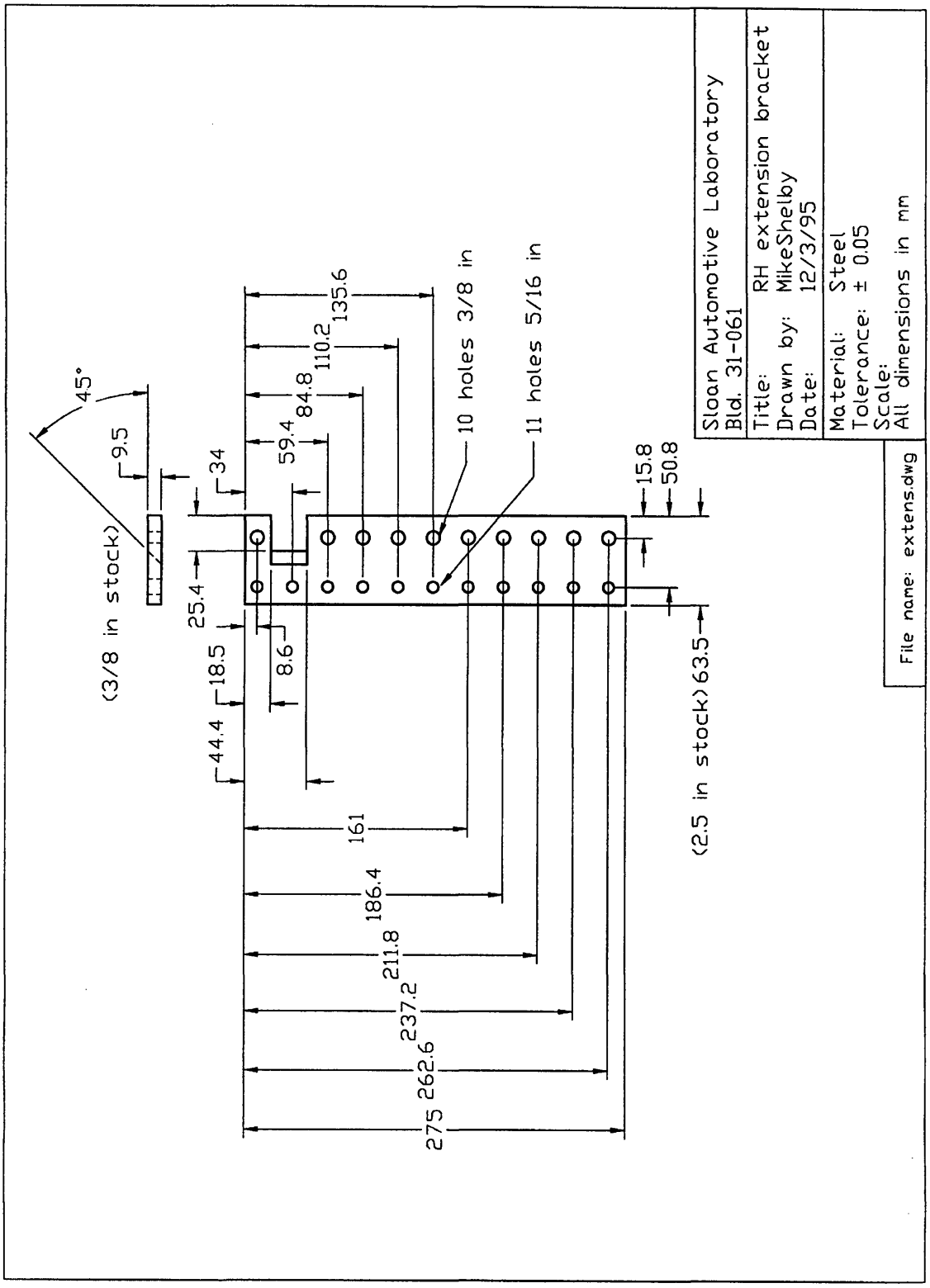

Figure A3.3 Right extension bracket drawing

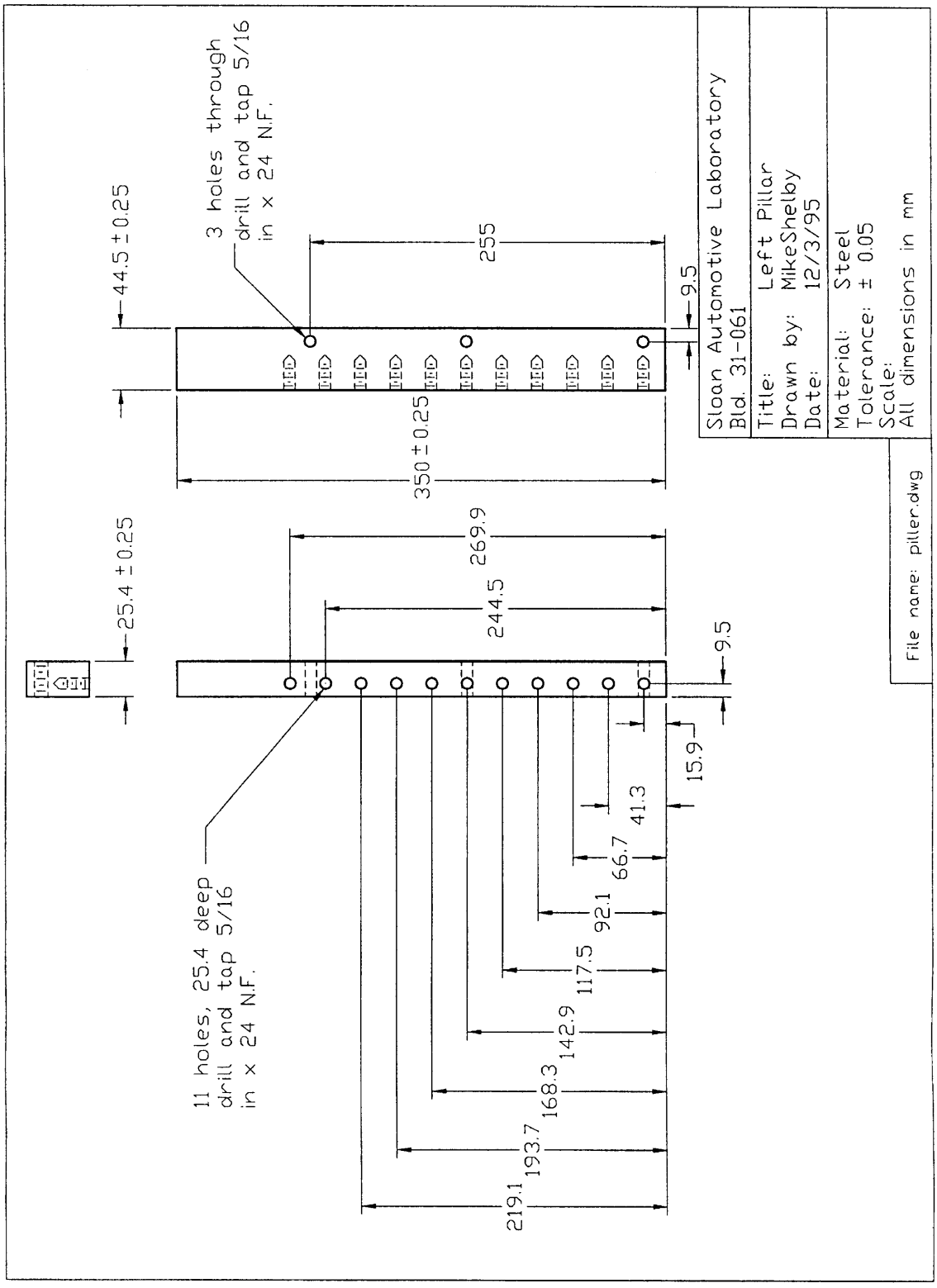

Figure A3.4 Left engine pillar drawing

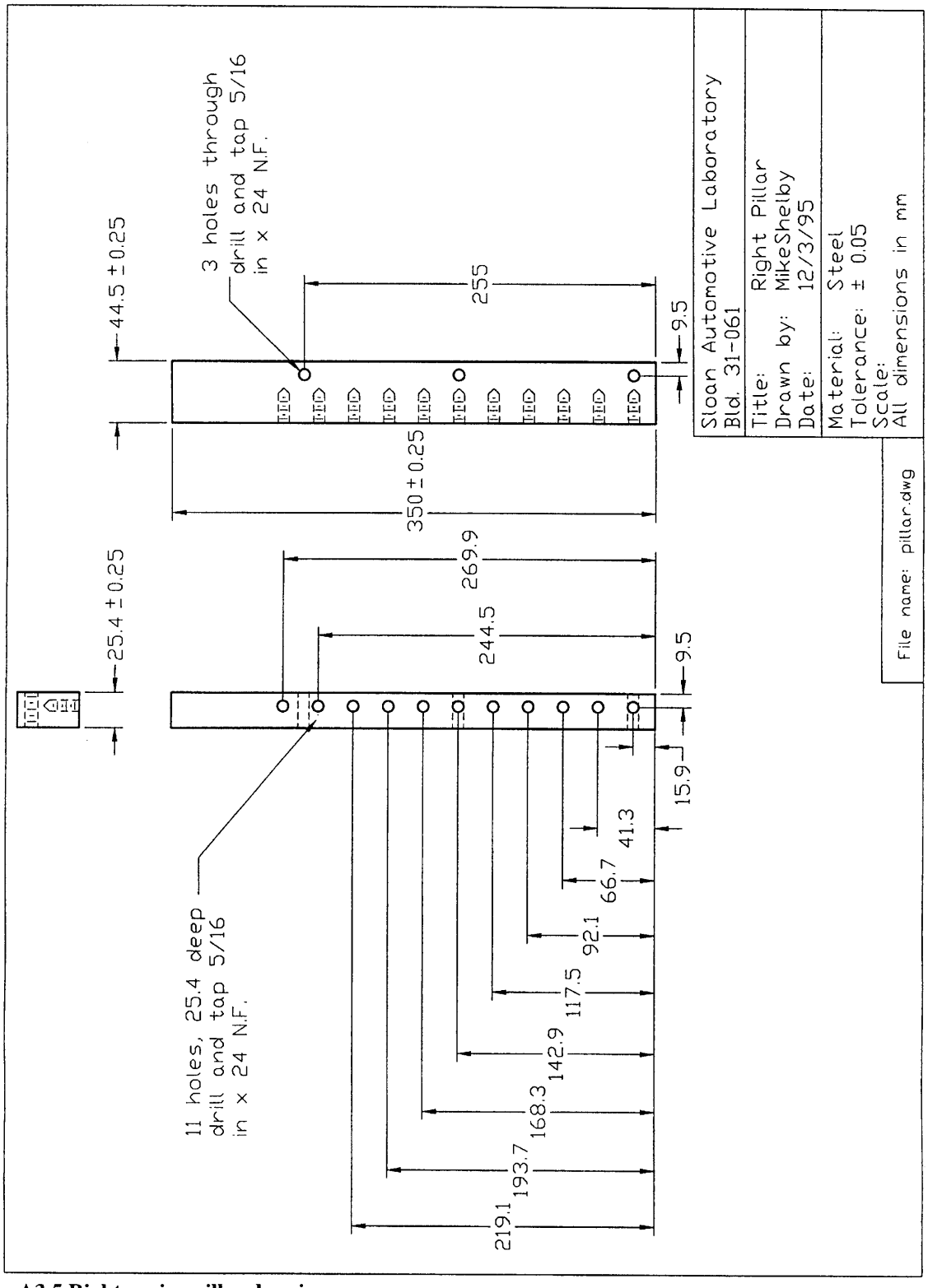

Figure A3.5 Right engine pillar drawing

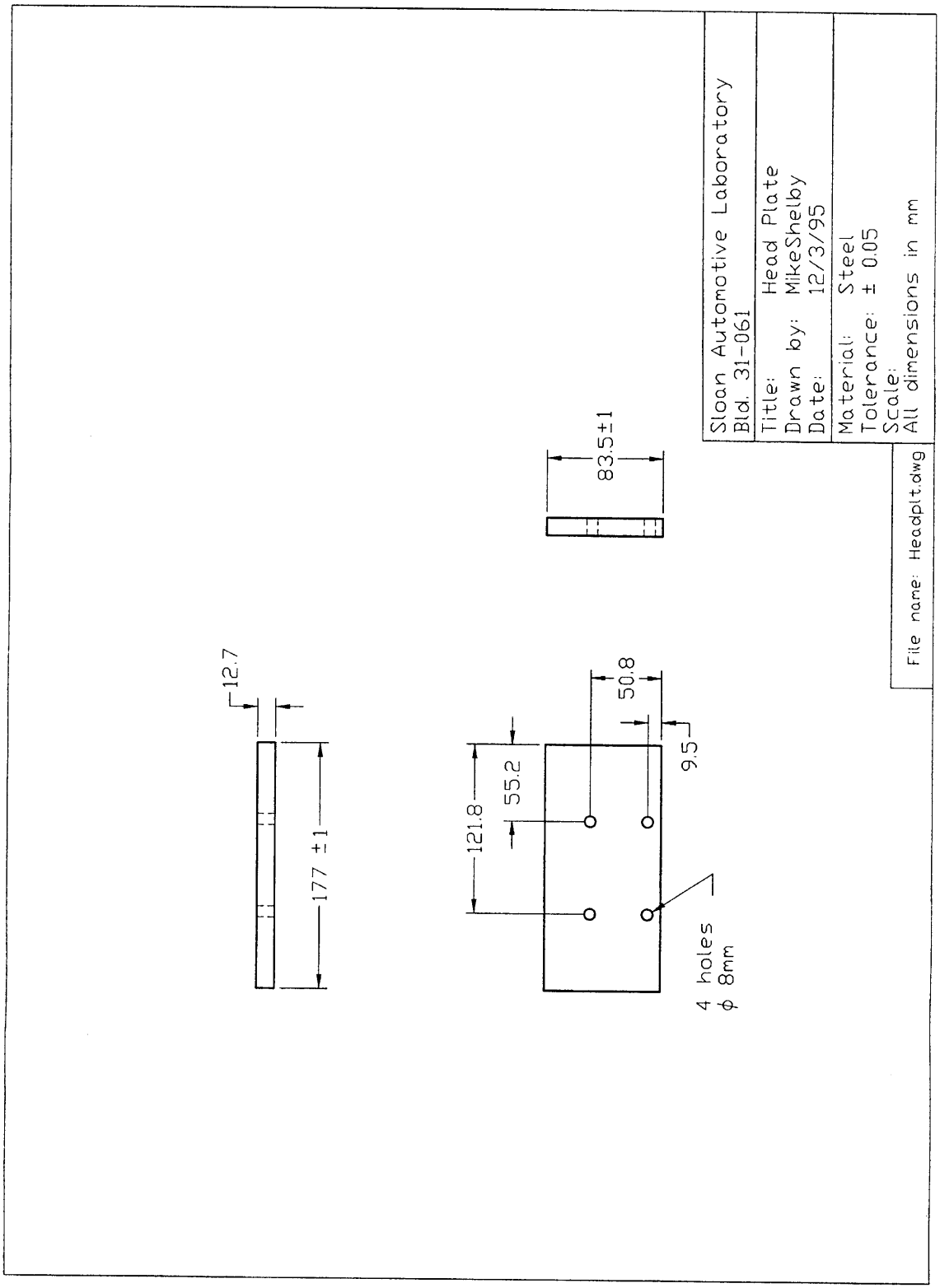

Figure A3.6 Head plate drawing

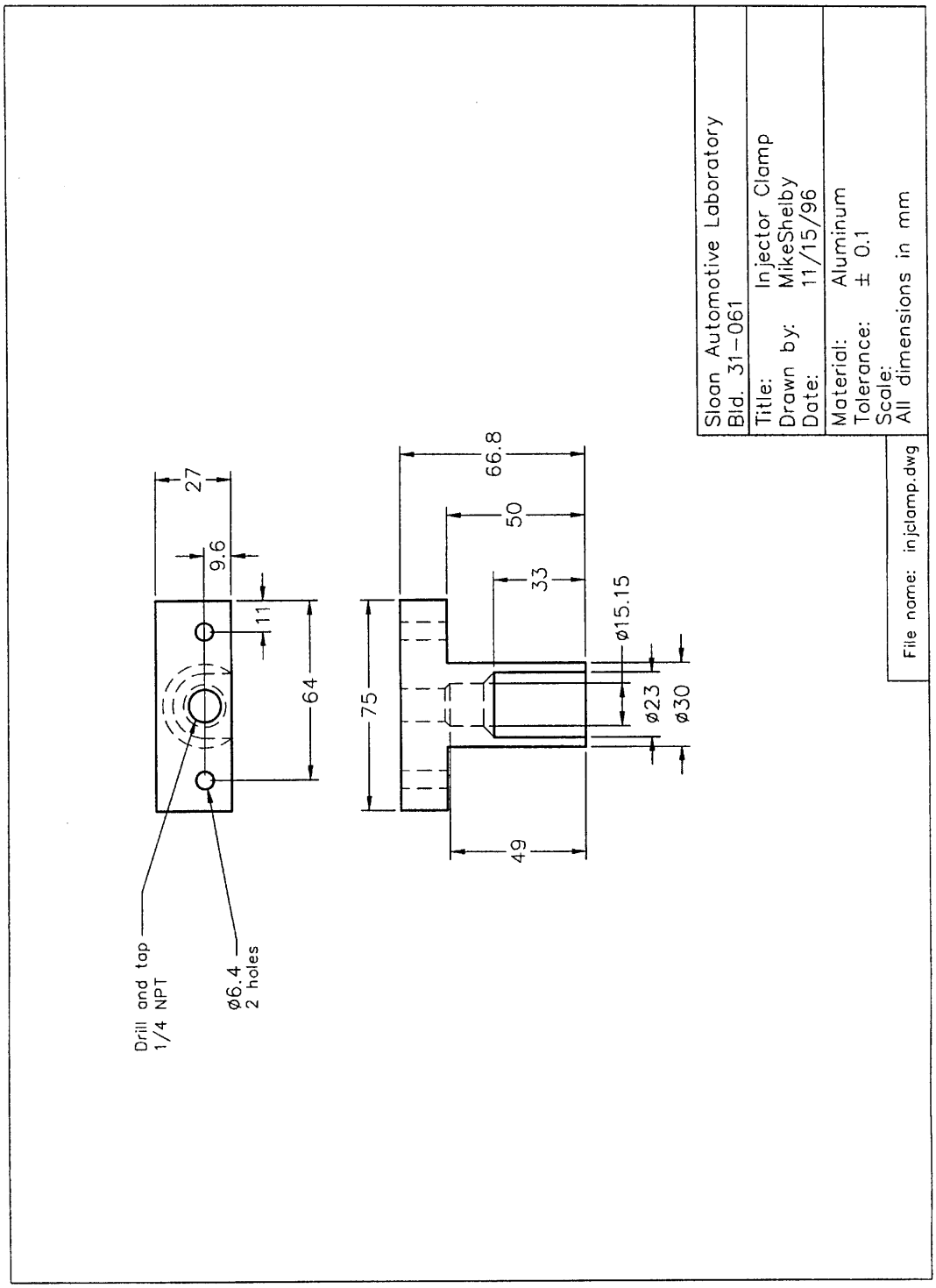

Figure A3.7 Zexel injector clamp drawing

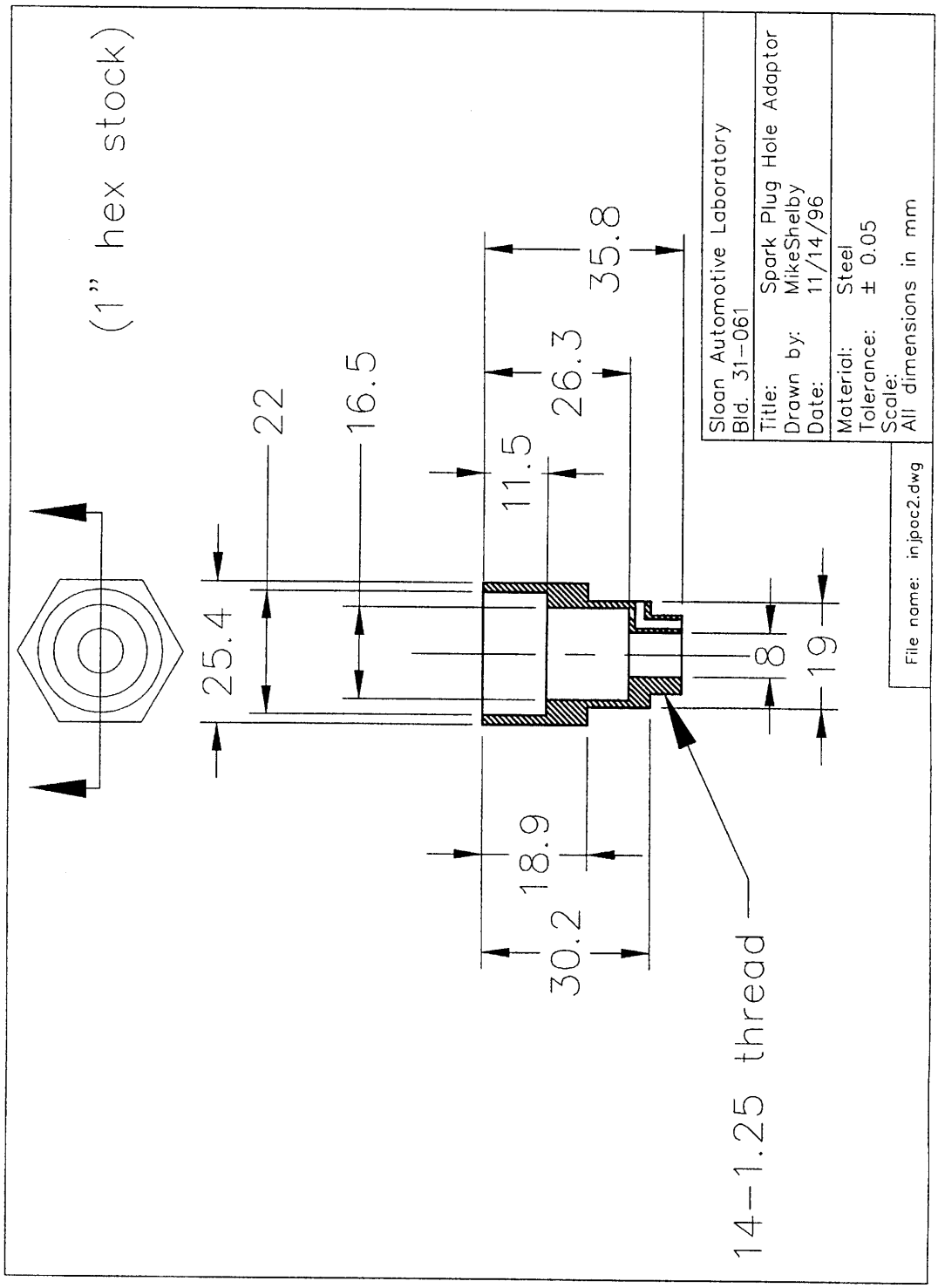

Figure A3.8 Spark plug hole adapter drawing

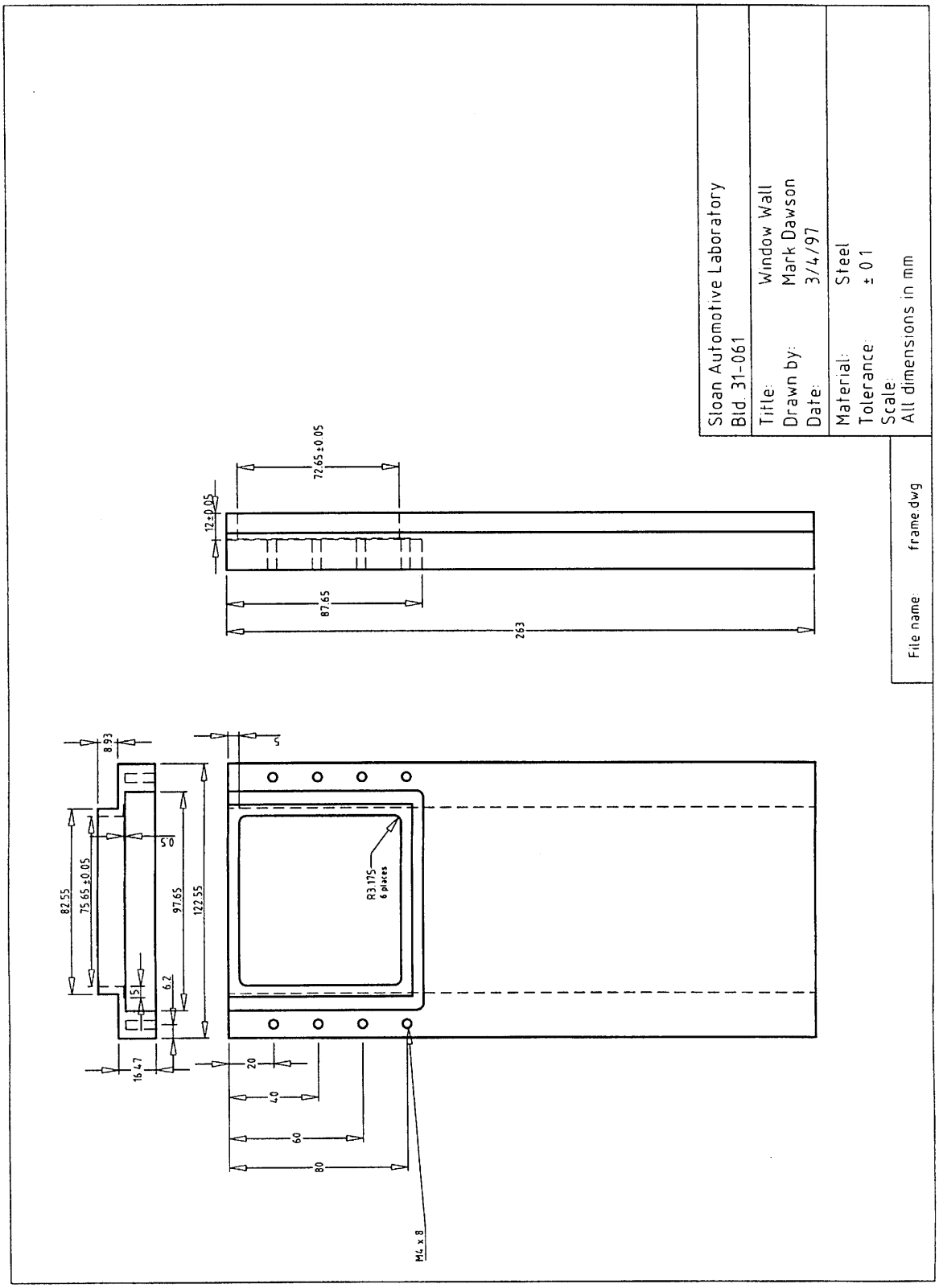

Figure A3.9 Third window frame drawing

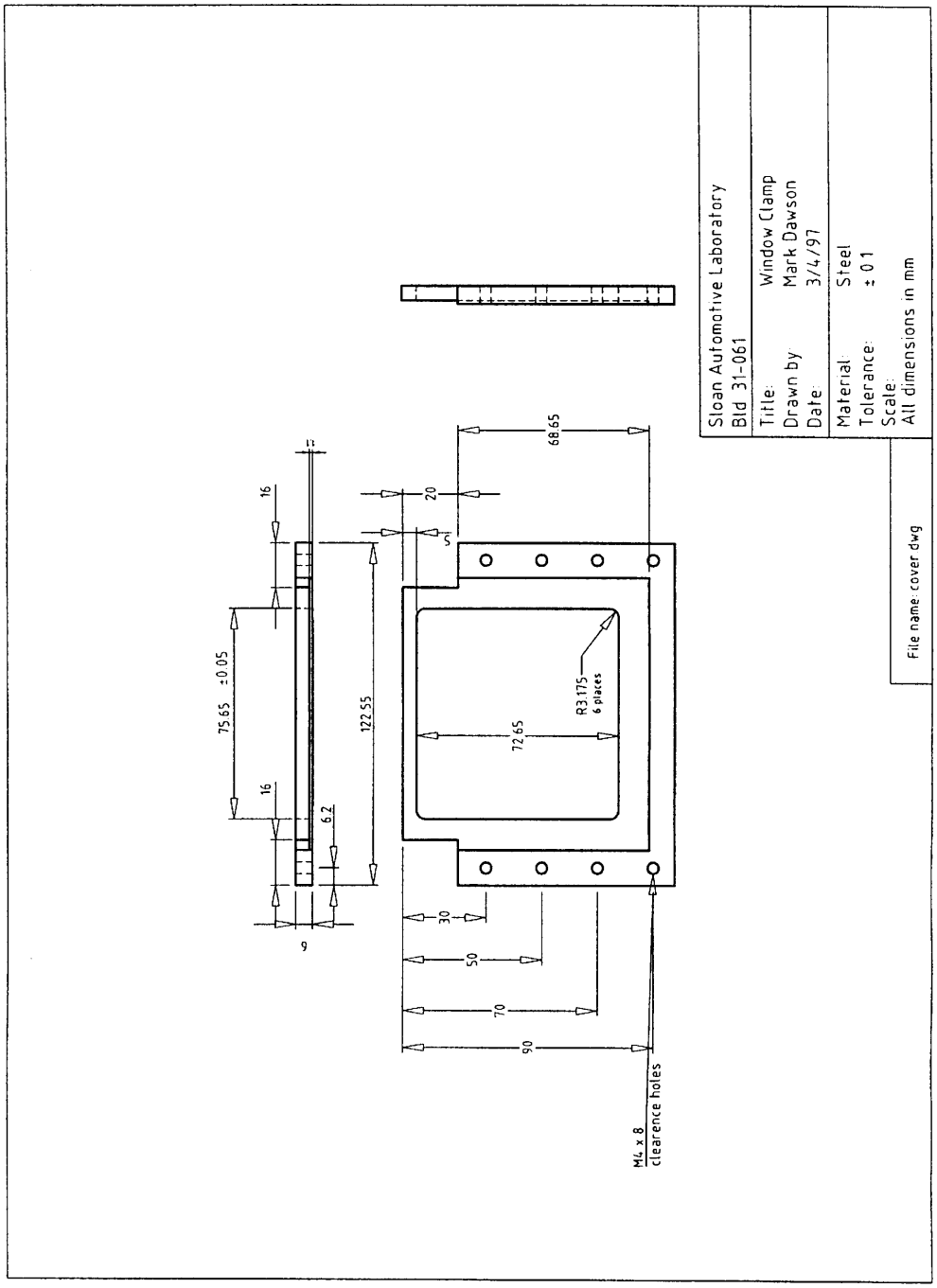

Figure A3.10 Window clamp drawing

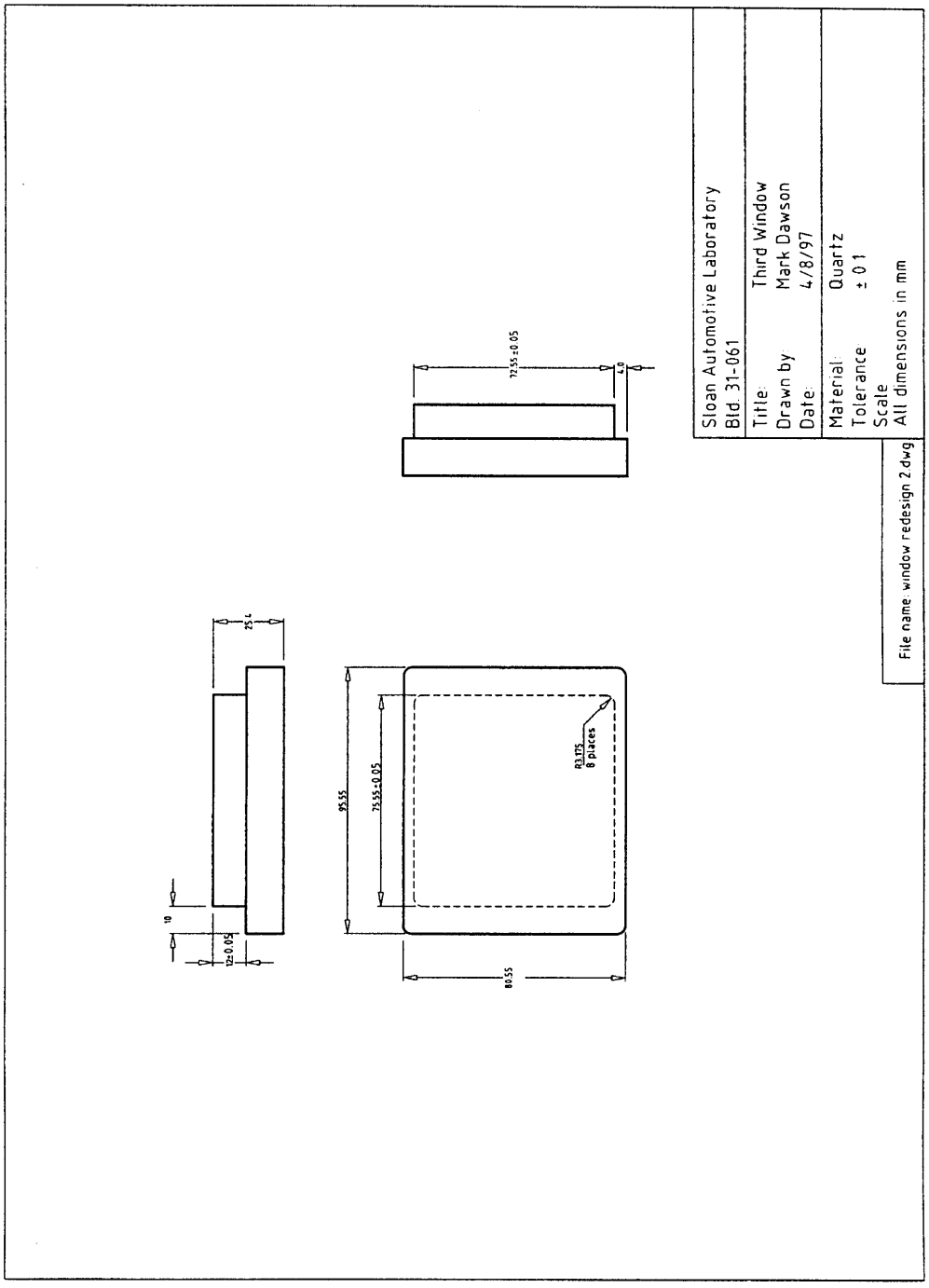

Figure A3.11 Third window drawing